WCAP-16149-NP
Revision 2

July 2007

Analysis of Capsule V from the South Texas Project Nuclear Operating Company, South Texas Unit 1 Reactor Vessel Radiation Surveillance Program

Westinghouse

WESTINGHOUSE NON-PROPRIETARY CLASS 3

WCAP-16149-NP, Revision 2

Analysis of Capsule V from the South Texas Project Nuclear Operating Company, South Texas Unit 1 Reactor Vessel Radiation Surveillance Program

B. N. Burgos*

July 2007

Approved by: J. S. Carlson, Manager*
Primary Component Asset Management

** Electronically approved records are authenticated in the Electronic Document Management System.*

Westinghouse Electric Company LLC
Energy Systems
P.O. Box 355
Pittsburgh, PA 15230-0355

TABLE OF CONTENTS

LIST OF TABLES

LIST OF TABLES (Cont.)

LIST OF FIGURES

LIST OF FIGURES (Cont.)

PREFACE

Revision 2 has been technically reviewed by:

Reviewer (Revision 2): F.C. Gift*

RECORD OF REVISIONS

Revision 0: Original Issue

Revision 1: Appendix D text was updated to reflect the correct plant name. This change was editorial in nature only.

Revision 2: Additional formatting changes were made to be consistent with the current standards of EDMS. These changes were editorial in nature only.

** Electronically approved records are authenticated in the Electronic Document Management System.*

EXECUTIVE SUMMARY

The purpose of this report is to document the results of the testing of surveillance Capsule V from South Texas Unit 1. Capsule V was removed at 11.13 EFPY and post irradiation mechanical tests of the Charpy V-notch and tensile specimens were performed. A fluence evaluation utilizing the recently released neutron transport and dosimetry cross-section libraries was derived from the ENDF/B-VI data-base. Capsule V received a fluence of 2.62 x 10^{19} n/cm^2 (E > 1.0 MeV) after irradiation to 11.13 EFPY. The peak clad/base metal interface vessel fluence after 11.13 EFPY of plant operation was 8.60 x 10^{18} n/cm^2 (E > 1.0 MeV).

This evaluation lead to the following conclusions: 1) The measured 30 ft-lb shift in transition temperature values of the intermediate shell plate R1606-2 contained in capsule V (transverse) is less than the Regulatory Guide 1.99, Revision 2[1], predictions. 2) The measured 30 ft-lb shift in transition temperature values of the intermediate shell plate R1606-2 contained in capsule V (longitudinal) is greater than the Regulatory Guide 1.99, Revision 2, predictions. However, the shift value is less than two sigma allowance by Regulatory Guide 1.99, Revision 2. 3) The measured 30 ft-lb shift in transition temperature values of the weld metal contained in capsule V is less than the Regulatory Guide 1.99, Revision 2, predictions. 4) The measured percent decrease in upper shelf energy for all the surveillance materials of Capsules V contained in the South Texas Unit 1 surveillance program are less than the Regulatory Guide 1.99, Revision 2 predictions. 5) All beltline materials exhibit a more than adequate upper shelf energy level for continued safe plant operation and are predicted to maintain an upper shelf energy greater than 50 ft-lb throughout the current license (34 EFPY) as required by 10CFR50, Appendix G [2]. 6) The South Texas Unit 1 surveillance data was found to be credible. This evaluation can be found in Appendix D.

Lastly, a brief summary of the Charpy V-notch testing can be found in Section 1. All Charpy V-notch data was plotted using a symmetric hyperbolic tangent curve fitting program.

1 SUMMARY OF RESULTS

The analysis of the reactor vessel materials contained in surveillance Capsule V, the third capsule removed and tested from the South Texas Unit 1 reactor pressure vessel, led to the following conclusions:

- The Charpy V-notch data presented in WCAP-14847 [3] were based on a re-plot of all capsule data from WCAP-9492 [4] and WCAP-12629 [5] using CVGRAPH, Version 4.1, which is a symmetric hyperbolic tangent curve-fitting program. The results presented herein only for the Capsule V test results, which are also based on using CVGRAPH, Version 4.1. This report also shows the composite plots that show the results from the previous capsules. Appendix C presents the CVGRAPH, Version 4.1, Charpy V-notch plots and the program input data.

- Capsule V received an average fast neutron fluence (E> 1.0 MeV) of 2.62 x 10^{19} n/cm^2 after 11.13 effective full power years (EFPY) of plant operation.

- Irradiation of the reactor vessel intermediate shell plate R1606-2 Charpy specimens, oriented with the longitudinal axis of the specimen parallel to the major working direction (longitudinal orientation), resulted in an irradiated 30 ft-lb transition temperature of -12.17°F and an irradiated 50 ft-lb transition temperature of 21.34°F. This results in a 30 ft-lb transition temperature increase of 40.15°F and a 50 ft-lb transition temperature increase of 41.78°F for the longitudinal oriented specimens.

- Irradiation of the reactor vessel intermediate shell plate R1606-2 Charpy specimens, oriented with the longitudinal axis of the specimen perpendicular to the major working direction (transverse orientation), resulted in an irradiated 30 ft-lb transition temperature of 17.78°F and an irradiated 50 ft-lb transition temperature of 56.11°F. This results in a 30 ft-lb transition temperature increase of 23.84°F and a 50 ft-lb transition temperature increase of 29.26°F for the longitudinal oriented specimens.

- Irradiation of the weld metal (heat number V89476) Charpy specimens resulted in an irradiated 30 ft-lb transition temperature of -29.41°F and an irradiated 50 ft-lb transition temperature of 15.64°F. This results in a 30 ft-lb transition temperature increase of 26.61°F and a 50 ft-lb transition temperature increase of 32.47°F.

- Irradiation of the weld Heat-Affected-Zone (HAZ) metal Charpy specimens resulted in an irradiated 30 ft-lb transition temperature of -75.34°F and an irradiated 50 ft-lb transition temperature of -35.75°F. This results in a 30 ft-lb transition temperature increase of 58.82°F and a 50 ft-lb transition temperature increase of 50.42°F.

- The average upper shelf energy of the intermediate shell plate R1606-2 (longitudinal orientation) resulted in an average energy decrease of 7 ft-lb after irradiation. This results in an irradiated average upper shelf energy of 131 ft-lb for the longitudinal oriented specimens.

- The average upper shelf energy of the Intermediate Shell Plate R1606-2 (transverse orientation) resulted in an average energy decrease of 7 ft-lb after irradiation. This results in an irradiated average upper shelf energy of 106 ft-lb for the longitudinal oriented specimens.

- The average upper shelf energy of the weld metal Charpy specimens resulted in no energy decrease after irradiation. This results in an irradiated average upper shelf energy of 86 ft-lb for the weld metal specimens.

- The average upper shelf energy of the weld HAZ metal Charpy specimens resulted in no energy decrease after irradiation. This results in an irradiated average upper shelf energy of 105 ft-lb for the weld HAZ metal.

- A comparison, as presented in Table 5-10, of the South Texas Unit 1 reactor vessel surveillance material test results with the Regulatory Guide 1.99, Revision 2[1] predictions led to the following conclusions:

  — The measured 30 ft-lb shift in transition temperature value of the intermediate shell plate R1606-2 contained in capsule V (longitudinal) is greater than the Regulatory Guide 1.99, Revision 2, prediction. However, the shift value is less than the two sigma allowance by Regulatory Guide 1.99, Revision 2.

  — The measured 30 ft-lb shift in transition temperature value of the intermediate shell plate R1606-2 contained in capsule V (transverse) is less than the Regulatory Guide 1.99, Revision 2, prediction.

  — The measured 30 ft-lb shift in transition temperature value of the weld metal contained in capsule V is less than the Regulatory Guide 1.99, Revision 2, prediction.

  — The measured percent decrease in upper shelf energy for all the surveillance materials of Capsules V contained in the South Texas Unit 1 surveillance program are less than the Regulatory Guide 1.99, Revision 2 prediction.

- All beltline materials exhibit a more than adequate upper shelf energy level for continued safe plant operation and are predicted to maintain an upper shelf energy greater than 50 ft-lb throughout the end of the current license (34 EFPY) as required by 10CFR50, Appendix G [2].

- The calculated end-of-license (34 EFPY) neutron fluence (E> 1.0 MeV) at the core midplane for the South Texas Unit 1 reactor vessel using the Regulatory Guide 1.99, Revision 2 attenuation formula (i.e., Equation #3 in the guide) are as follows:

<u>Calculated:</u> Vessel inner radius* = 2.46×10^{19} n/cm^2
Vessel 1/4 thickness = 1.47×10^{19} n/cm^2
Vessel 3/4 thickness = 5.20×10^{18} n/cm^2

*Clad/base metal interface. (Interpolated From Table 6-2)

2 INTRODUCTION

This report presents the results of the examination of Capsule V, the third capsule removed from the reactor in the continuing surveillance program which monitors the effects of neutron irradiation on the South Texas Project Nuclear Operating Company, South Texas Unit 1 reactor pressure vessel materials under actual operating conditions.

The surveillance program for the South Texas Project Nuclear Operating Company South Texas Unit 1 reactor pressure vessel materials was designed and recommended by the Westinghouse Electric Corporation. A description of the surveillance program and the pre-irradiation mechanical properties of the reactor vessel materials are presented in WCAP-9492, "South Texas Utilities South Texas Project Unit No. 1 Reactor Vessel Radiation Surveillance Program"[4]. The surveillance program was planned to cover the 40-year design life of the reactor pressure vessel and was based on ASTM E185-73, "Standard Recommended Practice for Surveillance Tests for Nuclear Reactor Vessels."[17] Capsule V was removed from the reactor after 11.13 EFPY of exposure and shipped to the Westinghouse Science and Technology Department Hot Cell Facility, where the post-irradiation mechanical testing of the Charpy V-notch impact and tensile surveillance specimens was performed.

This report summarizes the testing of and the post-irradiation data obtained from surveillance capsule V removed from the South Texas Project Nuclear Operating Company South Texas Unit 1 reactor vessel and discusses the analysis of the data.

3 BACKGROUND

The ability of the large steel pressure vessel containing the reactor core and its primary coolant to resist fracture constitutes an important factor in ensuring safety in the nuclear industry. The beltline region of the reactor pressure vessel is the most critical region of the vessel because it is subjected to significant fast neutron bombardment. The overall effects of fast neutron irradiation on the mechanical properties of low alloy, ferritic pressure vessel steels such as SA533 Grade B Class 1 (base material of the South Texas Unit 1 reactor pressure vessel beltline) are well documented in the literature. Generally, low alloy ferritic materials show an increase in hardness and tensile properties and a decrease in ductility and toughness during high-energy irradiation.

A method for ensuring the integrity of reactor pressure vessels has been presented in "Fracture Toughness Criteria for Protection Against Failure," Appendix G to Section XI of the ASME Boiler and Pressure Vessel Code [7]. The method uses fracture mechanics concepts and is based on the reference nil-ductility transition temperature (RT_{NDT}).

RT_{NDT} is defined as the greater of either the drop weight nil-ductility transition temperature (NDTT per ASTM E-208[6]) or the temperature 60°F less than the 50 ft-lb (and 35-mil lateral expansion) temperature as determined from Charpy specimens oriented perpendicular (transverse) to the major working direction of the plate. The RT_{NDT} of a given material is used to index that material to a reference stress intensity factor curve (K_{Ic} curve) which appears in Appendix G to the ASME Code[7]. The K_{Ic} curve is a lower bound of static fracture toughness results obtained from several heats of pressure vessel steel. When a given material is indexed to the K_{Ic} curve, allowable stress intensity factors can be obtained for this material as a function of temperature. Allowable operating limits can then be determined using these allowable stress intensity factors.

RT_{NDT} and, in turn, the operating limits of nuclear power plants can be adjusted to account for the effects of radiation on the reactor vessel material properties. The changes in mechanical properties of a given reactor pressure vessel steel, due to irradiation, can be monitored by a reactor vessel surveillance program, such as the South Texas Unit 1 reactor vessel radiation surveillance program[4], in which a surveillance capsule is periodically removed from the operating nuclear reactor and the encapsulated specimens tested. The increase in the average Charpy V-notch 30 ft-lb temperature (ΔRT_{NDT}) due to irradiation is added to the initial RT_{NDT}, along with a margin (M) to cover uncertainties, to adjust the RT_{NDT} (ART) for radiation embrittlement. This ART (RT_{NDT} initial + M + ΔRT_{NDT}) is used to index the material to the K_{Ic} curve and, in turn, to set operating limits for the nuclear power plant that take into account the effects of irradiation on the reactor vessel materials.

4 DESCRIPTION OF PROGRAM

Six surveillance capsules for monitoring the effects of neutron exposure on the South Texas Unit 1 reactor pressure vessel core region (beltline) materials were inserted in the reactor vessel prior to initial plant start-up. The six capsules were positioned in the reactor vessel between the neutron pads and the vessel wall as shown in Figure 4-1. The vertical center of the capsules is opposite the vertical center of the core. The capsules contain specimens made from intermediate shell plate R1606-2, weld metal fabricated with weld wire Type B4, Heat Number V89476 and Linde Type 124 flux, Lot Number 1061, which is identical to that used in the actual fabrication of the intermediate to lower shell circumferential weld seam. The surveillance weld was fabricated with the same heat of weld wire as all beltline region welds and is therefore representative of all of the reactor vessel beltline region welds.

Capsule V was removed after 11.13 effective full power years (EFPY) of plant operation. This capsule contained Charpy V-notch, tensile, and 1/2T-CT fracture mechanics specimens made from Intermediate Shell Plate R1606-2 and submerged arc weld metal representative of all the reactor vessel beltline region weld seams. In addition, this capsule contained Charpy V-notch specimens from the weld Heat-Affected-Zone (HAZ) metal of plate R1606-2.

Test material obtained from the intermediate shell course plate (after thermal heat treatment and forming of the plate) was taken at least one plate thickness from the quenched edges of the plate. All test specimens were machined from the ¼ thickness location of the plate after performing a simulated post-weld stress-relieved treatment on the test material and also from weld and heat-affected-zone metal of a stress-relieved weldment joining intermediate shell plate R1606-2 and adjacent intermediate shell plate R1606-3. All heat-affected-zone specimens were obtained from the weld heat-affected-zone of the Intermediate Shell Plate R1606-2.

Charpy V-notch impact specimens from intermediate shell plate R1606-2 were machined in the longitudinal orientation (longitudinal axis of the specimen parallel to the major working direction) and also in the transverse orientation (longitudinal axis of the specimen perpendicular to the major working direction). The core region weld Charpy impact specimens were machined from the weldment such that the long dimension of each Charpy specimen was perpendicular to the weld direction. The notch of the weld metal Charpy specimens was machined such that the direction of crack propagation in the specimen was in the welding direction.

Tensile specimens from intermediate shell plate R1606-2 were machined in both the longitudinal and transverse orientations. Tensile specimens from the weld metal were oriented with the long dimension of the specimen perpendicular to the weld direction.

Compact tension test specimens from intermediate shell plate R1606-2 were machined in the longitudinal and transverse orientations. Compact tension test specimens from the weld metal were machined perpendicular to the weld direction with the notch oriented in the direction of welding. All specimens were fatigue pre-cracked according to ASTM E399.

The chemical composition and heat treatment of the unirradiated surveillance materials are presented in Tables 4-1 and 4-2, respectively. The data in Table 4-1 and 4-2 was obtained from the unirradiated surveillance program report, WCAP-9492[4], Appendix A.

Capsule V contained dosimeter wires of pure iron, copper, nickel, and aluminum-0.15 weight percent cobalt (cadmium-shielded and unshielded). In addition, cadmium shielded dosimeters of neptunium (Np^{237}) and uranium (U^{238}) were placed in the capsule to measure the integrated flux at specific neutron energy levels.

The capsule contained thermal monitors made from two low-melting-point eutectic alloys and sealed in Pyrex tubes. These thermal monitors were used to define the maximum temperature attained by the test specimens during irradiation. The composition of the two eutectic alloys and their melting points are as follows:

2.5% Ag, 97.5% Pb	Melting Point: 579°F (304°C)
1.75% Ag, 0.75% Sn, 97.5% Pb	Melting Point: 590°F (310°C)

The arrangement of the various mechanical specimens, dosimeters and thermal monitors contained in Capsule V is shown in Figure 4-2.

Table 4-1 Chemical Composition (wt%) of the South Texas Unit 1 Reactor Vessel Surveillance Materials (Unirradiated)[a]

Element	Intermediate Shell Plate R1606-2	Weld Metal [b]
C	0.190	0.120
S	0.013	0.010
N_2	0.008	0.004
Co	0.012	0.009
Cu	0.040	0.020
Si	0.190	0.420
Mo	0.530	0.530
Ni	0.610	0.090
Mn	1.180	1.360
Cr	0.030	0.020
V	0.004	0.003
P	0.008	0.009
Sn	0.002	0.003
B	<0.001	0.001
Cb	<0.010	<0.010
Ti	<0.010	<0.010
W	<0.010	0.020
As	0.003	0.004
Zr	<0.001	<0.001
Pb	Not Dectected	<0.001
Ar	0.017	0.008

Notes:

(a) Data obtained from WCAP-9492[4] and duplicated herein for completeness.

(b) Weld wire Type B4, Heat Number V89476, Flux Type Linde 124, and Flux Lot Number 1061. Surveillance weldment is from a weld between the intermediate shell plates R1606-2 and R1606-3 and is identical to the intermediate to lower shell circumferential weld seam.

Table 4-2 Heat Treatment History of the South Texas Unit 1 Reactor Vessel Surveillance Materials[a]

Material	Temperature (°F)	Time	Coolant
Intermediate Shell Plate R1606-2	Austenitized @ 1600 ± 25	4 hrs.	Water-Quench
	Tempered @ 1225 ± 25	4 hrs.	Air-cooled
	Stress Relieved @ 1150 ± 50	14 hrs. 43 min.	Furnace Cooled
Weld Metal (heat # 89476)	Stress Relieved[b] @ 1150 ± 50	13 hrs. 15 min.	Furnace Cooled

Notes:

(a) This table was taken from WCAP-9492[4].

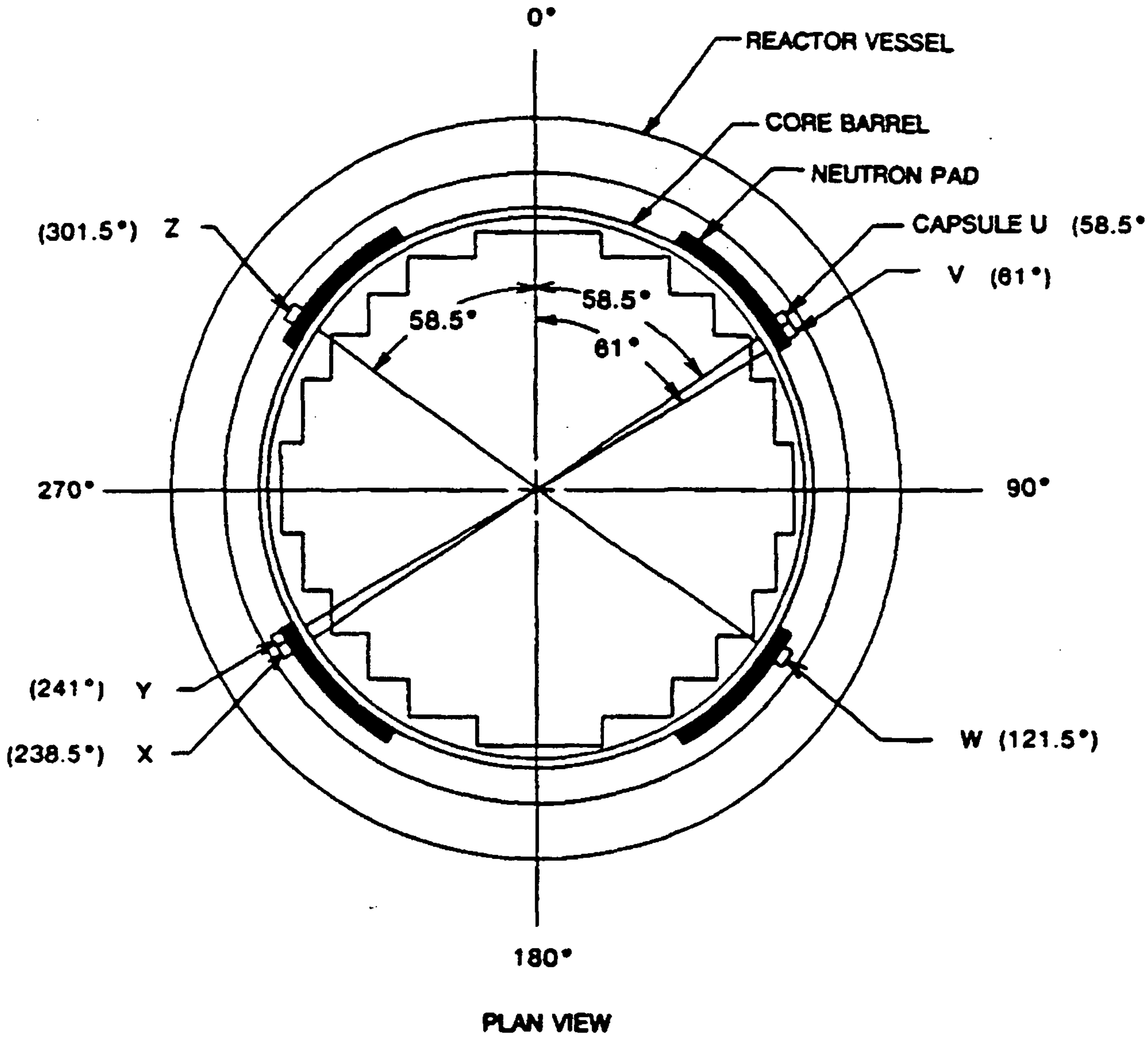

Figure 4-1 Arrangement of Surveillance Capsules in the South Texas Unit 1 Reactor Vessel

LEGEND:

GL - INTERMEDIATE SHELL PLATE R1606-2 (HT. - B8120-1 LONGITUDINAL)

GT - INTERMEDIATE SHELL PLATE R1606-2 (HT. - B8120-1 TRANSVERSE)

GW - WELD METAL

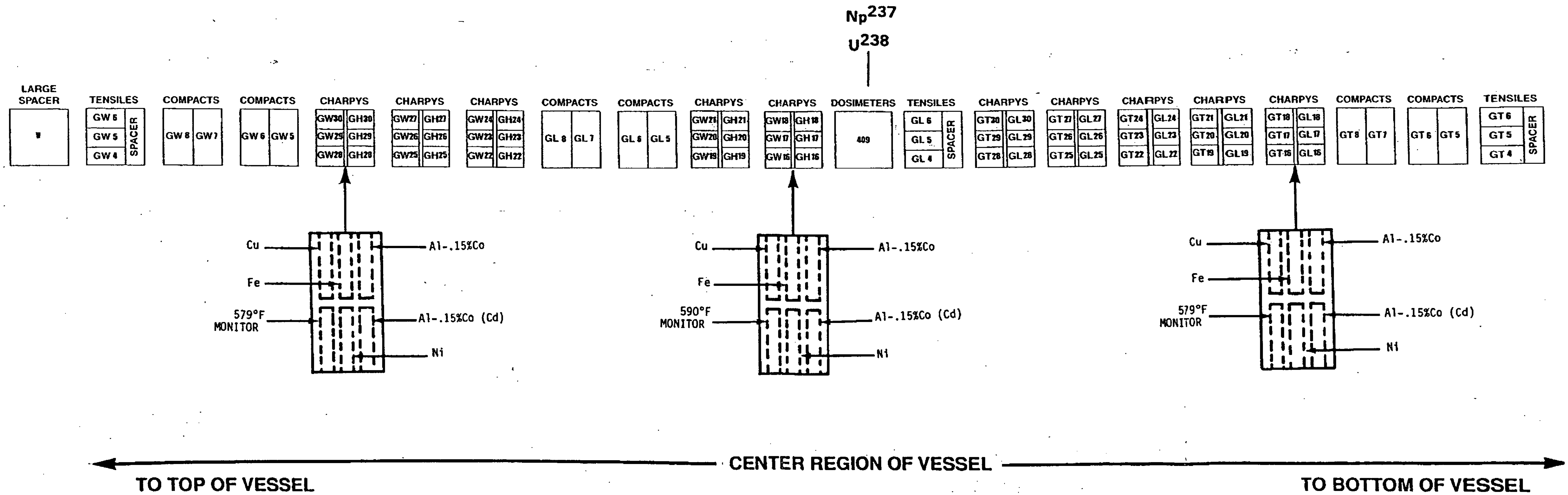

Figure 4-2 Capsule V Diagram Showing The Location of Specimens, Thermal Monitors, and Dosimeters

5 TESTING OF SPECIMENS FROM CAPSULE V

5.1 OVERVIEW

The post-irradiation mechanical testing of the Charpy V-notch impact specimens and tensile specimens was performed in the Remote Metallographic Facility (RMF) at the Westinghouse Research and Technology Park. Testing was performed in accordance with 10CFR50, Appendices G and H[2], ASTM Specification E185-82[8], and Westinghouse Procedure RMF 8402[9], Revision 2 as modified by Westinghouse RMF Procedures 8102[10], Revision 1, and 8103[11], Revision 1.

Upon receipt of the capsule at the hot cell laboratory, the specimens and spacer blocks were carefully removed, inspected for identification number, and checked against the master list in WCAP-9492[4]. No discrepancies were found.

Examination of the two low-melting point 579°F (304°C) and 590°F (310°C) eutectic alloys indicated no melting of either type of thermal monitor. Based on this examination, the maximum temperature to which the test specimens were exposed was less than 579°F (304°C).

The Charpy impact tests were performed per ASTM Specification E23-98[12] and RMF Procedure 8103, Rev. 1, on a Tinius-Olsen Model 74, 358J machine. The tup (striker) of the Charpy impact test machine is instrumented with a GRC 930-I instrumentation system, feeding information into an IBM compatible computer. With this system, load-time and energy-time signals can be recorded in addition to the standard measurement of Charpy energy (E_D). From the load-time curve (Appendix B), the load of general yielding (P_{GY}), the time to general yielding (t_{GY}), the maximum load (P_M), and the time to maximum load (t_M) can be determined. Under some test conditions, a sharp drop in load indicative of fast fracture was observed. The load at which fast fracture was initiated is identified as the fast fracture load (P_F), and the load at which fast fracture terminated is identified as the arrest load (P_A).

The energy at maximum load (E_M) was determined by comparing the energy-time record and the load-time record. The energy at maximum load is approximately equivalent to the energy required to initiate a crack in the specimen. Therefore, the propagation energy for the crack (E_p) is the difference between the total energy to fracture (E_D) and the energy at maximum load (E_M).

The yield stress (σ_Y) was calculated from the three-point bend formula having the following expression:

$$\sigma_Y = (P_{GY} * L) / [B * (W - a)^2 * C] \quad (1)$$

where:
- L = distance between the specimen supports in the impact machine
- B = the width of the specimen measured parallel to the notch
- W = height of the specimen, measured perpendicularly to the notch
- a = notch depth

The constant C is dependent on the notch flank angle (ϕ), notch root radius (ρ) and the type of loading (i.e., pure bending or three-point bending). In three-point bending, for a Charpy specimen in which ϕ = 45° and ρ = 0.010 inch, Equation 1 is valid with C = 1.21. Therefore, (for L = 4W),

$$\sigma_Y = (P_{GY} * L) / [B * (W-a)^2 * 1.21] = (3.305 * P_{GY} * W) / [B * (W-a)^2] \qquad (2)$$

For the Charpy specimen, B = 0.394 inch, W = 0.394 inch and a = 0.079 inch. Equation 2 then reduces to:

$$\sigma_Y = 33.3 * P_{GY} \qquad (3)$$

where σ_y is in units of psi and P_{GY} is in units of lbs. The flow stress was calculated from the average of the yield and maximum loads, also using the three-point bend formula.

The symbol A in columns 4, 5, and 6 of Tables 5-5 through 5-8 is the cross-section area under the notch of the Charpy specimens:

$$A = B * (W - a) = 0.1241 \text{ sq.in.} \qquad (4)$$

Percent shear was determined from post-fracture photographs using the ratio-of-areas methods in compliance with ASTM Specification E23-98 and A370-97a[13]. The lateral expansion was measured using a dial gage rig similar to that shown in the same specification.

Tensile tests were performed on a 20,000-pound Instron, split-console test machine (Model 1115) per ASTM Specification E8-99[14] and E21-92 (1998)[15], and Procedure RMF 8102, Rev. 1. All pull rods, grips, and pins were made of Inconel 718. The upper pull rod was connected through a universal joint to improve axiality of loading. The tests were conducted at a constant crosshead speed of 0.05 inches per minute throughout the test.

Extension measurements were made with a linear variable displacement transducer extensometer. The extensometer knife-edges were spring-loaded to the specimen and operated through specimen failure. The extensometer gage length was 1.00 inch. The extensometer is rated as Class B-2 per ASTM E83-93[16].

Elevated test temperatures were obtained with a three-zone electric resistance split-tube furnace with a 9-inch hot zone. All tests were conducted in air. Because of the difficulty in remotely attaching a thermocouple directly to the specimen, the following procedure was used to monitor specimen temperatures. Chromel-Alumel thermocouples were positioned at the center and at each end of the gage section of a dummy specimen and in each tensile machine griper. In the test configuration, with a slight load on the specimen, a plot of specimen temperature versus upper and lower tensile machine griper and controller temperatures was developed over the range from room temperature to 550°F. During the actual testing, the grip temperatures were used to obtain desired specimen temperatures. Experiments have indicated that this method is accurate to $\pm$2°F.

The yield load, ultimate load, fracture load, total elongation, and uniform elongation were determined directly from the load-extension curve. The yield strength, ultimate strength, and fracture strength were calculated using the original cross-sectional area. The final diameter and final gage length were determined from post-fracture photographs. The fracture area used to calculate the fracture stress (true stress at fracture) and percent reduction in area was computed using the final diameter measurement.

5.2 CHARPY V-NOTCH IMPACT TEST RESULTS

The results of the Charpy V-notch impact tests performed on the various materials contained in Capsule V, which received a fluence of 2.62 x 10^{19} n/cm^2(E> 1.0 MeV) in 11.13 EFPY of operation, are presented in Tables 5-1 through 5-8 and are compared with unirradiated results[4] as shown in Figures 5-1 through 5-12.

The transition temperature increases and upper shelf energy decreases for the Capsule V materials are summarized in Table 5-9 and led to the following results:

- The Charpy V-notch data presented in WCAP-14847 [3] were based on a re-plot of all capsule data from WCAP-9492 [4] and WCAP-12629 [5] using CVGRAPH, Version 4.1, which is a symmetric hyperbolic tangent curve-fitting program. The results presented herein only for the Capsule V test results, which are also based on using CVGRAPH, Version 4.1. This report also shows the composite plots that show the results from the previous capsules. Appendix C presents the CVGRAPH, Version 4.1, Charpy V-notch plots and the program input data.

- Capsule V received an average fast neutron fluence (E> 1.0 MeV) of 2.62 x 10^{19} n/cm^2 after 11.13 effective full power years (EFPY) of plant operation.

- Irradiation of the reactor vessel intermediate shell plate R1606-2 Charpy specimens, oriented with the longitudinal axis of the specimen parallel to the major working direction (longitudinal orientation), resulted in an irradiated 30 ft-lb transition temperature of -12.17°F and an irradiated 50 ft-lb transition temperature of 21.34°F. This results in a 30 ft-lb transition temperature increase of 40.15°F and a 50 ft-lb transition temperature increase of 41.78°F for the longitudinal oriented specimens.

- Irradiation of the reactor vessel intermediate shell plate R1606-2 Charpy specimens, oriented with the longitudinal axis of the specimen perpendicular to the major working direction (transverse orientation), resulted in an irradiated 30 ft-lb transition temperature of 17.78°F and an irradiated 50 ft-lb transition temperature of 56.11°F. This results in a 30 ft-lb transition temperature increase of 23.84°F and a 50 ft-lb transition temperature increase of 29.26°F for the longitudinal oriented specimens.

- Irradiation of the weld metal (heat number 89476) Charpy specimens resulted in an irradiated 30 ft-lb transition temperature of -29.41°F and an irradiated 50 ft-lb transition temperature of 15.64°F. This results in a 30 ft-lb transition temperature increase of 26.61°F and a 50 ft-lb transition temperature increase of 32.47°F.

- Irradiation of the weld Heat-Affected-Zone (HAZ) metal Charpy specimens resulted in an irradiated 30 ft-lb transition temperature of -75.34°F and an irradiated 50 ft-lb transition temperature of -35.75°F. This results in a 30 ft-lb transition temperature increase of 58.82°F and a 50 ft-lb transition temperature increase of 50.42°F.

- The average upper shelf energy of the intermediate shell plate R1606-2 (longitudinal orientation) resulted in an average energy decrease of 7 ft-lb after irradiation. This results in an irradiated average upper shelf energy of 131 ft-lb for the longitudinal oriented specimens.

- The average upper shelf energy of the Intermediate Shell Plate R1606-2 (transverse orientation) resulted in an average energy decrease of 7 ft-lb after irradiation. This results in an irradiated average upper shelf energy of 106 ft-lb for the longitudinal oriented specimens.

- The average upper shelf energy of the weld metal Charpy specimens resulted in no energy decrease after irradiation. This results in an irradiated average upper shelf energy of 86 ft-lb for the weld metal specimens.

- The average upper shelf energy of the weld HAZ metal Charpy specimens resulted in no energy decrease after irradiation. This results in an irradiated average upper shelf energy of 105 ft-lb for the weld HAZ metal.

- A comparison, as presented in Table 5-10, of the South Texas Unit 1 reactor vessel surveillance material test results with the Regulatory Guide 1.99, Revision 2[1] predictions led to the following conclusions:

  — The measured 30 ft-lb shift in transition temperature value of the intermediate shell plate R1606-2 contained in capsule V (longitudinal) is greater than the Regulatory Guide 1.99, Revision 2, prediction. However, the shift value is less than the two sigma allowance by Regulatory Guide 1.99, Revision 2.

  — The measured 30 ft-lb shift in transition temperature value of the intermediate shell plate R1606-2 contained in capsule V (transverse) is less than the Regulatory Guide 1.99, Revision 2, prediction.

  — The measured 30 ft-lb shift in transition temperature value of the weld metal contained in capsule V is less than the Regulatory Guide 1.99, Revision 2, prediction.

  — The measured percent decrease in upper shelf energy for all the surveillance materials of Capsules V contained in the South Texas Unit 1 surveillance program are less than the Regulatory Guide 1.99, Revision 2 prediction.

All beltline materials exhibit a more than adequate upper shelf energy level for continued safe plant operation and are predicted to maintain an upper shelf energy greater than 50 ft-lb throughout the end of the current license (34 EFPY) as required by 10CFR50, Appendix G [2].

The fracture appearance of each irradiated Charpy specimen from the various surveillance Capsule V materials is shown in Figures 5-13 through 5-16 and shows an increasingly ductile or tougher appearance with increasing test temperature.

The load-time records for individual instrumented Charpy specimen tests are shown in Appendix B.

The Charpy V-notch data presented in WCAP-14847 [3] were based on a re-plot of all capsule data from WCAP-9492 [4] and WCAP-12629 [5] using CVGRAPH, Version 4.1, which is a symmetric hyperbolic tangent curve-fitting program. The results presented herein only for the Capsule V test results, which are also based on using CVGRAPH, Version 4.1. This report also shows the composite plots that show the results from the previous capsules. Appendix C presents the CVGRAPH, Version 4.1, Charpy V-notch plots and the program input data for Capsule V.

5.3 TENSILE TEST RESULTS

The results of the tensile tests performed on the various materials contained in Capsule V irradiated to 2.62×10^{19} n/cm^2 (E> 1.0 MeV) are presented in Table 5-11 and are compared with unirradiated results[4] as shown in Figures 5-17 through 5-19.

The results of the tensile tests performed on the intermediate shell plate R1606-2 (longitudinal orientation) indicated that irradiation to 2.62×10^{19} n/cm^2 (E> 1.0 MeV) caused approximately a 2 to 6 ksi increase in the 0.2 percent offset yield strength and approximately a 1 to 4 ksi increase in the ultimate tensile strength when compared to unirradiated data[4]. See Figure 5-17.

The results of the tensile tests performed on the intermediate shell plate R1606-2 (transverse orientation) indicated that irradiation to 2.62×10^{19} n/cm^2 (E> 1.0 MeV) caused approximately a 2 to 6 ksi increase in the 0.2 percent offset yield strength and approximately a 1 to 4 ksi increase in the ultimate tensile strength when compared to unirradiated data[4]. See Figure 5-18.

The results of the tensile tests performed on the surveillance weld metal indicated that irradiation to 2.62×10^{19} n/cm^2 (E> 1.0 MeV) caused approximately a 1 to 8 ksi increase in the 0.2 percent offset yield strength and approximately a 2 to 5 ksi increase in the ultimate tensile strength when compared to unirradiated data[4]. See Figure 5-19.

The fractured tensile specimens for the intermediate shell plate R1606-2 material are shown in Figures 5-20 and 5-21, while the fractured tensile specimens for the surveillance weld metal are shown in Figure 5-22. The engineering stress-strain curves for the tensile tests are shown in Figures 5-23 through 5-25.

5.4 1/2T COMPACT TENSION SPECIMEN TESTS

Per the surveillance capsule testing contract, the 1/2T Compact Tension Specimens were not tested and are being stored at the Westinghouse Research and Technology Park Hot Cell facility.

Table 5-1 Charpy V-notch Data for the South Texas Unit 1 Intermediate Shell Plate R1606-2 Irradiated to a Fluence of 2.62 x 10^{19} n/cm^2 (E> 1.0 MeV) (Longitudinal Orientation)							
Sample	**Temperature**		**Impact Energy**		**Lateral Expansion**		**Shear**
Number	**°F**	**°C**	**ft-lbs**	**Joules**	**mils**	**mm**	**%**
GL29	-75	-59	4	5	0	0.00	2
GL16	-25	-32	29	39	15	0.38	10
GL21	-25	-32	29	39	18	0.46	5
GL17	0	-18	16	22	9	0.23	15
GL24	10	-12	29	39	16	0.41	15
GL23	25	-4	53	72	36	0.91	25
GL18	30	-1	69	94	42	1.07	40
GL19	50	10	95	129	58	1.47	55
GL25	100	38	92	125	58	1.47	70
GL20	125	52	104	141	66	1.68	80
GL27	150	66	115	156	70	1.78	90
GL22	175	79	123	167	74	1.88	100
GL30	225	107	133	180	71	1.80	100
GL28	250	121	141	191	75	1.91	100
GL26	250	121	127	172	78	1.98	100

Table 5-2 Charpy V-notch Data for the South Texas Unit 1 Intermediate Shell Plate R1606-2 Irradiated to a Fluence of 2.62 x 10^{19} n/cm^2 (E> 1.0 MeV) (Transverse Orientation)

Sample	Temperature		Impact Energy		Lateral Expansion		Shear
Number	°F	°C	ft-lbs	Joules	mils	mm	%
GT28	-100	-73	2	3	0	0.00	2
GT25	-50	-46	17	23	9	0.23	5
GT21	-25	-32	14	19	7	0.18	10
GT20	0	-18	22	30	13	0.33	15
GT30	25	-4	27	37	17	0.43	20
GT22	40	4	53	72	36	0.91	30
GT24	50	10	43	58	28	0.71	40
GT29	75	24	59	80	40	1.02	45
GT26	100	38	69	94	49	1.24	50
GT27	125	52	87	118	60	1.52	80
GT17	150	66	94	127	62	1.57	90
GT18	200	93	109	148	67	1.70	100
GT16	225	107	94	127	64	1.63	100
GT19	250	121	108	146	70	1.78	100
GT23	260	127	112	152	70	1.78	100

Table 5-3 Charpy V-notch Data for the South Texas Unit 1 Surveillance Weld Metal Irradiated to a Fluence of 2.62 x 10^{19} n/cm^2 (E> 1.0 MeV)

Sample Number	Temperature		Impact Energy		Lateral Expansion		Shear
	°F	°C	ft-lbs	Joules	mils	mm	%
GW16	-125	-87	3	4	0	0.00	2
GW17	-75	-59	29	39	15	0.38	10
GW25	-75	-59	6	8	0	0.00	20
GW26	-50	-46	16	22	9	0.23	20
GW19	-25	-32	28	38	16	0.41	30
GW28	0	-18	71	96	46	1.17	60
GW27	0	-18	32	43	25	0.64	45
GW20	25	-4	45	61	33	0.84	55
GW24	50	10	69	94	51	1.30	80
GW22	75	24	72	98	52	1.32	80
GW29	100	38	71	96	53	1.35	85
GW21	150	66	102	138	81	2.06	100
GW18	175	79	102	138	73	1.85	100
GW23	200	93	87	118	62	1.57	100
GW30	200	93	87	118	56	1.42	100

Table 5-4 Charpy V-notch Data for the South Texas Unit 1 Heat-Affected-Zone (HAZ) Material Irradiated to a Fluence of 2.62 x 10^{19} n/cm^2 (E> 1.0 MeV)

Sample	Temperature		Impact Energy		Lateral Expansion		Shear
Number	°F	°C	Ft-lbs	Joules	mils	mm	%
GH22	-150	-101	13	18	4	0.10	2
GH30	-75	-59	26	35	10	0.25	15
GH28	-50	-46	45	61	16	0.41	20
GH18	-25	-32	84	114	58	1.47	70
GH20	-25	-32	46	62	21	0.53	35
GH16	0	-18	32	43	16	0.41	40
GH21	10	-12	68	92	39	0.99	60
GH24	25	-4	105	142	57	1.45	75
GH26	25	-4	118	160	52	1.32	85
GH17	40	4	82	111	64	1.63	100
GH23	50	10	55	75	42	1.07	75
GH29	75	24	105	142	64	1.63	100
GH27	100	38	117	159	74	1.88	100
GH19	125	52	119	161	72	1.83	100
GH25	150	66	114	155	71	1.80	100

Table 5-5 Instrumented Charpy Impact Test Results for the South Texas Unit 1 Intermediate Shell Plate R1606-2 Irradiated to a Fluence of 2.62 x 10^{19} n/cm^2 (E>1.0 MeV) (Longitudinal Orientation)

Sample No.	Test Temp. (°F)	Charpy Energy E_D (ft-lb)	Normalized Energies (ft-lb/in^2)			Yield Load P_{GY} (lb)	Time to Yield t_{GY} (msec)	Max. Load P_M (lb)	Time to Max. t_M (msec)	Fast Fract. Load P_F (lb)	Arrest Load P_A (lb)	Yield Stress σ_Y (ksi)	Flow Stress (ksi)
			Charpy E_D/A	Max. E_M/A	Prop. E_p/A								
GL29	-75	4	32	14	18	1851	0.12	1851	0.12	1851	0	62	62
GL16	-25	29	234	193	41	3424	0.14	4401	0.45	4396	0	114	130
GL21	-25	29	234	193	40	3530	0.14	4459	0.44	4452	0	118	133
GL17	0	16	129	61	67	3486	0.15	4125	0.21	4084	0	116	127
GL24	10	29	234	184	50	3353	0.14	4299	0.43	4290	0	112	127
GL23	25	53	427	312	115	3502	0.15	4419	0.66	4286	0	117	132
GL18	30	69	556	227	329	3395	0.14	4386	0.51	4089	0	113	130
GL19	50	95	765	314	451	3214	0.14	4284	0.70	3338	351	107	125
GL25	100	92	741	218	523	3070	0.14	4198	0.52	3503	1329	102	121
GL20	125	104	838	298	540	3120	0.14	4182	0.68	3086	1426	104	122
GL27	150	115	927	293	634	3081	0.14	4144	0.68	3038	1735	103	120
GL22	175	123	991	289	702	3047	0.14	4096	0.67	n/a	n/a	101	119
GL30	225	133	1072	344	728	3069	0.15	4187	0.78	n/a	n/a	102	121
GL28	250	141	1136	284	852	2863	0.14	4008	0.68	n/a	n/a	95	114
GL26	250	127	1023	282	742	2900	0.14	4042	0.67	n/a	n/a	97	116

Table 5-6 Instrumented Charpy Impact Test Results for the South Texas Unit 1 Intermediate Shell Plate R1606-2 Irradiated to a Fluence of 2.62 x 10^{19} n/cm^2 (E>1.0 MeV) (Transverse Orientation)

Sample No.	Test Temp. (°F)	Charpy Energy E_D (ft-lb)	Normalized Energies (ft-lb/in^2) Charpy E_D/A	Max. E_M/A	Prop. E_p/A	Yield Load P_{GY} (lb)	Time to Yield t_{GY} (msec)	Max. Load P_M (lb)	Time to Max. t_M (msec)	Fast Fract. Load P_F (lb)	Arrest Load P_A (lb)	Yield Stress σ_Y (ksi)	Flow Stress (ksi)
GT28	-100	2	16	8	8	1135	0.10	1135	0.10	1135	0	38	38
GT25	-50	17	137	66	71	3639	0.15	4315	0.21	4225	0	121	132
GT21	-25	14	113	61	52	3480	0.14	4170	0.21	4144	0	116	127
GT20	0	22	177	66	111	3390	0.14	4086	0.22	4011	0	113	124
GT30	25	27	218	60	157	3272	0.14	3915	0.21	3799	336	109	120
GT22	40	53	427	221	206	3171	0.14	4293	0.52	4144	389	106	124
GT24	50	43	346	207	139	3224	0.15	4177	0.50	4151	673	107	123
GT29	75	59	475	299	177	3188	0.14	4261	0.66	4130	1126	106	124
GT26	100	69	556	287	269	3052	0.14	4100	0.66	3854	1451	102	119
GT27	125	87	701	284	417	3102	0.14	4044	0.66	3256	1763	103	119
GT17	150	94	757	720	38	2999	0.15	3970	0.76	3289	2400	100	116
GT18	200	109	878	283	595	2940	0.14	3994	0.68	n/a	n/a	98	115
GT16	225	94	757	282	475	2973	0.15	4015	0.68	n/a	n/a	99	116
GT19	250	108	870	295	575	3037	0.19	4012	0.72	n/a	n/a	101	117
GT23	260	112	902	317	585	2706	0.19	4003	0.78	n/a	n/a	90	112

Table 5-7 Instrumented Charpy Impact Test Results for the South Texas Unit 1 Surveillance Weld Metal Irradiated to a Fluence of 2.62 x 10^{19} n/cm^2 (E>1.0 MeV)

Sample No.	Test Temp. (°F)	Charpy Energy E_D (ft-lb)	Normalized Energies (ft-lb/in^2) Charpy E_D/A	Normalized Energies (ft-lb/in^2) Max. E_M/A	Normalized Energies (ft-lb/in^2) Prop. E_p/A	Yield Load P_{GY} (lb)	Time to Yield t_{GY} (msec)	Max. Load P_M (lb)	Time to Max. t_M (msec)	Fast Fract. Load P_F (lb)	Arrest Load P_A (lb)	Yield Stress σ_Y (ksi)	Flow Stress (ksi)
GW16	-125	3	24	11	14	1452	0.11	1452	0.11	1452	0	48	48
GW17	-75	29	234	189	45	3714	0.15	4517	0.42	4471	0	124	137
GW25	-75	6	48	11	37	1475	0.11	1475	0.11	1475	0	49	49
GW26	-50	16	129	60	69	3645	0.15	4247	0.20	4244	0	121	131
GW19	-25	28	226	155	71	3277	0.14	4182	0.38	4170	449	109	124
GW28	0	71	572	232	340	3537	0.14	4377	0.52	3827	888	118	132
GW27	0	32	258	154	104	3320	0.14	4173	0.38	4115	860	111	125
GW20	25	45	363	198	165	3228	0.14	4130	0.47	4046	1808	108	123
GW24	50	69	556	223	333	3311	0.14	4261	0.52	3664	1287	110	126
GW22	75	72	580	218	362	3138	0.14	4152	0.52	3674	1662	104	121
GW29	100	71	572	207	365	3052	0.14	4007	0.51	3088	1733	102	118
GW21	150	102	822	289	533	3074	0.14	4037	0.67	n/a	n/a	102	118
GW18	175	102	822	290	532	3102	0.14	4100	0.66	n/a	n/a	103	120
GW23	200	87	701	283	418	2982	0.14	3936	0.68	n/a	n/a	99	115
GW30	200	87	701	278	423	2908	0.14	3944	0.67	n/a	n/a	97	114

Table 5-8 Instrumented Charpy Impact Test Results for the South Texas Unit 1 Heat-Affected-Zone (HAZ) Metal Irradiated to a Fluence of 2.62 x 10^{19} n/cm^2 (E>1.0 MeV)

Sample No.	Test Temp. (°F)	Charpy Energy E_D (ft-lb)	Normalized Energies (ft-lb/in^2)			Yield Load P_{GY} (lb)	Time to Yield t_{GY} (msec)	Max. Load P_M (lb)	Time to Max. t_M (msec)	Fast Fract. Load P_F (lb)	Arrest Load P_A (lb)	Yield Stress σ_Y (ksi)	Flow Stress (ksi)
			Charpy E_D/A	Max. E_M/A	Prop. E_p/A								
GH22	-150	13	105	65	40	4850	0.17	5194	0.20	5194	0	162	167
GH30	-75	26	209	74	135	4244	0.17	4816	0.23	4634	0	141	151
GH28	-50	45	363	283	79	4093	0.17	4878	0.57	4829	0	136	149
GH18	-25	84	677	334	343	3912	0.15	4689	0.66	3873	748	130	143
GH20	-25	46	371	253	118	3822	0.15	4824	0.52	4809	668	127	144
GH16	0	32	258	69	189	3692	0.14	4527	0.21	4461	298	123	137
GH21	10	68	548	261	287	3679	0.15	4706	0.55	4165	824	123	140
GH24	25	105	846	248	598	3629	0.15	4630	0.53	3464	1709	121	137
GH26	25	118	951	336	615	3669	0.15	4662	0.68	3623	772	122	139
GH17	40	82	661	204	457	3503	0.14	4423	0.46	n/a	n/a	117	132
GH23	50	55	443	226	217	3521	0.14	4500	0.49	4241	1237	117	134
GH29	75	105	846	331	515	3679	0.16	4669	0.67	n/a	n/a	123	139
GH27	100	117	943	325	618	3547	0.15	4627	0.67	n/a	n/a	118	136
GH19	125	119	959	370	589	3422	0.15	4508	0.77	n/a	n/a	114	132
GH25	150	114	919	315	603	3305	0.14	4485	0.68	n/a	n/a	110	130

Table 5-9 Effect of Irradiation to 2.62 x 10^{19} n/cm^2 (E>1.0 MeV) on the Capsule U Notch Toughness Properties of the South Texas Unit 1 Reactor Vessel Surveillance Materials

Material	Average 30 (ft-lb)[a] Transition Temperature (°F)			Average 35 mil Lateral[b] Expansion Temperature (°F)			Average 50 ft-lb[a] Transition Temperature (°F)			Average Energy Absorption[a] at Full Shear (ft-lb)		
	Unirradiated	Irradiated	ΔT	Unirradiated	Irradiated	ΔT	Unirradiated	Irradiated	ΔT	Unirradiated	Irradiated	ΔE
Intermediate Shell Plate R1606-2 (Long.)	-52.32	-12.17	40.15	-22.91	26.04	48.96	-20.43	21.34	41.78	138	131	-7
Intermediate Shell Plate R1606-2 (Trans.)	-6.06	17.78	23.84	19.61	59.77	40.16	26.85	56.11	29.26	113	106	-7
Weld Metal (Heat # V89476)	-56.03	-29.41	26.61	-26.56	14.61	41.17	-16.82	15.64	32.47	86	95	+9
HAZ Metal	-134.16	-75.34	58.82	-58.73	-8.84	49.89	-86.18	-35.75	50.42	105	114	+9

a. "Average" is defined as the value read from the curve fit through the data points of the Charpy tests (see Figures 5-1, 5-4, 5-7 and 5-10).

b. "Average" is defined as the value read from the curve fit through the data points of the Charpy tests (see Figures 5-2, 5-5, 5-8 and 5-11).

Table 5-10 Comparison of the South Texas Unit 1 Surveillance Material 30 ft-lb Transition Temperature Shifts and Upper Shelf Energy Decreases with Regulatory Guide 1.99, Revision 2, Predictions

Material	Capsule	Fluence[d] (x 10^{19} n/cm², E > 1.0 MeV)	30 ft-lb Transition Temperature Shift		Upper Shelf Energy Decrease	
			Predicted (°F) [a]	Measured (°F) [b]	Predicted (%) [a]	Measured (%)[c]
Intermediate Shell	U	0.258	16.43	18.09	14	8
Plate R1606-2	Y	1.29	27.85	43.98	20	0.7
(Longitudinal)	V	2.62	32.71	40.15	24	5
Intermediate Shell	U	0.258	16.43	23.44	14	8
Plate R1606-2	Y	1.29	27.85	11.94	20	2
(Transverse)	V	2.62	32.71	23.84	24	6
Surveillance	U	0.258	14.73	33.58	14	0
Program	Y	1.29	24.95	37.89	20	0
Weld Metal	V	2.62	29.31	26.61	24	0
Heat Affected Zone	U	0.258	---	0.00[e]	---	0
Material	Y	1.29	---	19.20	---	0
	V	2.62	---	58.82	---	0

Notes:

a) Based on Regulatory Guide 1.99, Revision 2, methodology using the mean weight percent values of copper and nickel of the surveillance material.

b) Calculated using measured Charpy data plotted using CVGRAPH, Version 4.1 (See Appendix C)

c) Values are based on the definition of upper shelf energy given in ASTM E185-82.

d) The fluence values presented here are the calculated values, not the best estimate values.

e) Due to the scatter in the capsule V HAZ Charpy test results, a true Hyperbolic Tangent Curve fit resulted in ΔT_{30} values of −15.89°F, when compared to unirradiated Charpy test data. Physically this should not happen. Hence, based on engineering judgement a value of 0°F will be used in RT_{NDT} calculations.

Table 5-11 Tensile Properties of the South Texas Unit 1 Capsule V Reactor Vessel Surveillance Materials Irradiated to 2.62 x 10^{19} n/cm^2 (E > 1.0 MeV)

Material	Sample Number	Test Temp. (°F)	0.2% Yield Strength (ksi)	Ultimate Strength (ksi)	Fracture Load (kip)	Fracture Stress (ksi)	Fracture Strength (ksi)	Uniform Elongation (%)	Total Elongation (%)	Reduction in Area (%)
Inter. Shell Plate R1606-2 (Long.)	GL-4	75	70.3	88.5	2.68	175.1	54.6	12.0	27.9	69
	GL-5	300	62.6	81.3	2.25	144.5	45.8	12.0	24.4	68
	GL-6	550	60.1	84.2	2.84	173.7	57.9	11.5	23.6	67
Inter. Shell Plate R1606-2 (Trans.)	GT-4	75	67.8	86.2	2.93	170.7	59.8	11.5	27.6	65
	GT-6	300	64.7	81.6	2.57	116.7	52.3	11.0	23.0	65
	GT-5	550	62.3	85.5	3.00	159.8	61.1	11.8	22.5	62
Weld Metal	GW-6	75	74.4	89.8	2.81	178.2	57.2	12.0	26.6	68
	GW-5	300	68.2	81.5	2.66	181.2	54.2	10.2	22.0	70
	GW-4	550	62.1	83.6	2.79	164.6	56.8	10.9	21.9	65

PLATE R1606-2 (LONGITUDINAL)

CVGRAPH 4.1 Hyperbolic Tangent Curve Printed at 123421 on 08-15-2003

Results

Curve	Fluence	LSE	d-LSE	USE	d-USE	T @ 30	d-T @ 30	T @ 50	d-T @ 50
1	0	2.19	0	138	0	-52.32	0	-20.43	0
2	0	2.19	0	127	-11	-34.22	18.09	-1.17	19.26
3	0	2.19	0	137	-1	-8.34	43.98	23.9	44.33
4	0	2.19	0	131	-7	-12.17	40.15	21.34	41.78

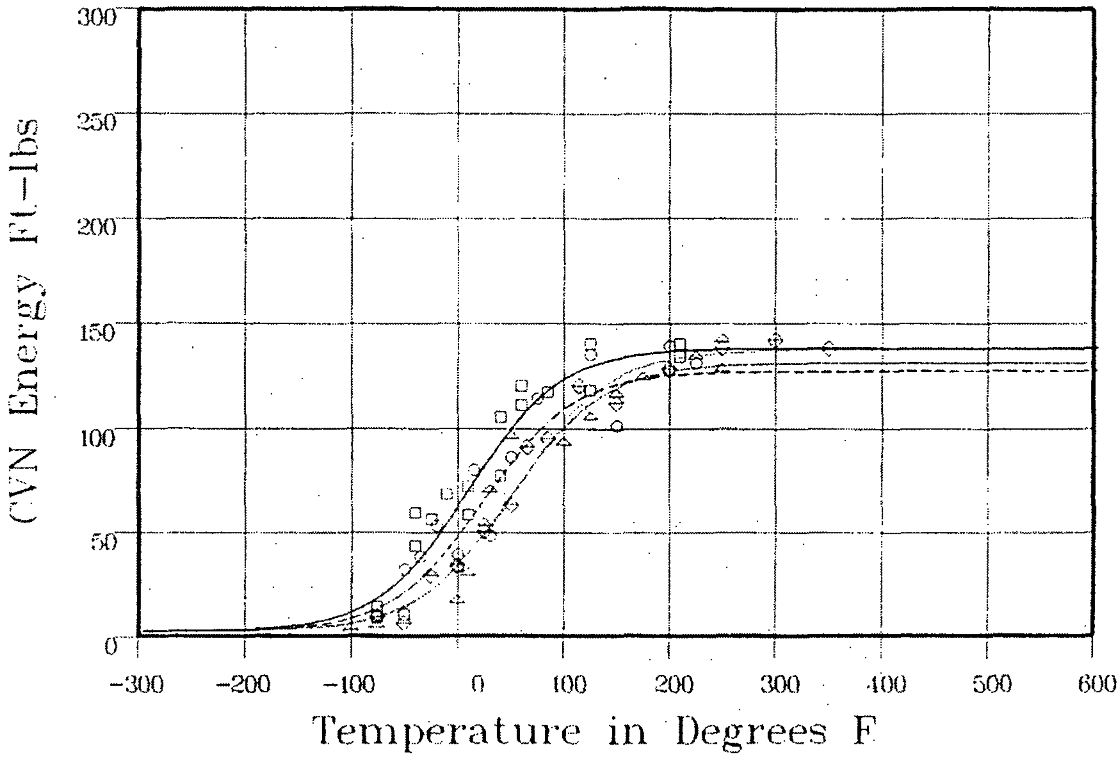

Curve Legend

1 □——— 2 ○--------- 3 ⊖ -·-·-· 4 △———

Data Set(s) Plotted

Curve	Plant	Capsule	Material	Ori.	Heat#
1	STI	UNIRR	PLATE SA533B1	LT	B8120-1
2	STI	U	PLATE SA533B1	LT	B8120-1
3	STI	Y	PLATE SA533B1	LT	B8120-1
4	STI	V	PLATE SA533B1	LT	B8120-1

Figure 5-1 Charpy V-Notch Impact Energy vs. Temperature for South Texas Unit 1 Reactor Vessel Intermediate Shell Plate R1606-2 (Longitudinal Orientation)

PLATE 1606-2 (LONGITUDINAL)

CVGRAPH 4.1 Hyperbolic Tangent Curve Printed at 12:40:57 on 08-15-2003

Results

Curve	Fluence	USE	d-USE	T @ LE35	d-T @ LE35
1	0	88.12	0	-22.91	0
2	0	82.8	-5.31	-6.4	16.5
3	0	75.63	-12.49	21.04	43.95
4	0	71.84	-16.28	26.04	48.96

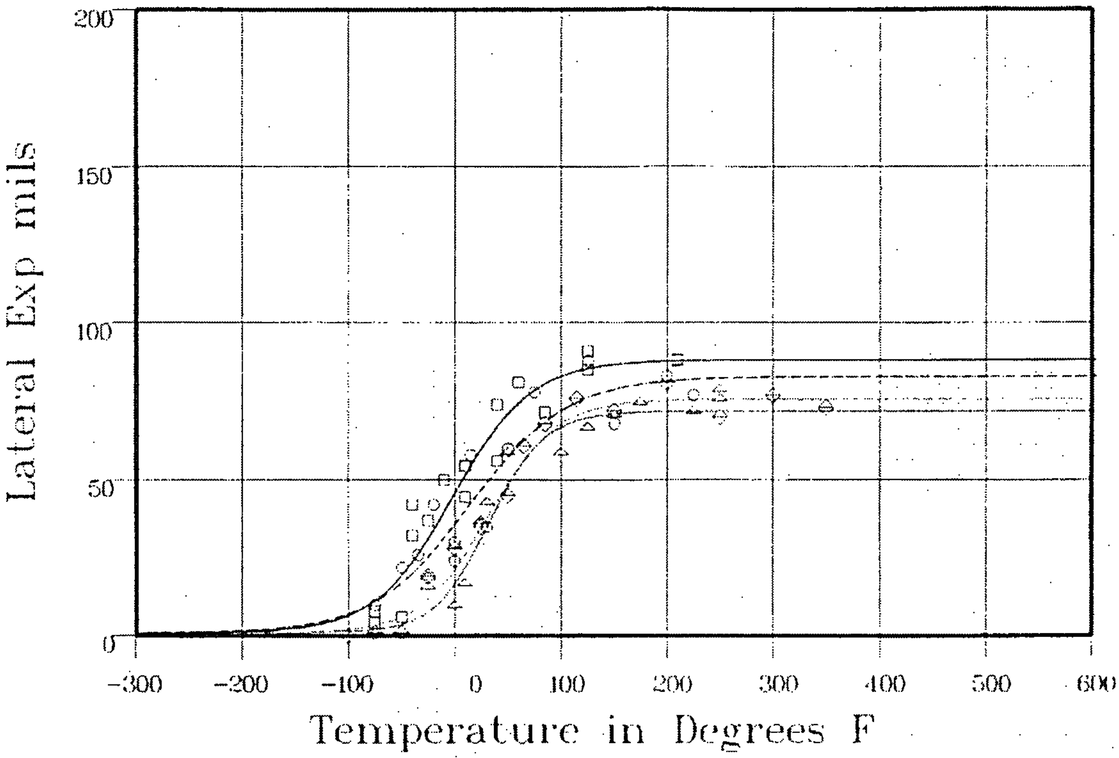

Curve Legend

1 □———— 2 ○- - - - - 3 ◇ - · - · - 4 △————

Data Set(s) Plotted

Curve	Plant	Capsule	Material	Ori.	Heat#
1	ST1	UNIRR	PLATE SA533B1	LT	B9120-1
2	ST1	U	PLATE SA533B1	LT	B9120-1
3	ST1	Y	PLATE SA533B1	LT	B9120-1
4	ST1	V	PLATE SA533B1	LT	B9120-1

Figure 5-2 Charpy V-Notch Lateral Expansion vs. Temperature for South Texas Unit 1 Reactor Vessel Intermediate Shell Plate R1606-2 (Longitudinal Orientation)

PLATE 1606-2 (LONGITUDINAL)

CVGRAPH 4.1 Hyperbolic Tangent Curve Printed at 22:14:38 on 08-15-2005

Results

Curve	Fluence	T @ 50% Shear	d-T @ 50% Shear
1	0	31.4	0
2	0	29.06	-2.34
3	0	72.65	41.25
4	0	58.59	27.18

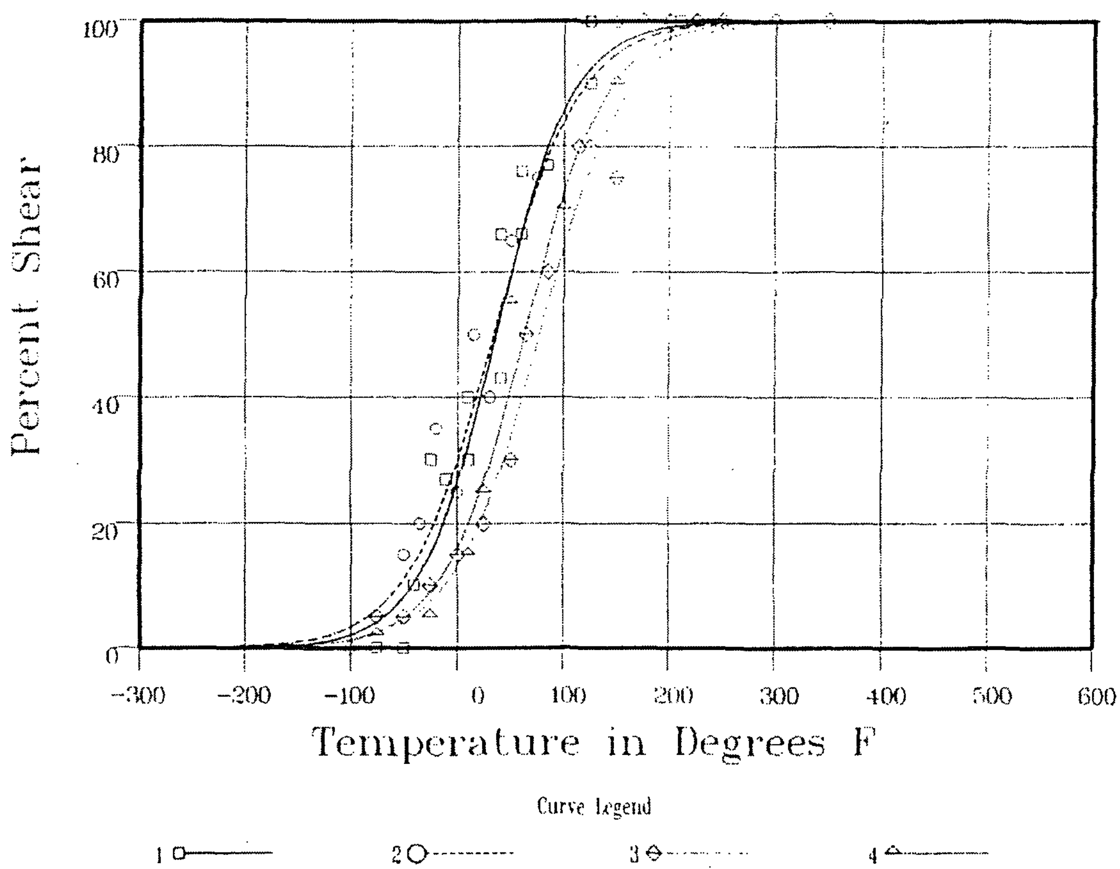

Data Set(s) Plotted

Curve	Plant	Capsule	Material	Ori.	Heat #
1	STI	UNIRR	PLATE SA533B1	LT	B8120-1
2	STI	U	PLATE SA533B1	LT	B8120-1
3	STI	Y	PLATE SA533B1	LT	B8120-1
4	STI	V	PLATE SA533B1	LT	B8120-1

Figure 5-3 Charpy V-Notch Percent Shear vs. Temperature for South Texas Unit 1 Reactor Vessel Intermediate Shell Plate R1606-2 (Longitudinal Orientation)

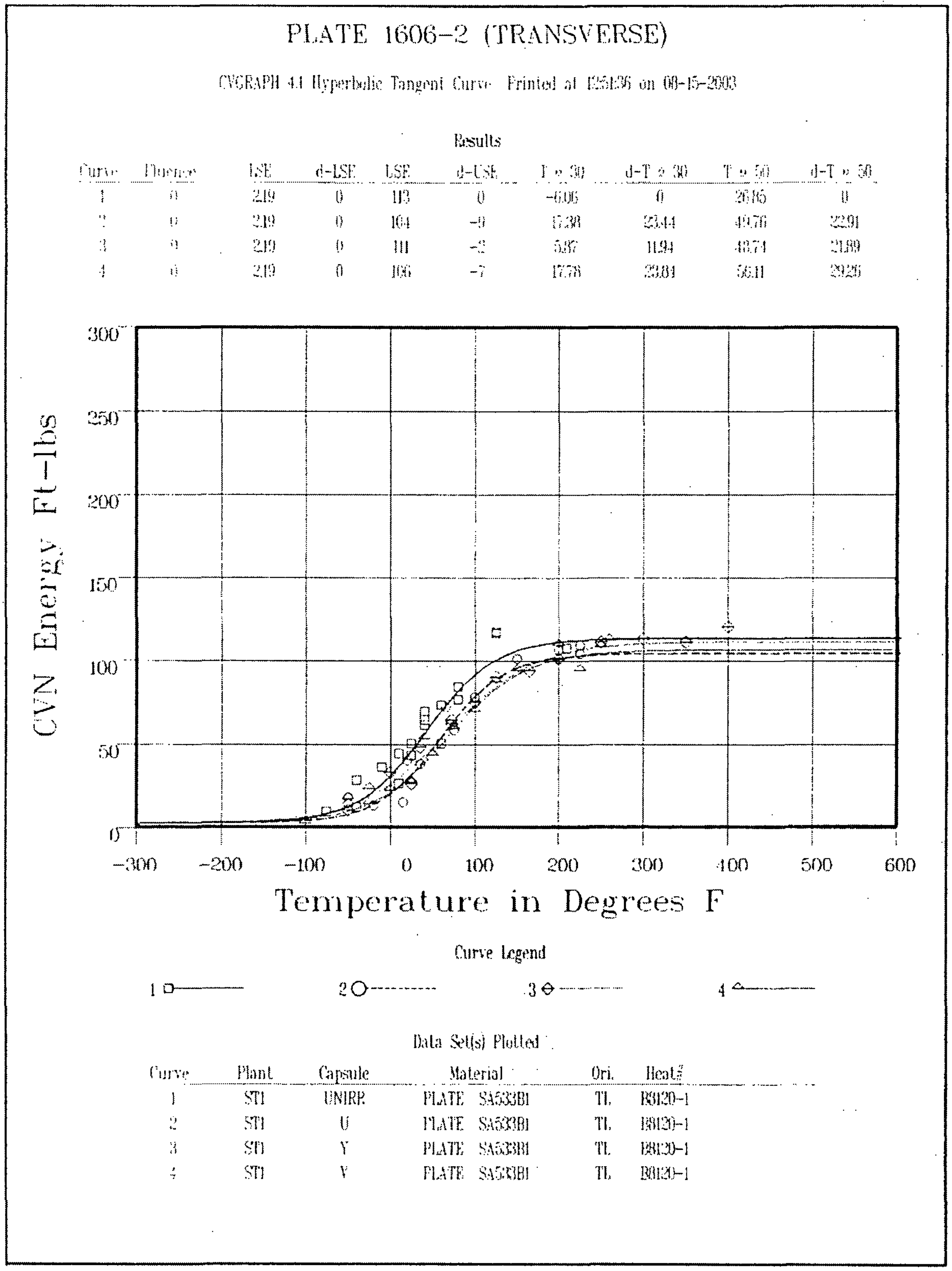

Figure 5-4 Charpy V-Notch Impact Energy vs. Temperature for South Texas Unit 1 Reactor Vessel Intermediate Shell Plate R1606-2 (Transverse Orientation)

PLATE R1606-2 (TRANSVERSE)

CVGRAPH 4.1 Hyperbolic Tangent Curve Printed at 13:28:48 on 08-15-2003

Results

Curve	Fluence	USE	d-USE	T @ LE35	d-T @ LE35
1	0	86.08	0	19.61	0
2	0	73.91	-12.16	30.61	10.99
3	0	72.3	-13.77	44.53	21.92
4	0	69.18	-16.89	59.77	40.16

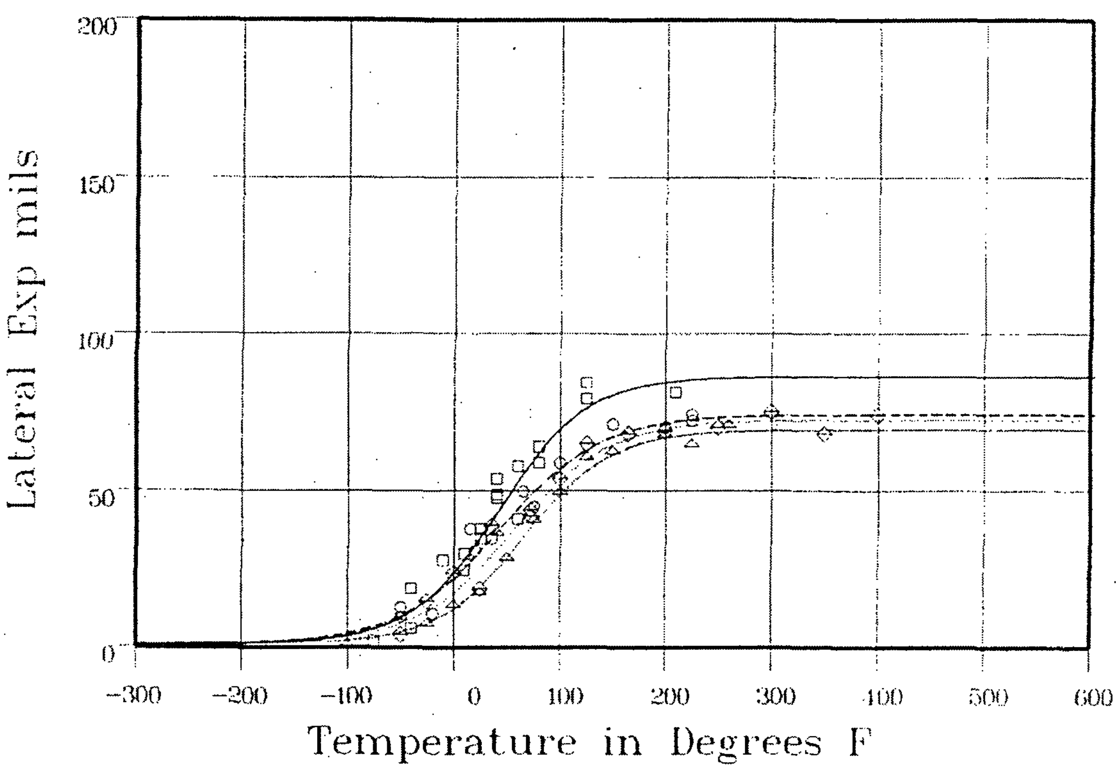

Curve Legend

1 □——— 2 ○- - - - 3 ◇······ 4 △······

Data Set(s) Plotted

Curve	Plant	Capsule	Material	Ori.	Heat#
1	ST1	UNIRR	PLATE SA533B1	TL	B8120-1
2	ST1	U	PLATE SA533B1	TL	B8120-1
3	ST1	Y	PLATE SA533B1	TL	B8120-1
4	ST1	V	PLATE SA533B1	TL	B8120-1

Figure 5-5 Charpy V-Notch Lateral Expansion vs. Temperature for South Texas Unit 1 Reactor Vessel Intermediate Shell Plate R1606-2 (Transverse Orientation)

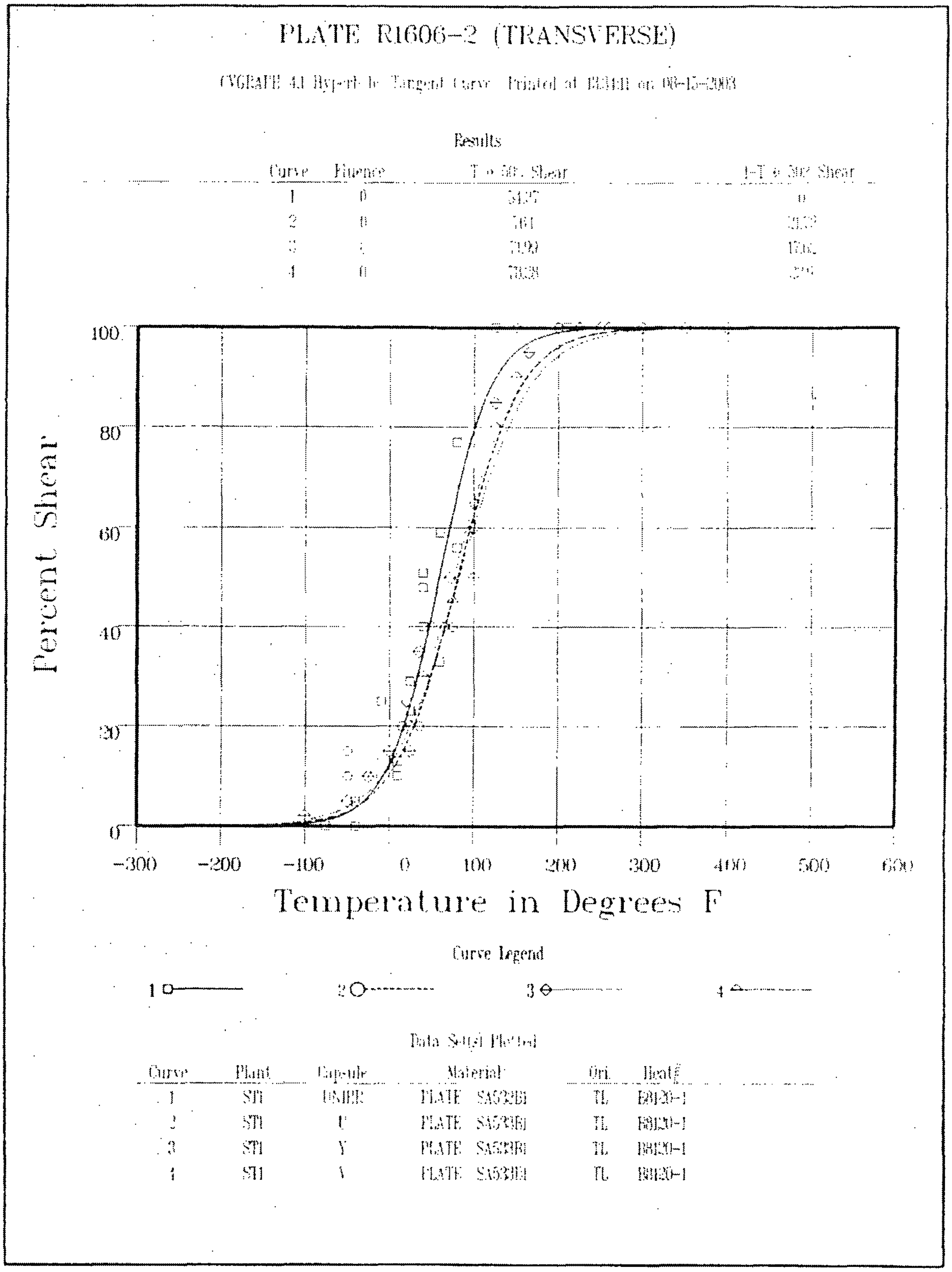

Figure 5-6 Charpy V-Notch Percent Shear vs. Temperature for South Texas Unit 1 Reactor Vessel Intermediate Shell Plate R1606-2 (Transverse Orientation)

WELD METAL

CVGRAPH 4.1 Hyperbolic Tangent Curve Printed at 13:14:31 on 08-15-2003

Results

Curve	Fluence	LSE	d-LSE	USE	d-USE	T @ 30	d-T @ 30	T @ 50	d-T @ 50
1	0	2.19	0	86	0	-56.03	0	-16.82	0
2	0	2.19	0	87	1	-22.45	33.58	2.92	19.74
3	0	2.19	0	96	10	-18.14	37.89	13.04	29.86
4	0	2.19	0	95	9	-29.41	26.61	15.65	32.47

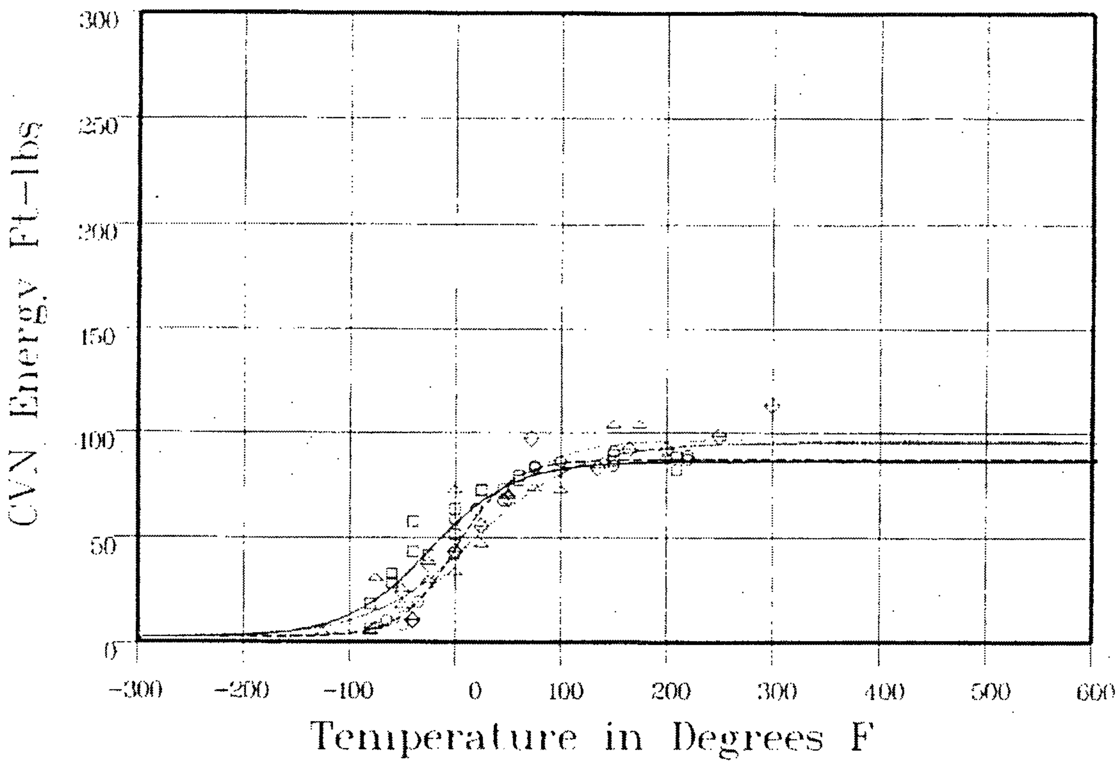

Curve Legend

1 □———— 2 ○-------- 3 ⊖ ······ 4 △—·—·—

Data Set(s) Plotted

Curve	Plant	Capsule	Material	Ori.	Heat #
1	STI	UNIRR	WELD		V89476
2	STI	U	WELD		V89476
3	STI	Y	WELD		V89476
4	STI	V	WELD		V89476

Figure 5-7 Charpy V-Notch Impact Energy vs. Temperature for South Texas Unit 1 Reactor Vessel Weld Metal

WELD METAL

CVGRAPH 4.1 Hyperbolic Tangent Curve Printed at 13:47:33 on 08-15-2003

Results

Curve	Fluence	USE	d-USE	T @ LE35	d-T @ LE35
1	0	77.31	0	-26.56	0
2	0	69.1	-8.21	-7.58	18.97
3	0	71.27	-6.04	3.23	29.79
4	0	66.98	-10.33	14.61	41.17

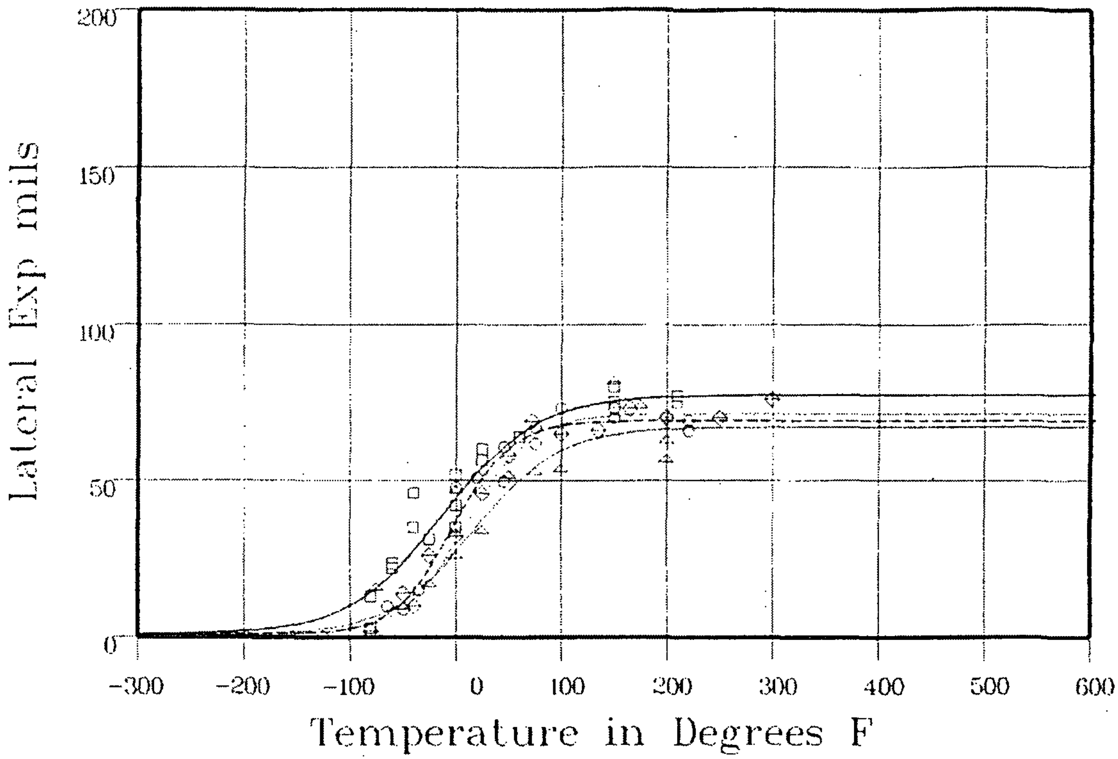

Curve Legend

1 □ ——— 2 ○ - - - - 3 ◇ · · · · 4 △ ———

Data Set(s) Plotted

Curve	Plant	Capsule	Material	Ori.	Heat#
1	ST1	UNIRR	WELD		V89476
2	ST1	U	WELD		V89476
3	ST1	Y	WELD		V89476
4	ST1	V	WELD		V89476

Figure 5-8 Charpy V-Notch Lateral Expansion vs. Temperature for South Texas Unit 1 Reactor Vessel Weld Metal

WELD METAL

CVGRAPH 4.1 Hyperbolic Tangent Curve Printed at 13:51:02 on 08-15-2003

Results

Curve	Fluence	T @ 50% Shear	d-T @ 50% Shear
1	0	-17.07	0
2	0	1.87	18.94
3	0	-.93	16.13
4	0	4.21	21.29

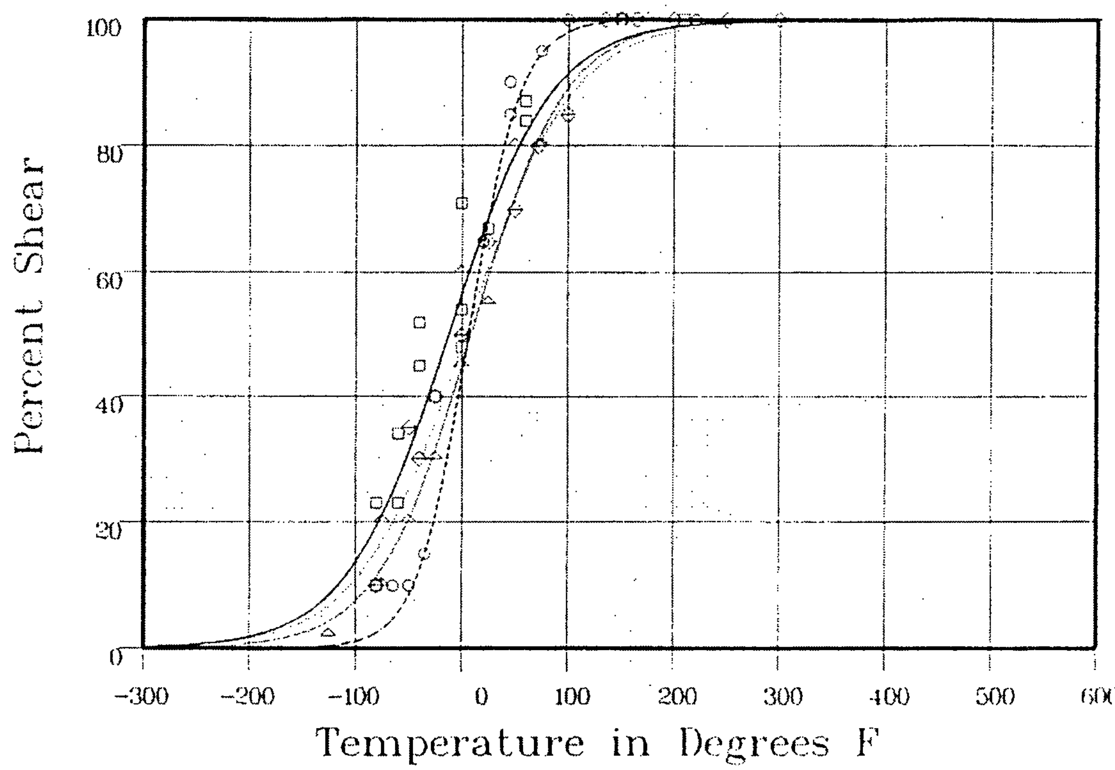

Curve Legend

1 □——— 2 ○--------- 3 ◇ ········· 4 △———

Data Set(s) Plotted

Curve	Plant	Capsule	Material	Ori.	Heat #
1	ST1	UNIRR	WELD		V89476
2	ST1	U	WELD		V89476
3	ST1	Y	WELD		V89476
4	ST1	V	WELD		V89476

Figure 5-9 Charpy V-Notch Percent Shear vs. Temperature for South Texas Unit 1 Reactor Vessel Weld Metal

HEAT AFFECTED ZONE

CVGRAPH 4.1 Hyperbolic Tangent Curve Printed at 12:21:19 on 08-18-2003

Results

Curve	Fluence	LSE	d-LSE	USE	d-USE	T @ 30	d-T @ 30	T @ 50	d-T @ 50
1	0	2.19	0	105	0	-134.16	0	-86.18	0
2	0	2.19	0	129	24	-150.05	-15.89	-87.4	-1.22
3	0	2.19	0	130	25	-114.96	19.2	-69.32	16.85
4	0	2.19	0	114	9	-75.34	58.82	-35.75	50.42

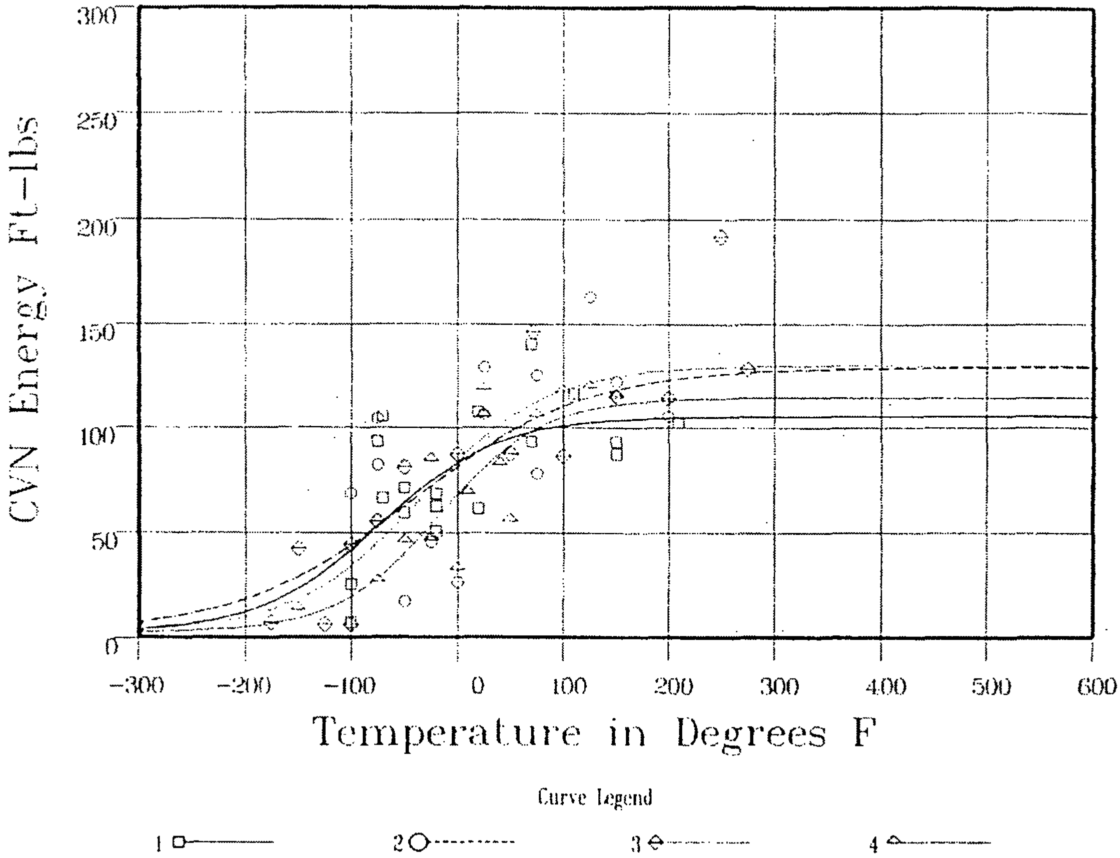

Data Set(s) Plotted

Curve	Plant	Capsule	Material	Ori.	Heat#
1	ST1	UNIRR	HEAT AFF'D ZONE		
2	ST1	U	HEAT AFF'D ZONE		
3	ST1	Y	HEAT AFF'D ZONE		
4	ST1	V	HEAT AFF'D ZONE		

Figure 5-10 Charpy V-Notch Impact Energy vs. Temperature for South Texas Unit 1 Reactor Vessel Heat-Affected-Zone Material

HEAT AFFECTED ZONE

CVGRAPH 4.1 Hyperbolic Tangent Curve Printed at 14:11:50 on 08-15-2003

Results

Curve	Fluence	USE	d-USE	T @ LE35	d-T @ LE35
1	0	74.02	0	-58.73	0
2	0	107.02	33	-75.26	-16.52
3	0	69.29	-4.73	-46.56	12.17
4	0	76.46	2.43	-8.84	49.89

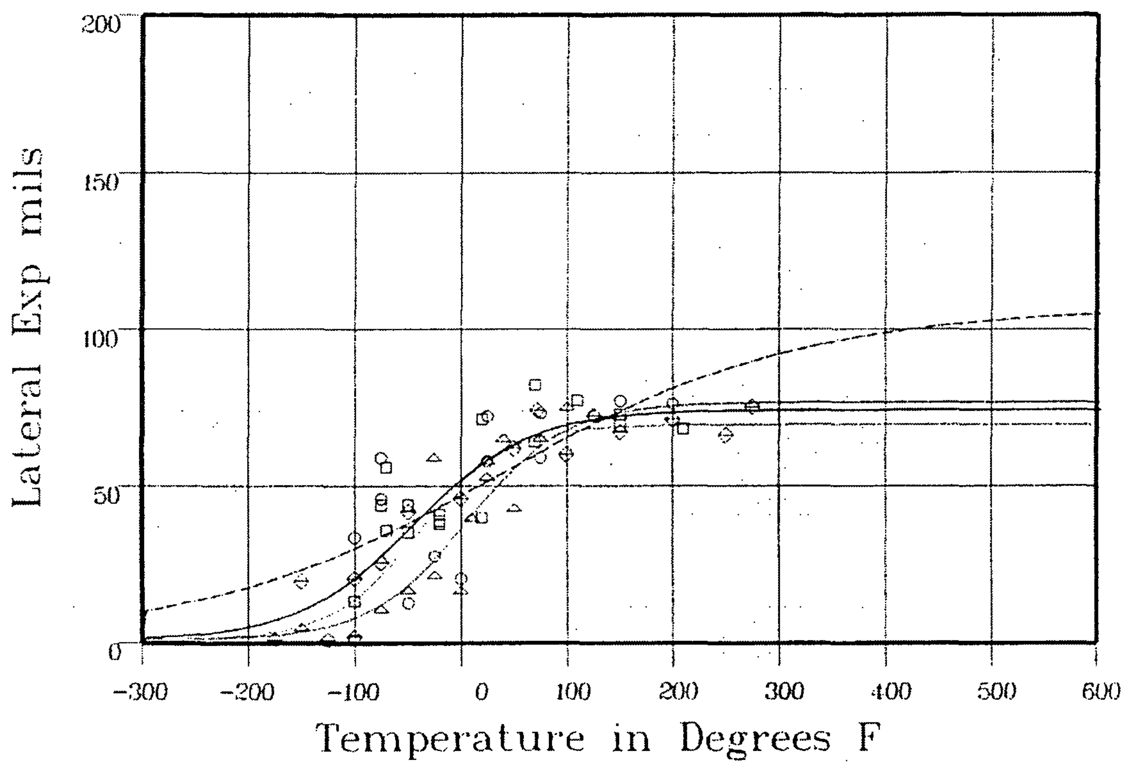

Curve Legend

1 □——— 2 ○--------- 3 ◇——— 4 △———

Data Set(s) Plotted

Curve	Plant	Capsule	Material	Ori.	Heat#
1	ST1	UNIRR	HEAT AFFD ZONE		
2	ST1	U	HEAT AFFD ZONE		
3	ST1	Y	HEAT AFFD ZONE		
4	ST1	V	HEAT AFFD ZONE		

Figure 5-11 Charpy V-Notch Lateral Expansion vs. Temperature for South Texas Unit 1 Reactor Vessel Heat-Affected-Zone Material

HEAT AFFECTED ZONE

CVGRAPH 4.1 Hyperbolic Tangent Curve Printed at 14:34:08 on 08-15-2003

Results

Curve	Fluence	T @ 50% Shear	d-T @ 50% Shear
1	0	-31.4	0
2	0	-2.76	28.63
3	0	-33.95	-2.54
4	0	-14.53	16.87

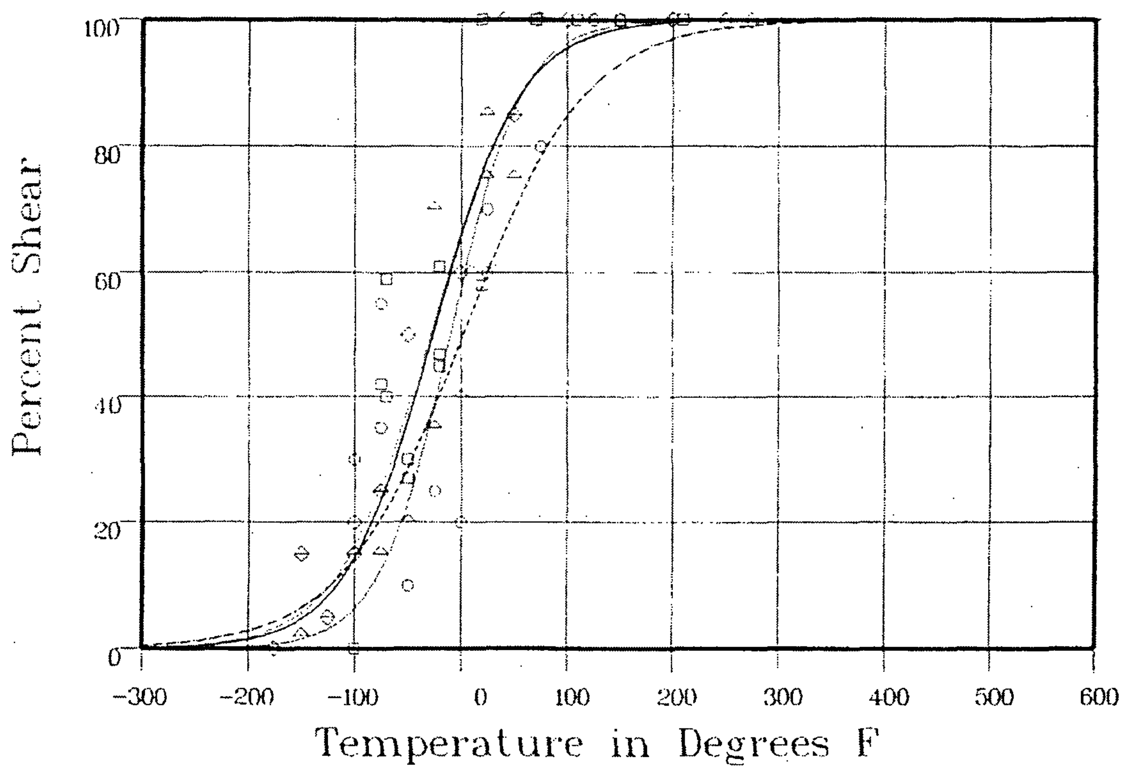

Curve Legend

1 □——— 2 ○--------- 3 ◇--------- 4 △———

Data Set(s) Plotted

Curve	Plant	Capsule	Material	Ori.	Heat#
1	ST1	UNIRR	HEAT AFFD ZONE		
2	ST1	U	HEAT AFFD ZONE		
3	ST1	Y	HEAT AFFD ZONE		
4	ST1	V	HEAT AFFD ZONE		

Figure 5-12 Charpy V-Notch Percent Shear vs. Temperature for South Texas Unit 1 Reactor Vessel Heat-Affected-Zone Material

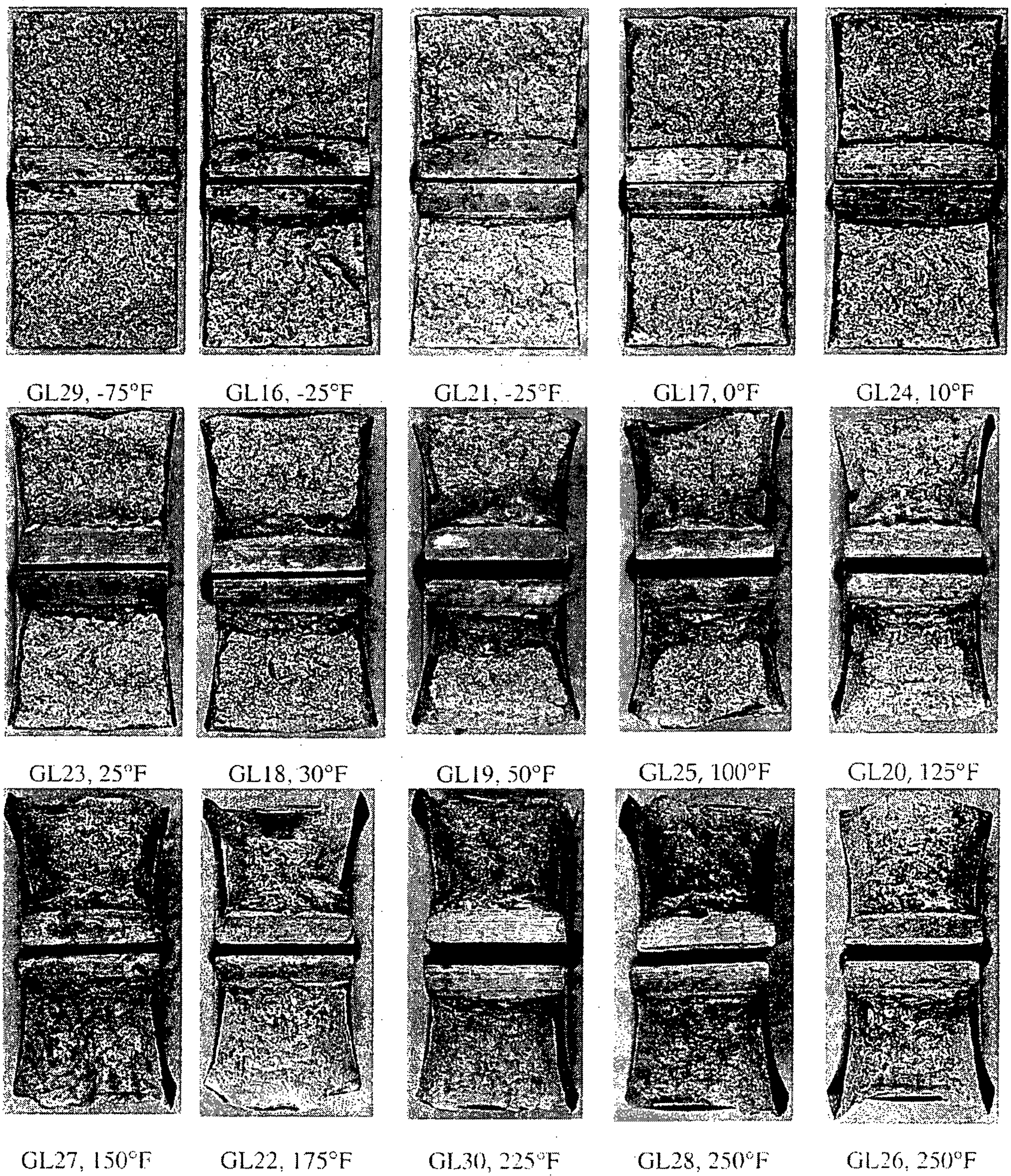

Figure 5-13 Charpy Impact Specimen Fracture Surfaces for South Texas Unit 1 Reactor Vessel Intermediate Shell Plate R1606-2 (Longitudinal Orientation)

Figure 5-14 Charpy Impact Specimen Fracture Surfaces for South Texas Unit 1 Reactor Vessel Intermediate Shell Plate R1606-2 (Transverse Orientation)

Figure 5-15 Charpy Impact Specimen Fracture Surfaces for South Texas Unit 1 Reactor Vessel Weld Metal

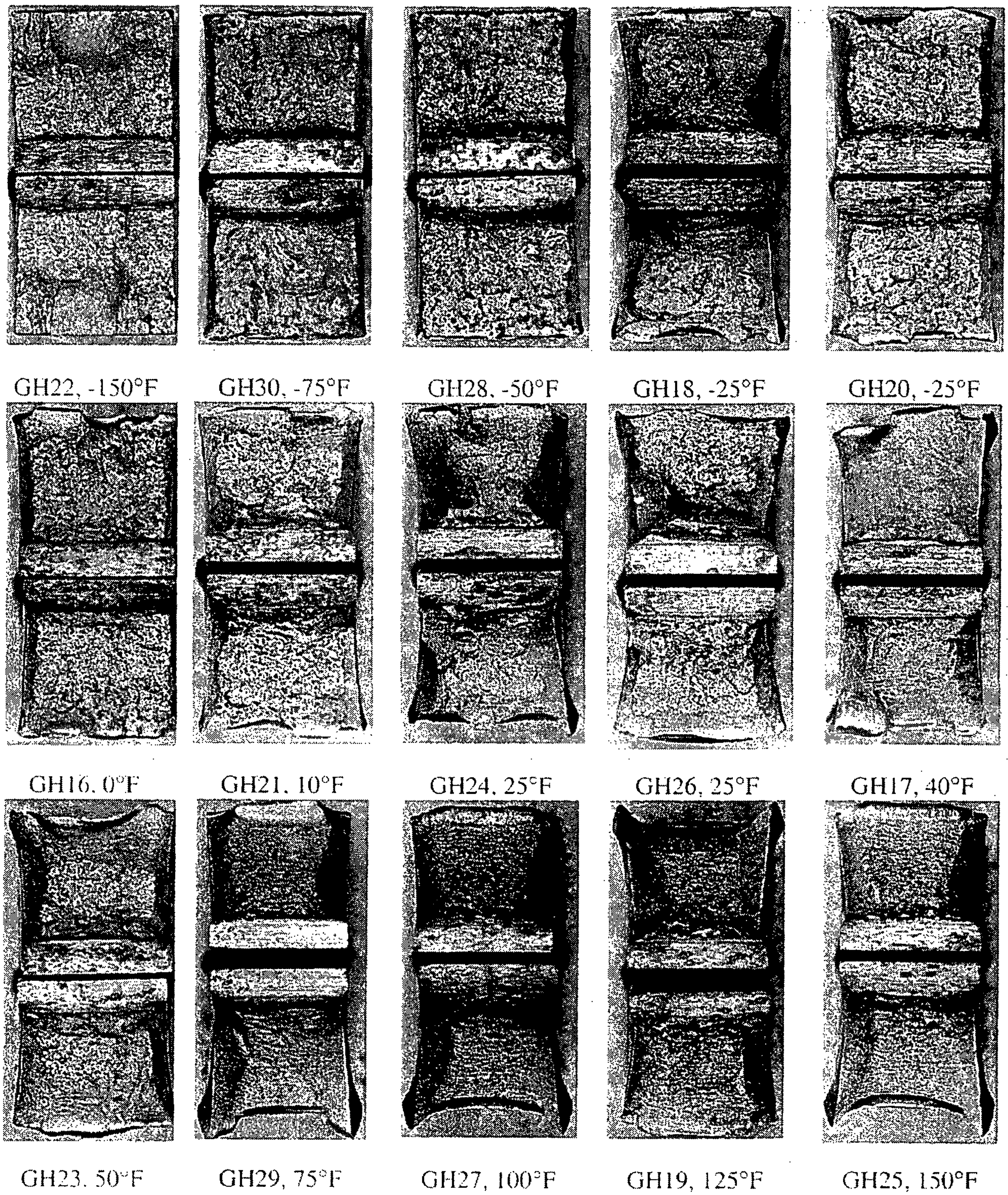

Figure 5-16 Charpy Impact Specimen Fracture Surfaces for South Texas Unit 1 Reactor Vessel Heat-Affected-Zone Metal

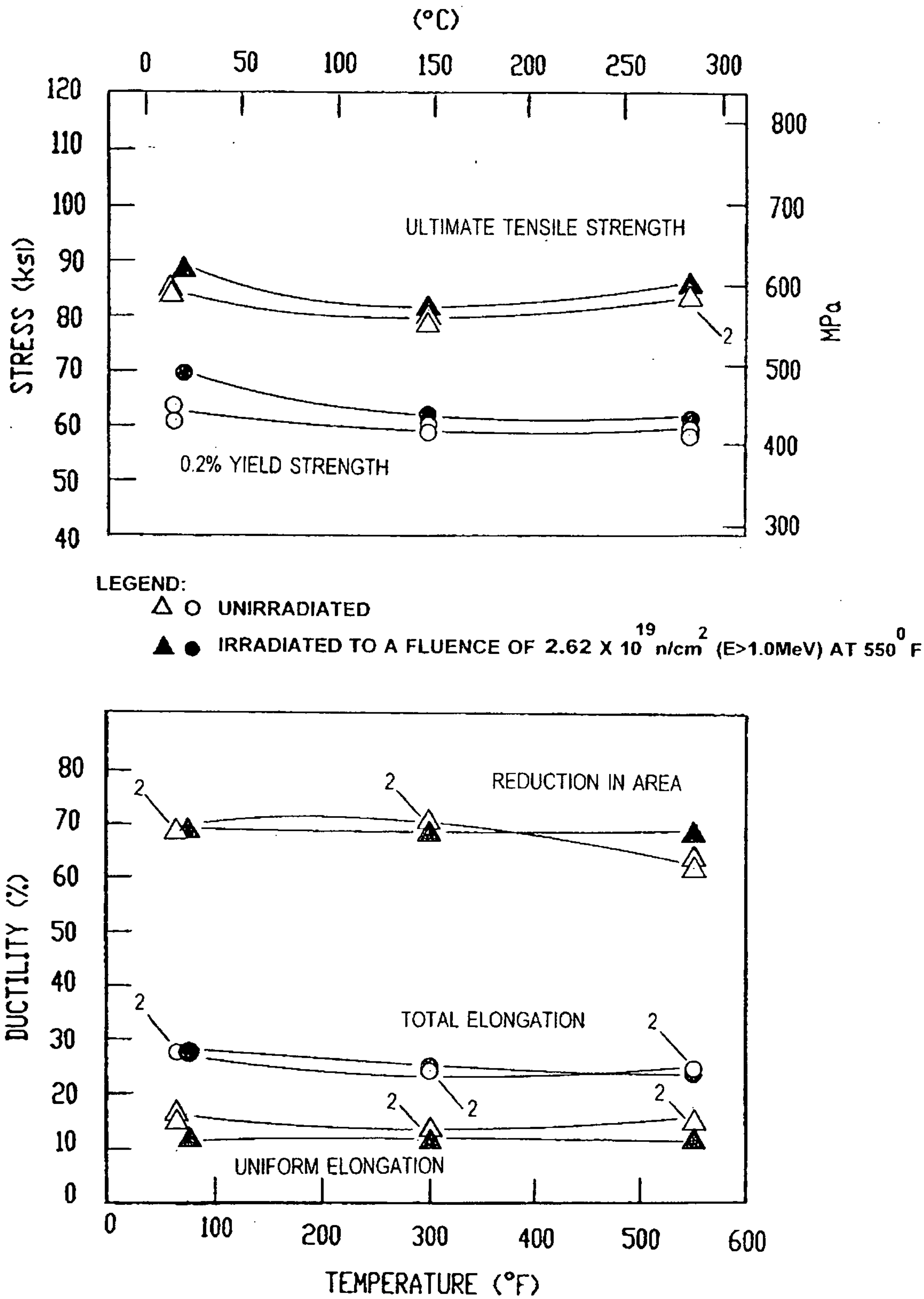

Figure 5-17 Tensile Properties for South Texas Unit 1 Reactor Vessel Intermediate Shell Plate R1606-2 (Longitudinal Orientation)

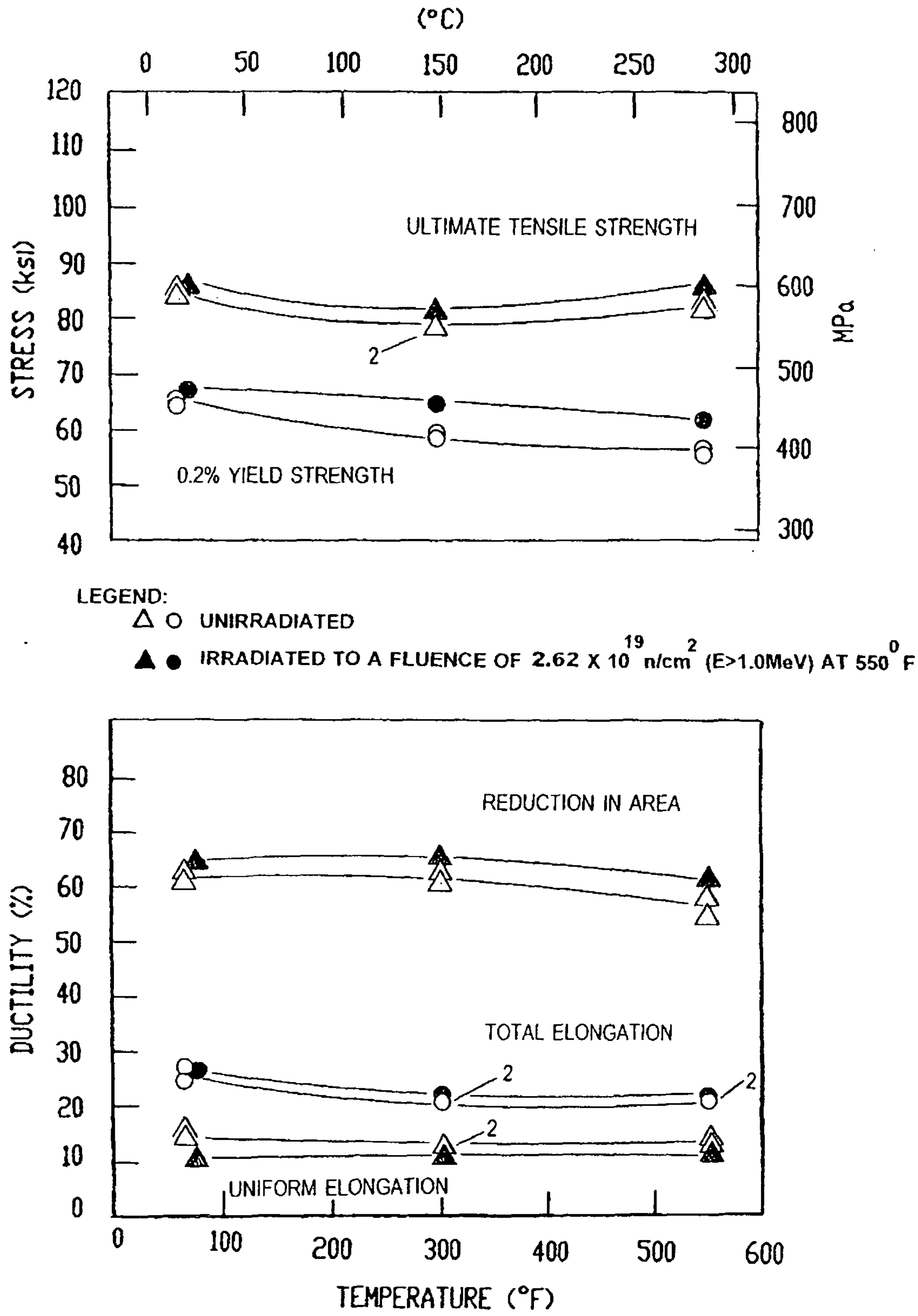

Figure 5-18 Tensile Properties for South Texas Unit 1 Reactor Vessel Intermediate Shell Plate R1606-2 (Transverse Orientation)

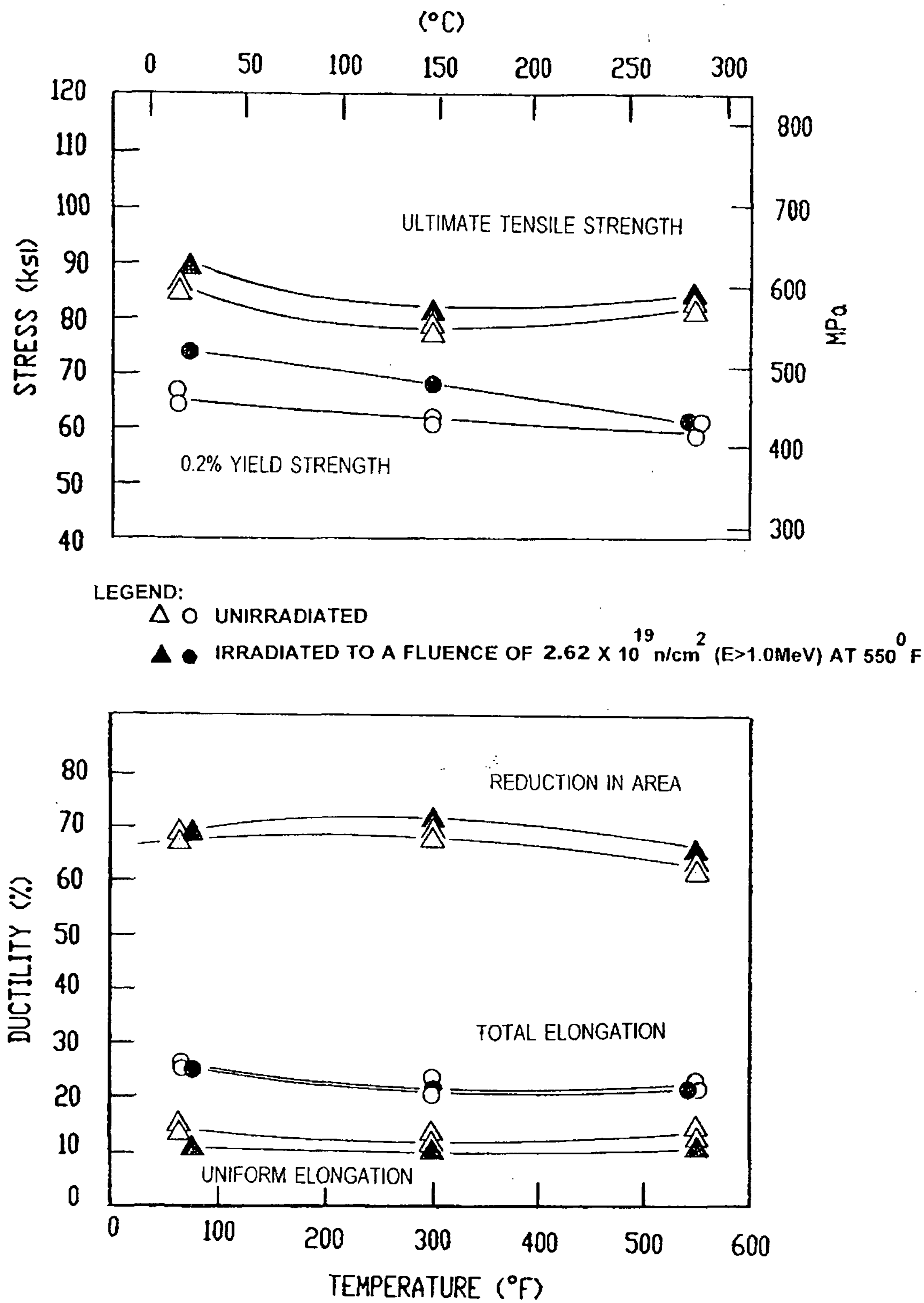

Figure 5-19 Tensile Properties for South Texas Unit 1 Reactor Vessel Weld Metal

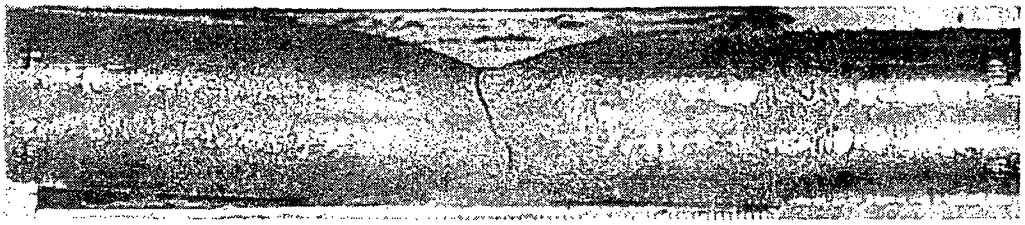

Specimen GL-4 Tested at 75°F

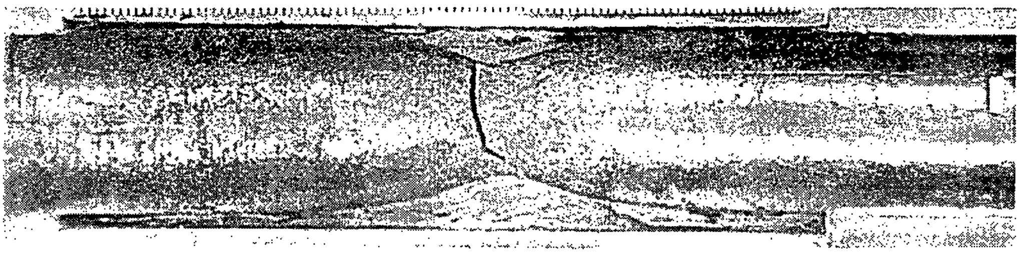

Specimen GL-5 Tested at 300°F

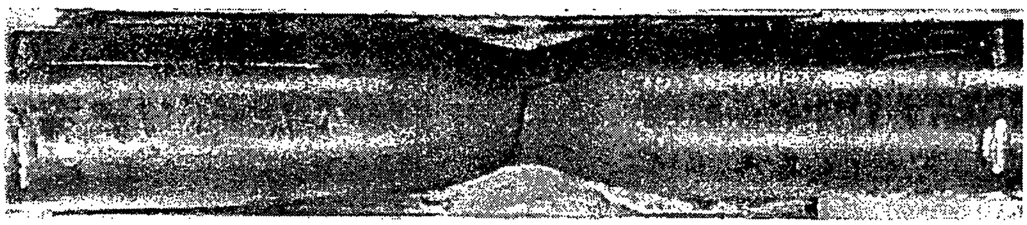

Specimen GL-6 Tested at 550°F

Figure 5-20 Fractured Tensile Specimens from South Texas Unit 1 Reactor Vessel Lower Shell Plate R1606-2 (Longitudinal Orientation)

Specimen GT-4 Tested at 75°F

Specimen GT-6 Tested at 300°F

Specimen GT-5 Tested at 550°F

Figure 5-21 Fractured Tensile Specimens from South Texas Unit 1 Reactor Vessel Lower Shell Plate R1606-2 (Transverse Orientation)

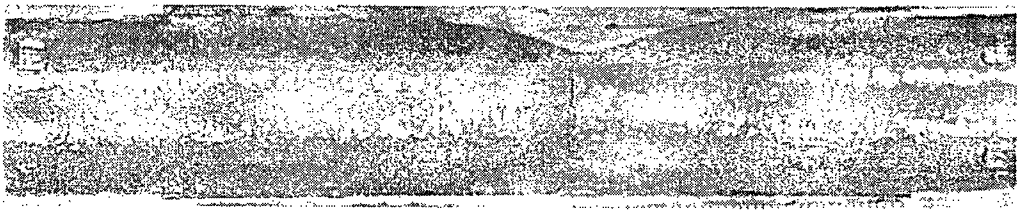

Specimen GW-6 Tested at 75°F

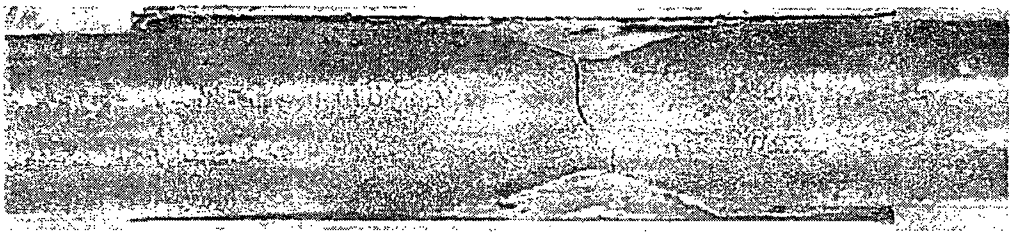

Specimen GW-5 Tested at 300°F

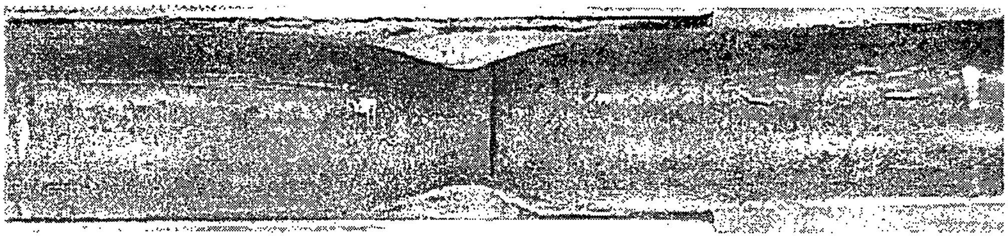

Specimen GW-4 Tested at 550°F

Figure 5-22 Fractured Tensile Specimens from South Texas Unit 1 Reactor Vessel Weld Metal

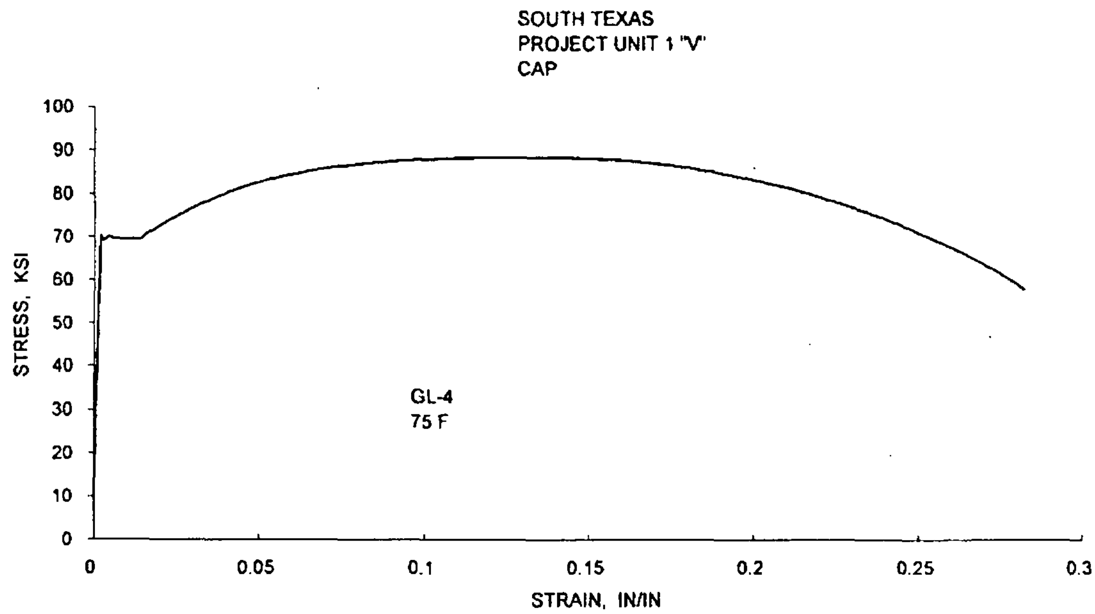

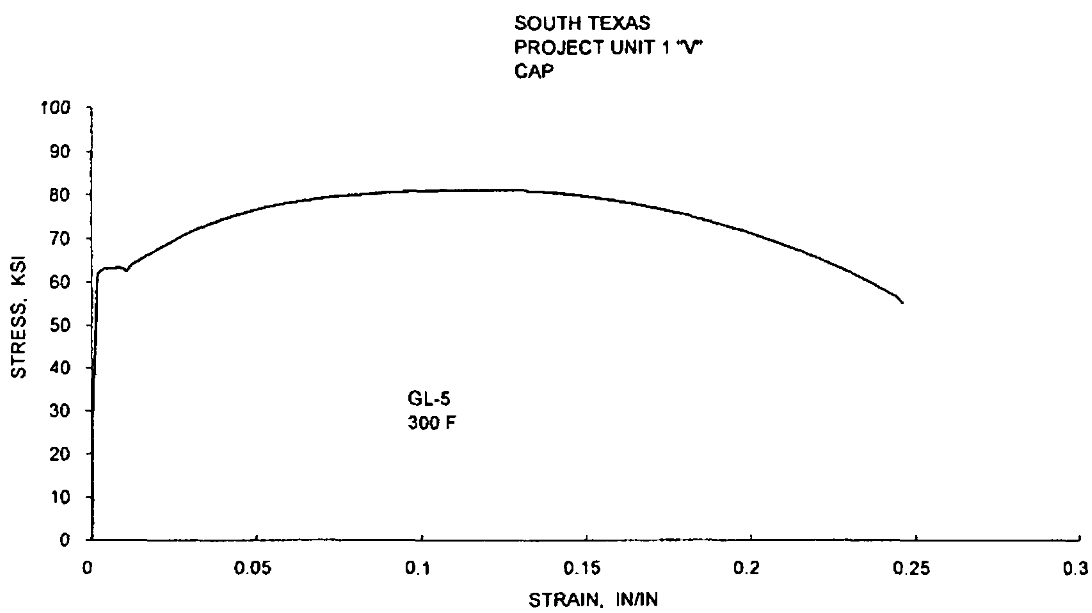

Figure 5-23 Engineering Stress-Strain Curves for South Texas Unit 1 Intermediate Shell Plate R1606-2 Tensile Specimens GL-4, GL-5 and GL-6 (Longitudinal Orientation)

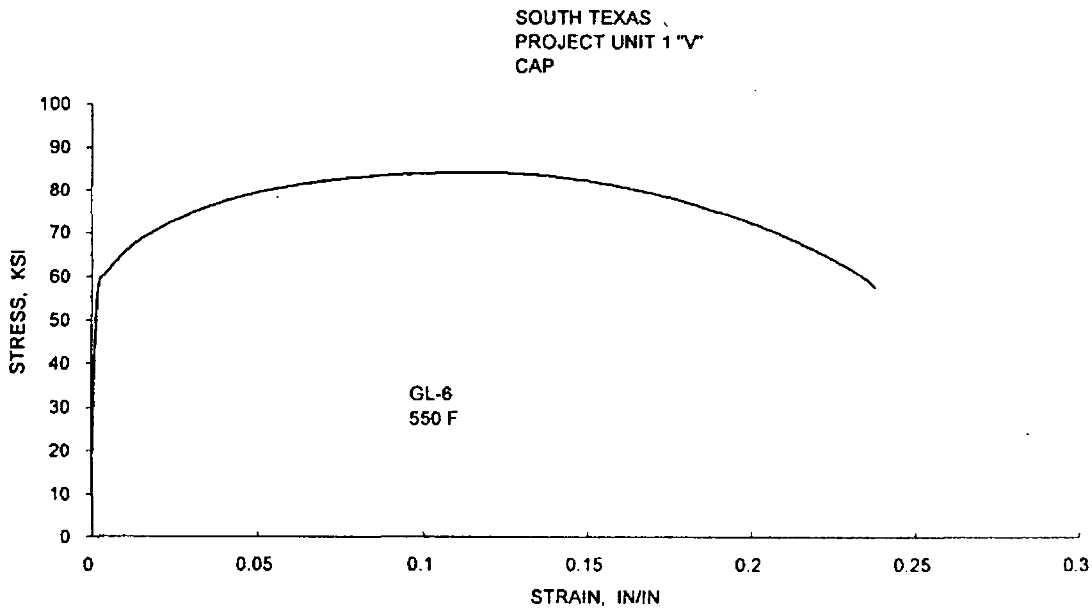

Figure 5-23 - Continued

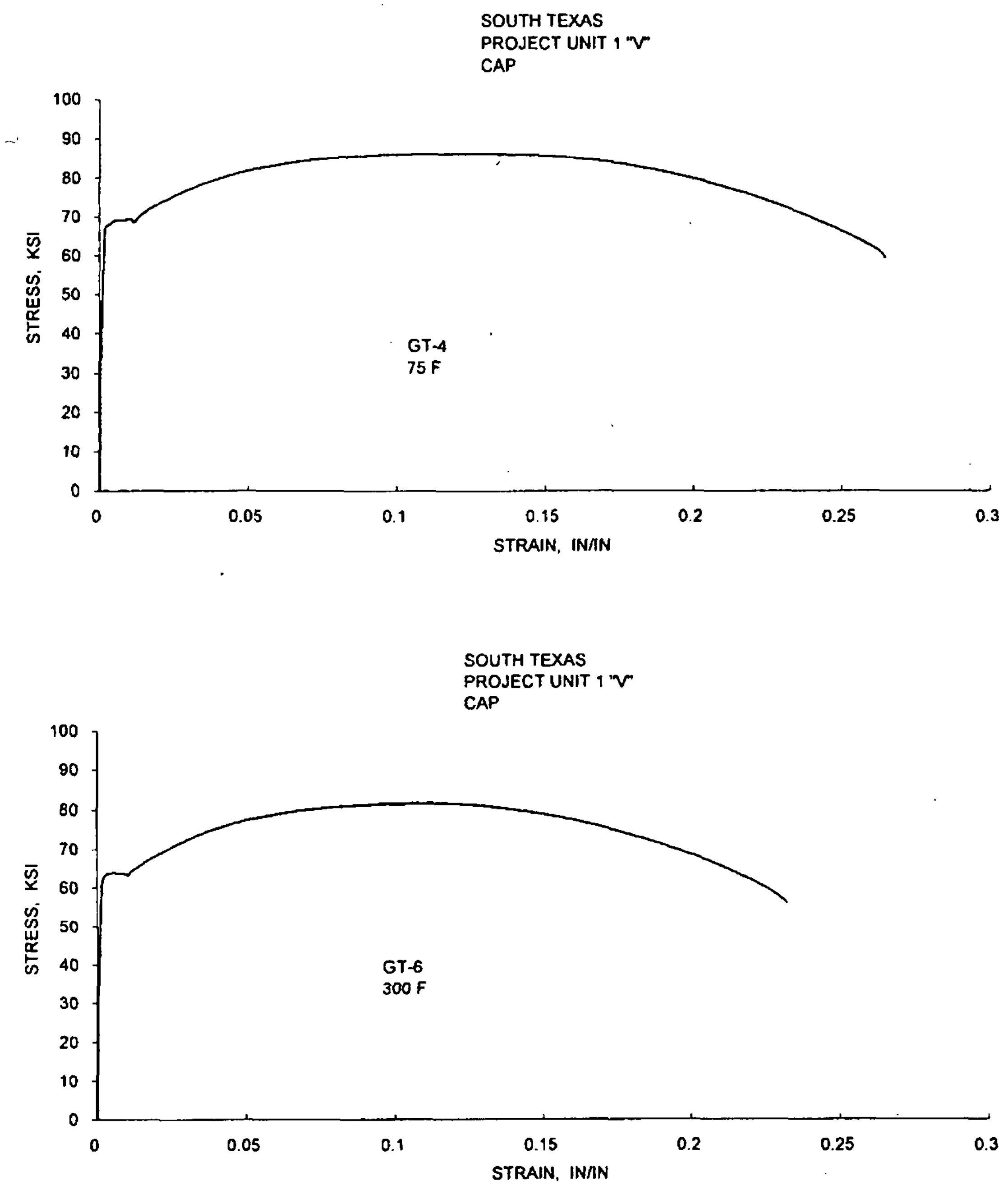

Figure 5-24 Engineering Stress-Strain Curves for South Texas Unit 1 Intermediate Shell Plate R1606-2 Tensile Specimens GT-4, GT-5 and GT-6 (Transverse Orientation)

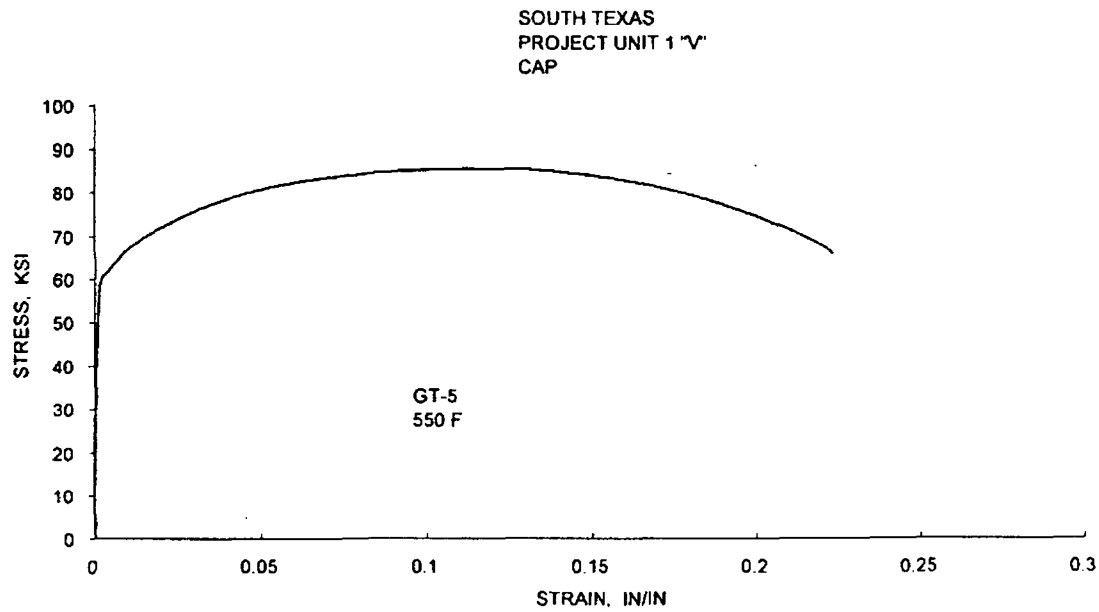

Figure 5-24 - Continued

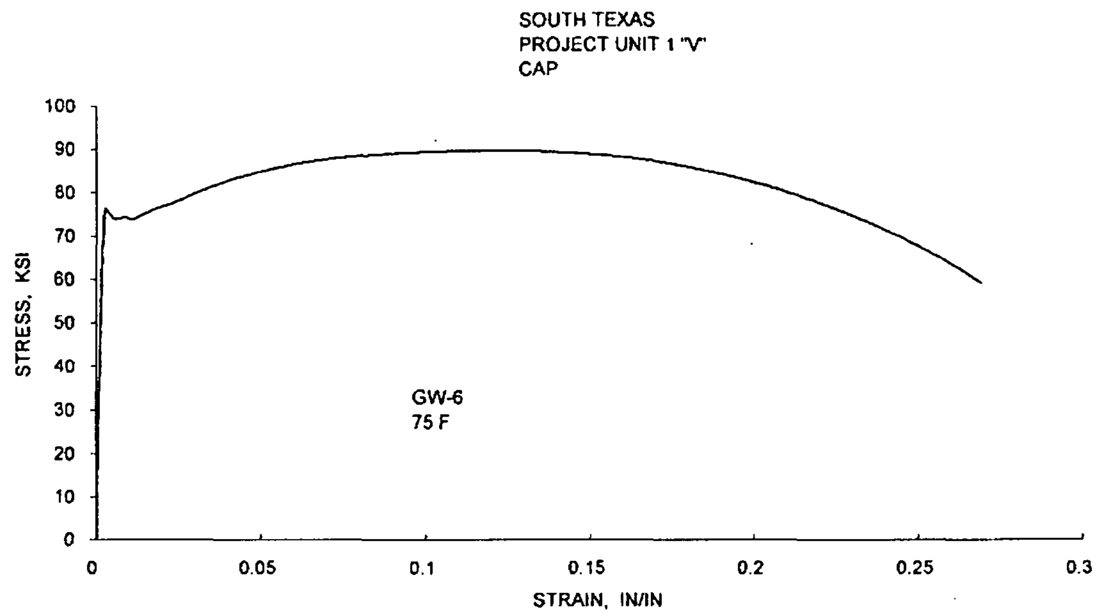

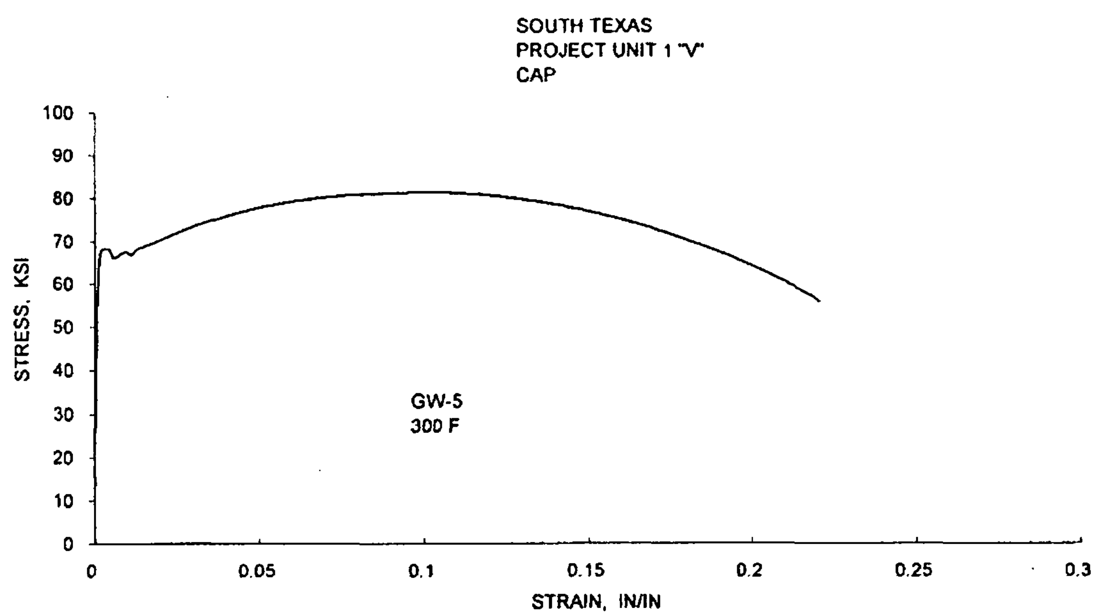

Figure 5-25 Engineering Stress-Strain Curves for Weld Metal Tensile Specimens GW-4, GW-5 and GW-6

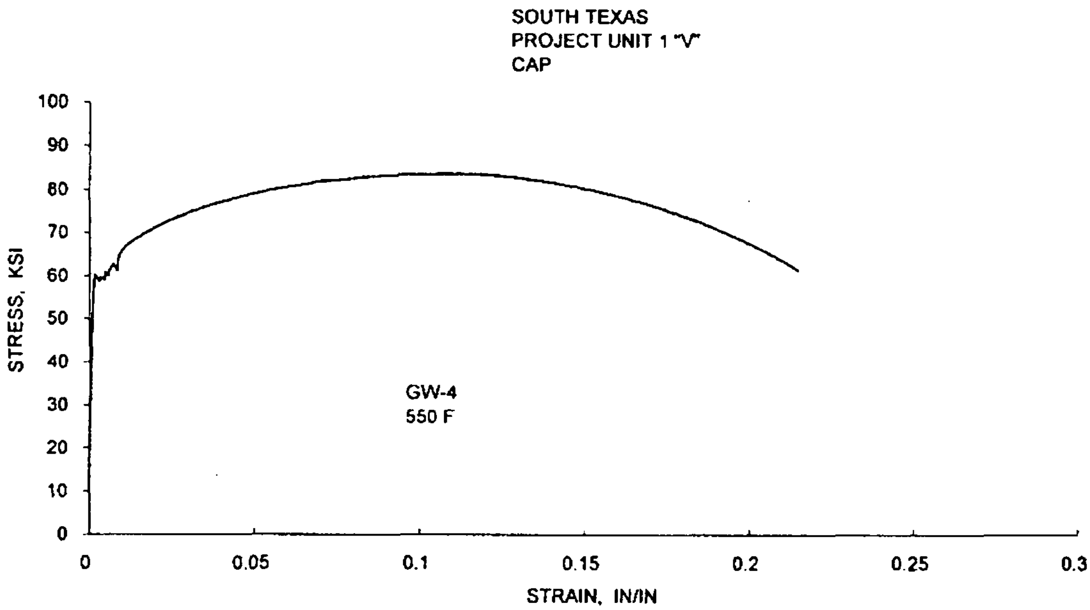

Figure 5-25 - Continued

6 RADIATION ANALYSIS AND NEUTRON DOSIMETRY

6.1 INTRODUCTION

This section describes a discrete ordinates S_n transport analysis performed for the South Texas Project Unit 1 reactor to determine the neutron radiation environment within the reactor pressure vessel and surveillance capsules. In this analysis, fast neutron exposure parameters in terms of fast neutron fluence (E > 1.0 MeV) and iron atom displacements (dpa) were established on a plant and fuel cycle specific basis. An evaluation of the most recent dosimetry sensor set from Capsule V, withdrawn at the end of the eleventh plant operating cycle, is provided. In addition, to provide an up-to-date data base applicable to the South Texas Project Unit 1 reactor, sensor sets from previously withdrawn capsules (U and Y) were re-analyzed using the current dosimetry evaluation methodology. These dosimetry updates are presented in Appendix A of this report. Comparisons of the results from these dosimetry evaluations with the analytical predictions served to validate the plant specific neutron transport calculations. These validated calculations subsequently formed the basis for providing projections of the neutron exposure of the reactor pressure vessel for operating periods extending to 54 Effective Full Power Years (EFPY). These projections also account for the plant uprating, from 3800 MWt to 3853 MWt, which occurred during mid-Cycle 11 operation and assumed thereafter.

The use of fast neutron fluence (E > 1.0 MeV) to correlate measured material property changes to the neutron exposure of the material has traditionally been accepted for the development of damage trend curves as well as for the implementation of trend curve data to assess the condition of the vessel. In recent years, however, it has been suggested that an exposure model that accounts for differences in neutron energy spectra between surveillance capsule locations and positions within the vessel wall could lead to an improvement in the uncertainties associated with damage trend curves and improved accuracy in the evaluation of damage gradients through the reactor vessel wall.

Because of this potential shift away from a threshold fluence toward an energy dependent damage function for data correlation, ASTM Standard Practice E853, "Analysis and Interpretation of Light-Water Reactor Surveillance Results," recommends reporting displacements per iron atom (dpa) along with fluence (E > 1.0 MeV) to provide a database for future reference. The energy dependent dpa function to be used for this evaluation is specified in ASTM Standard Practice E693, "Characterizing Neutron Exposures in Iron and Low Alloy Steels in Terms of Displacements per Atom." The application of the dpa parameter to the assessment of embrittlement gradients through the thickness of the reactor vessel wall has already been promulgated in Revision 2 to Regulatory Guide 1.99, "Radiation Embrittlement of Reactor Vessel Materials."

All of the calculations and dosimetry evaluations described in this section and in Appendix A were based on the latest available nuclear cross-section data derived from ENDF/B-VI and made use of the latest available calculational tools. Furthermore, the neutron transport and dosimetry evaluation methodologies follow the guidance and meet the requirements of Regulatory Guide 1.190, "Calculational and Dosimetry Methods for Determining Pressure Vessel Neutron Fluence."[19] Additionally, the methods used to develop the calculated pressure vessel fluence are consistent with the NRC approved methodology described in WCAP-14040-NP-A, "Methodology Used to Develop Cold Overpressure Mitigating System Setpoints and RCS Heatup and Cooldown Limit Curves," January 1996.[20] The specific calculational

methods applied are also consistent with those described in WCAP-15557, "Qualification of the Westinghouse Pressure Vessel Neutron Fluence Evaluation Methodology."[21]

6.2 DISCRETE ORDINATES ANALYSIS

A plan view of the South Texas Project Unit 1 reactor geometry at the core midplane is shown in Figure 4-1. Six irradiation capsules attached to the neutron pad are included in the reactor design that constitutes the reactor vessel surveillance program. The capsules are located at azimuthal angles of 58.5°, 61°, 121.5°, 238.5°, 241°, and 301.5° as shown in Figure 4-1. These full-core positions correspond to the following octant symmetric capsule locations represented in Figure 6-1: 29° from the core cardinal axis (for the 61° and 241° dual surveillance capsule holder locations) and 31.5° from the core cardinal axes (for the 121.5° and 301.5° single surveillance capsule holder locations, and for the 58.5° and 238.5° dual surveillance capsule holder locations). The stainless steel specimen containers are 1.182-inch by 1-inch and are approximately 56 inches in height. The containers are positioned axially such that the test specimens are centered on the core midplane, thus spanning the central 5 feet of the 14-foot high reactor core.

From a neutronic standpoint, the surveillance capsules and associated support structures are significant. The presence of these materials has a marked effect on both the spatial distribution of neutron flux and the neutron energy spectrum in the water annulus between the neutron pads and the reactor vessel. In order to determine the neutron environment at the test specimen location, the capsules themselves must be included in the analytical model.

In performing the fast neutron exposure evaluations for the South Texas Project Unit 1 reactor vessel and surveillance capsules, a series of fuel cycle specific forward transport calculations were carried out using the following three-dimensional flux synthesis technique:

$$\phi(r,\theta,z) = \phi(r,\theta) * \frac{\phi(r,z)}{\phi(r)}$$

where $\phi(r,\theta,z)$ is the synthesized three-dimensional neutron flux distribution, $\phi(r,\theta)$ is the transport solution in r,θ geometry, $\phi(r,z)$ is the two-dimensional solution for a cylindrical reactor model using the actual axial core power distribution, and $\phi(r)$ is the one-dimensional solution for a cylindrical reactor model using the same source per unit height as that used in the r,θ two-dimensional calculation. This synthesis procedure was carried out for each operating cycle at South Texas Project Unit 1.

For the South Texas Project Unit 1 transport calculations, the r,θ models depicted in Figure 6-1 were utilized since, with the exception of the neutron pads, the reactor is octant symmetric. These r,θ models include the core, the reactor internals, the neutron pads -- including explicit representations of octants not containing surveillance capsules and octants with surveillance capsules at 29° and 31.5°, the pressure vessel cladding and vessel wall, the insulation external to the pressure vessel, and the primary biological shield wall. These models formed the basis for the calculated results and enabled making comparisons to the surveillance capsule dosimetry evaluations. In developing these analytical models, nominal design dimensions were employed for the various structural components. Likewise, water temperatures, and hence, coolant densities in the reactor core and downcomer regions of the reactor were taken to be

representative of full power operating conditions. The coolant densities were treated on a fuel cycle specific basis. The reactor core itself was treated as a homogeneous mixture of fuel, cladding, water, and miscellaneous core structures such as fuel assembly grids, guide tubes, et cetera. The geometric mesh description of the r,θ reactor models consisted of 183 radial by 99 azimuthal intervals. Mesh sizes were chosen to assure that proper convergence of the inner iterations was achieved on a pointwise basis. The pointwise inner iteration flux convergence criterion utilized in the r,θ calculations was set at a value of 0.001.

The r,z models used for the South Texas Project Unit 1 calculations are shown in Figure 6-2 and extend radially from the centerline of the reactor core out to a location interior to the primary biological shield and over an axial span from an elevation 3-feet below the active fuel to approximately 5-feet above the active fuel. (Note that the only difference between these r,z models, and the corresponding r models, is the inclusion or exclusion of the neutron pads. R,Z / R synthesis factors with the neutron pad were used for the capsule locations and the 45° vessel location, whereas the corresponding synthesis factors without the neutron pad were used for the 0°, 15°, and 30° azimuthal locations of the pressure vessel.) As in the case of the r,θ models, nominal design dimensions and full power coolant densities were employed in the calculations. In this case, the homogenous core region was treated as an equivalent cylinder with a volume equal to that of the active core zone. The stainless steel former plates located between the core baffle and core barrel regions were also explicitly included in the model. The r,z geometric mesh description of these reactor models consisted of 137 radial by 191 axial intervals. As in the case of the r,θ calculations, mesh sizes were chosen to assure that proper convergence of the inner iterations was achieved on a point-wise basis. The point-wise inner iteration flux convergence criterion utilized in the r,z calculations was also set at a value of 0.001.

The one-dimensional radial models used in the synthesis procedure consisted of the same 137 radial mesh intervals included in the r,z models. Thus, radial synthesis factors could be determined on a mesh-wise basis throughout the entire geometry.

The core power distributions used in the plant specific transport analysis were taken from the appropriate South Texas Project Unit 1 fuel cycle design reports. The data extracted from the design reports represented cycle dependent fuel assembly enrichments, burnups, and axial power distributions. This information was used to develop spatial and energy dependent core source distributions averaged over each individual fuel cycle. Therefore, the results from the neutron transport calculations provided data in terms of fuel cycle averaged neutron flux, which when multiplied by the appropriate fuel cycle length, generated the incremental fast neutron exposure for each fuel cycle. In constructing these core source distributions, the energy distribution of the source was based on an appropriate fission split for uranium and plutonium isotopes based on the initial enrichment and burnup history of individual fuel assemblies. From these assembly dependent fission splits, composite values of energy release per fission, neutron yield per fission, and fission spectrum were determined.

All of the transport calculations supporting this analysis were carried out using the DORT discrete ordinates code Version 3.1[22] and the BUGLE-96 cross-section library.[23] The BUGLE-96 library provides a 67 group coupled neutron-gamma ray cross-section data set produced specifically for light water reactor (LWR) applications. In these analyses, anisotropic scattering was treated with a P_5 legendre expansion and angular discretization was modeled with an S_{16} order of angular quadrature.

Energy and space dependent core power distributions, as well as system operating temperatures, were treated on a fuel cycle specific basis.

Selected results from the neutron transport analyses are provided in Tables 6-1 through 6-7. In Table 6-1, the calculated exposure rates and integrated exposures, expressed in terms of both neutron fluence (E > 1.0 MeV) and dpa, are given at the radial and azimuthal center of the octant symmetric surveillance capsule positions, i.e., for the 29° dual capsule, 31.5° dual capsule, and 31.5° single capsule. These results, representative of the axial midplane of the active core, establish the calculated exposure of the surveillance capsules withdrawn to date as well as projected into the future. Similar information is provided in Tables 6-2 and 6-3 for the reactor vessel inner radius. The vessel data given in Table 6-2 are representative of the axial location of the maximum neutron exposure at each of the four azimuthal locations. Maximum integrated neutron exposure results for key vessel plate and weld materials are subsequently given in Table 6-3 for the end of Cycle 11 and beyond. It is also important to note that the data for the vessel inner radius were taken at the clad/base metal interface, and thus, represent the maximum calculated exposure levels of the vessel plates and welds.

Both calculated fluence (E > 1.0 MeV) and dpa data are provided in Table 6-1 through Table 6-3. These data tabulations include both plant and fuel cycle specific calculated neutron exposures at the end of the eleventh operating fuel cycle as well as projections for the current operating fuel cycle, i.e., Cycle 12, and future projections to 16, 32, 48, and 54 effective full power years (EFPY). The projections were based on the assumption that the core power distributions and associated plant operating characteristics from Cycle 12 were representative of future plant operation. The future projections are also based on the current reactor power level of 3853 MWt.

Radial gradient information applicable to fast (E > 1.0 MeV) neutron fluence and dpa are given in Tables 6-4 and 6-5, respectively. The data, based on the cumulative integrated exposures from Cycles 1 through 12, are presented on a relative basis for each exposure parameter at several azimuthal locations. Exposure distributions through the vessel wall may be obtained by multiplying the calculated exposure at the vessel inner radius by the gradient data listed in Tables 6-4 and 6-5.

The calculated fast neutron exposures for the three surveillance capsules withdrawn from the South Texas Project Unit 1 reactor are provided in Table 6-6. These assigned neutron exposure levels are based on the plant and fuel cycle specific neutron transport calculations performed for the South Texas Project Unit 1 reactor.

Updated lead factors for the South Texas Project Unit 1 surveillance capsules are provided in Table 6-7. The capsule lead factor is defined as the ratio of the calculated fluence (E > 1.0 MeV) at the geometric center of the surveillance capsule to the corresponding maximum calculated fluence at the pressure vessel clad/base metal interface. In Table 6-7, the lead factors for capsules that have been withdrawn from the reactor (U, Y, and V) were based on the calculated fluence values for the irradiation period corresponding to the time of withdrawal for the individual capsules. For the capsules remaining in the reactor (W, X, and Z), the lead factors correspond to the calculated fluence values at the end of Cycle 12, the current operating fuel cycle for South Texas Project Unit 1.

6.3 NEUTRON DOSIMETRY

The validity of the calculated neutron exposures previously reported in Section 6.2 is demonstrated by a direct comparison against the measured sensor reaction rates and via a least squares evaluation performed for each of the capsule dosimetry sets. However, since the neutron dosimetry measurement data merely serves to validate the calculated results, only the direct comparison of measured-to-calculated results for the most recent surveillance capsule removed from service is provided in this section of the report. For completeness, the assessment of all measured dosimetry removed to date, based on both direct and least squares evaluation comparisons, is documented in Appendix A.

The direct comparison of measured versus calculated fast neutron threshold reaction rates for the sensors from Capsule V, that was withdrawn from South Texas Project Unit 1 at the end of the eleventh fuel cycle, is summarized below.

Reaction	Reaction Rates (rps/atom)		M/C Ratio
	Measured	Calculated	
$^{63}Cu(n,\alpha)^{60}Co$	4.26E-17	4.01E-17	1.06
$^{54}Fe(n,p)^{54}Mn$	4.47E-15	4.43E-15	1.01
$^{58}Ni(n,p)^{58}Co$	6.40E-15	6.21E-15	1.03
$^{238}U(n,p)^{137}Cs$ (Cd)	2.78E-14	2.38E-14	1.17
$^{237}Np(n,f)^{137}Cs$ (Cd)	2.49E-13	2.32E-13	1.07
		Average:	1.07
		% Standard Deviation:	5.7

The measured-to-calculated (M/C) reaction rate ratios for the Capsule V threshold reactions range from 1.01 to 1.17, and the average M/C ratio is 1.07 ± 5.7% (1σ). This direct comparison falls well within the ± 20% criterion specified in Regulatory Guide 1.190; furthermore, it is consistent with the full set of comparisons given in Appendix A for all measured dosimetry removed to date from the South Texas Project Unit 1 reactor. These comparisons validate the current analytical results described in Section 6.2; therefore, the calculations are deemed applicable for South Texas Project Unit 1.

6.4 CALCULATIONAL UNCERTAINTIES

The uncertainty associated with the calculated neutron exposure of the South Texas Project Unit 1 surveillance capsule and reactor pressure vessel is based on the recommended approach provided in Regulatory Guide 1.190. In particular, the qualification of the methodology was carried out in the following four stages:

1 - Comparison of calculations with benchmark measurements from the Pool Critical Assembly (PCA) simulator at the Oak Ridge National Laboratory (ORNL).

2 - Comparisons of calculations with surveillance capsule and reactor cavity measurements from the H. B. Robinson power reactor benchmark experiment.

3 - An analytical sensitivity study addressing the uncertainty components resulting from important input parameters applicable to the plant specific transport calculations used in the neutron exposure assessments.

4 - Comparisons of the plant specific calculations with all available dosimetry results from the South Texas Project Unit 1 surveillance program.

The first phase of the methods qualification (PCA comparisons) addressed the adequacy of basic transport calculation and dosimetry evaluation techniques and associated cross-sections. This phase, however, did not test the accuracy of commercial core neutron source calculations nor did it address uncertainties in operational or geometric variables that impact power reactor calculations. The second phase of the qualification (H. B. Robinson comparisons) addressed uncertainties in these additional areas that are primarily methods related and would tend to apply generically to all fast neutron exposure evaluations. The third phase of the qualification (analytical sensitivity study) identified the potential uncertainties introduced into the overall evaluation due to calculational methods approximations as well as to a lack of knowledge relative to various plant specific input parameters. The overall calculational uncertainty applicable to the South Texas Project Unit 1 analysis was established from results of these three phases of the methods qualification.

The fourth phase of the uncertainty assessment (comparisons with South Texas Project Unit 1 measurements) was used solely to demonstrate the validity of the transport calculations and to confirm the uncertainty estimates associated with the analytical results. The comparison was used only as a check and was not used in any way to modify the calculated surveillance capsule and pressure vessel neutron exposures previously described in Section 6.2. As such, the validation of the South Texas Project Unit 1 analytical model based on the measured plant dosimetry is completely described in Appendix A.

The following summarizes the uncertainties developed from the first three phases of the methodology qualification. Additional information pertinent to these evaluations is provided in Reference 21.

	Capsule	Vessel IR
PCA Comparisons	3%	3%
H. B. Robinson Comparisons	3%	3%
Analytical Sensitivity Studies	10%	11%
Additional Uncertainty for Factors not Explicitly Evaluated	5%	5%
Net Calculational Uncertainty	12%	13%

The net calculational uncertainty was determined by combining the individual components in quadrature. Therefore, the resultant uncertainty was treated as random and no systematic bias was applied to the analytical results.

The plant specific measurement comparisons described in Appendix A support these uncertainty assessments for South Texas Project Unit 1.

Figure 6-1

South Texas Project Unit 1 r,θ Reactor Geometry with a 12.5° Neutron Pad
at the Core Midplane

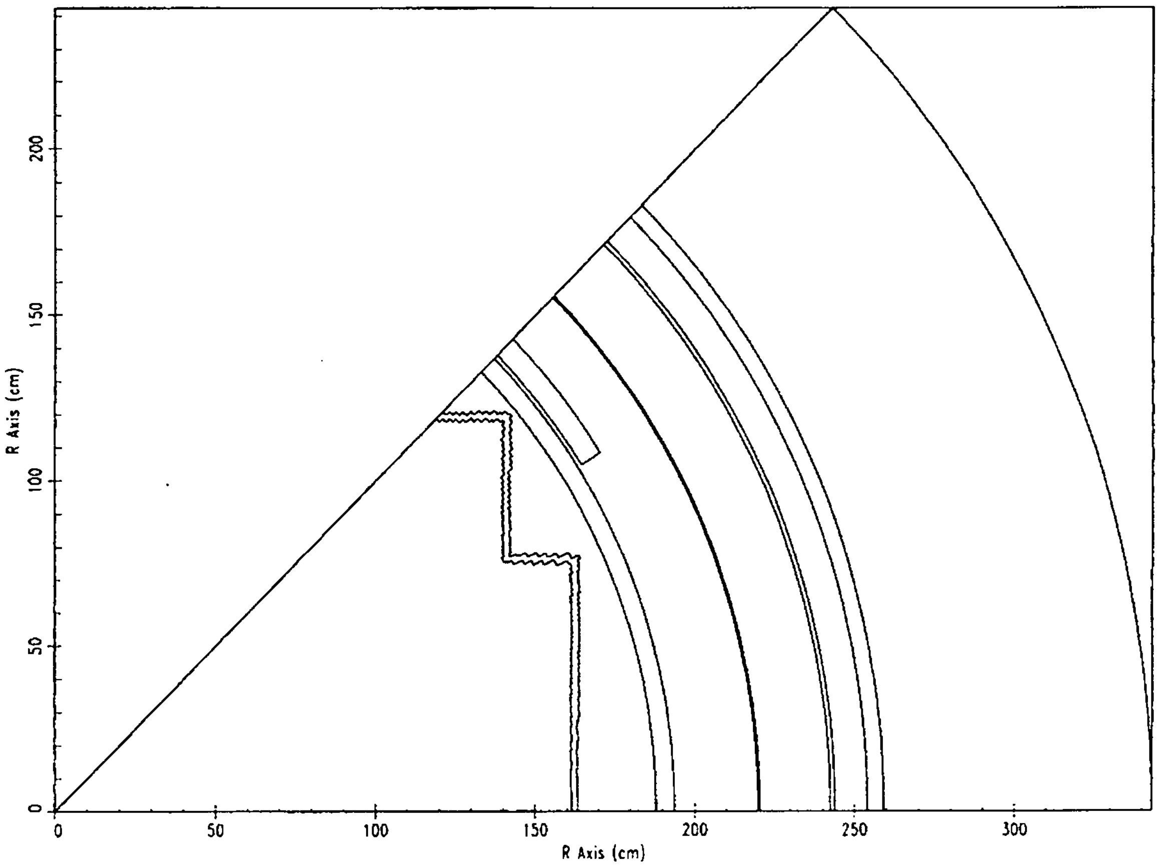

Figure 6-1 (continued)

South Texas Project Unit 1 r,θ Reactor Geometry with a 20.0° Neutron Pad at the Core Midplane

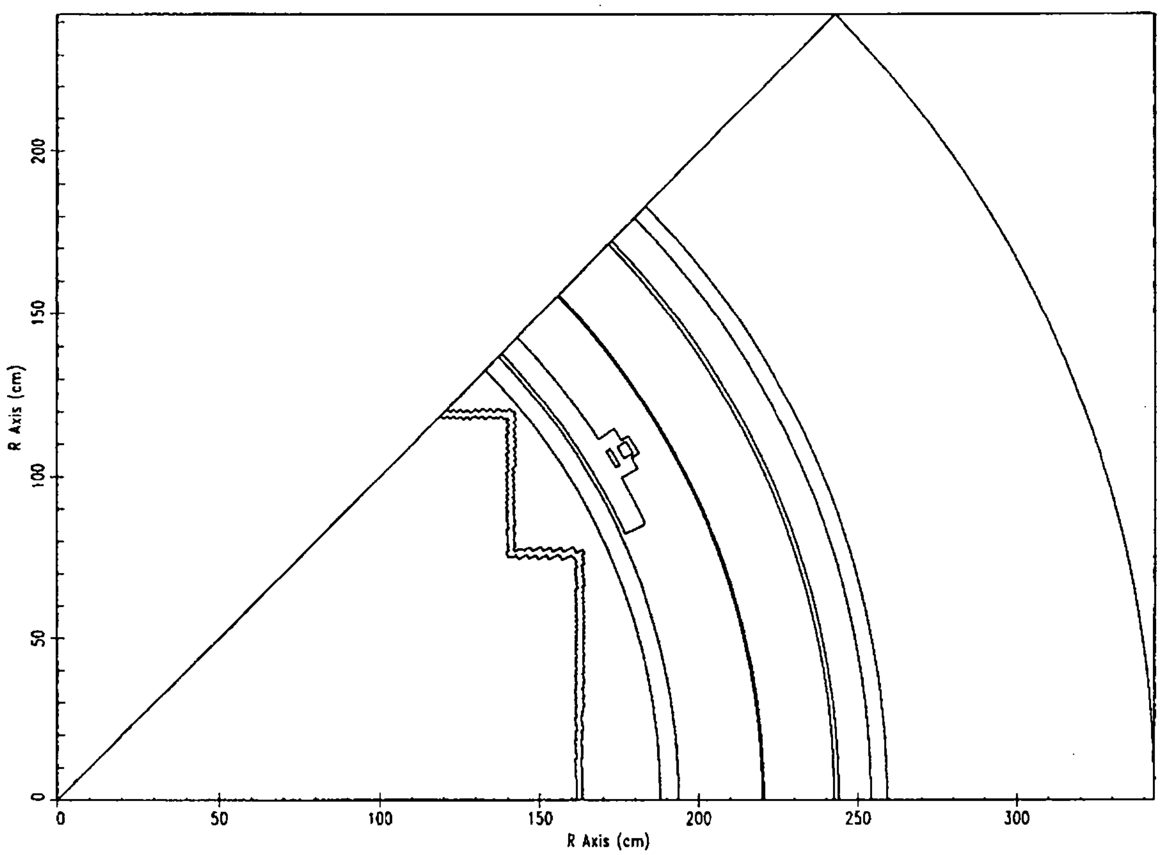

Figure 6-1 (continued)

South Texas Project Unit 1 r,θ Reactor Geometry with a 22.5° Neutron Pad at the Core Midplane

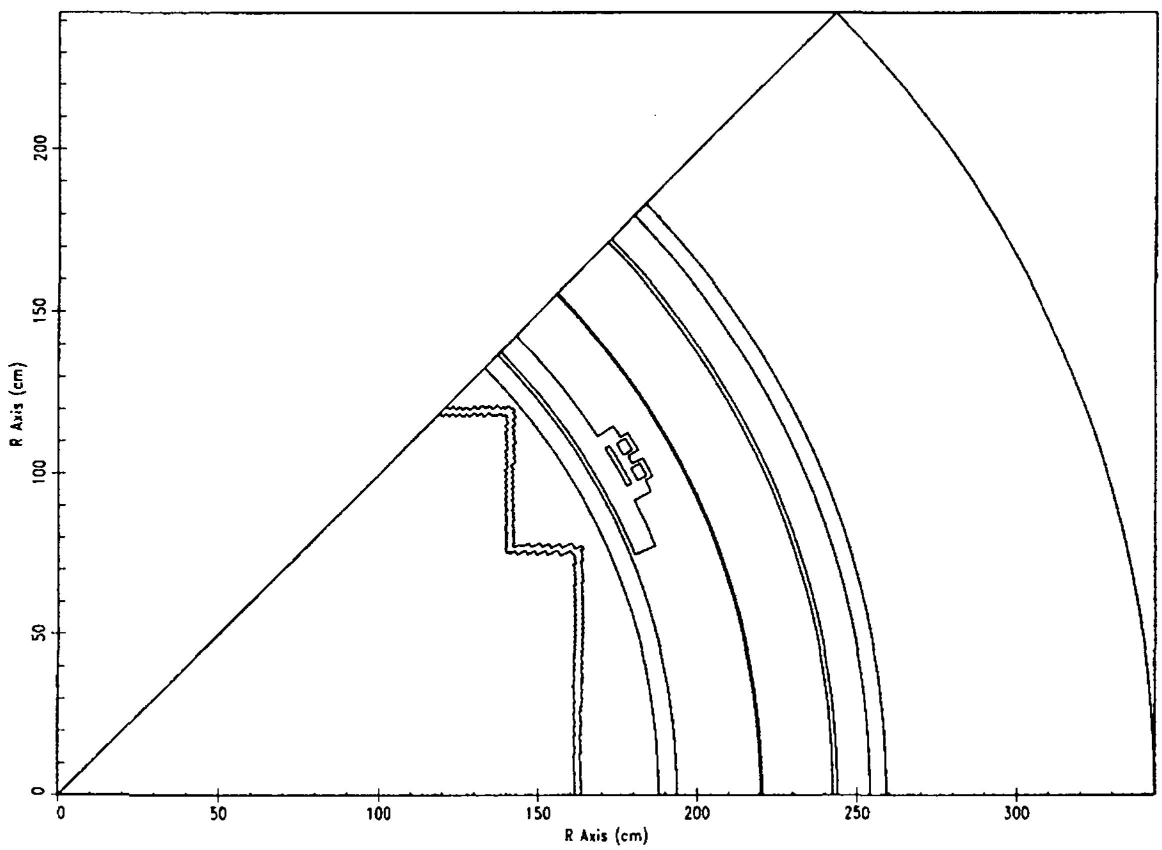

Figure 6-2

South Texas Project Unit 1 r,z Reactor Geometry with Neutron Pad

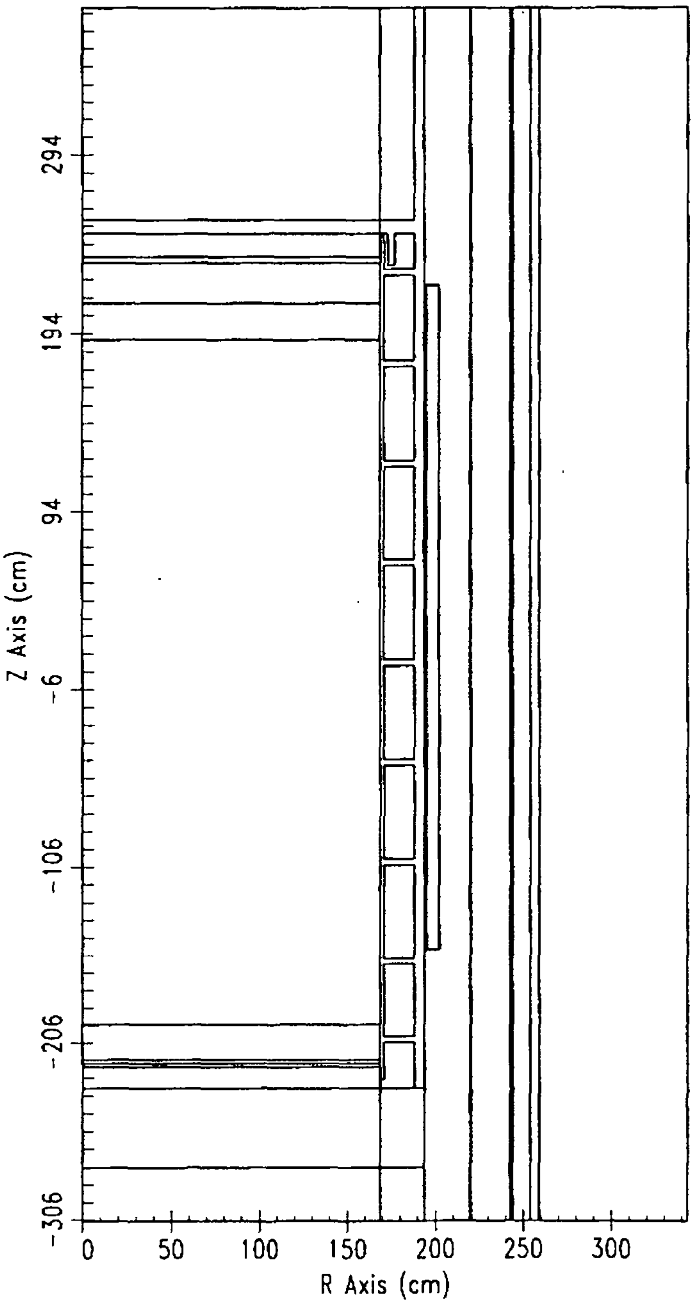

Note: This model was used in the assessment of the surveillance capsule neutron exposures and reactor vessel neutron exposures at the 45° azimuthal location only.

Figure 6-2 (continued)

South Texas Project Unit 1 r,z Reactor Geometry without Neutron Pad

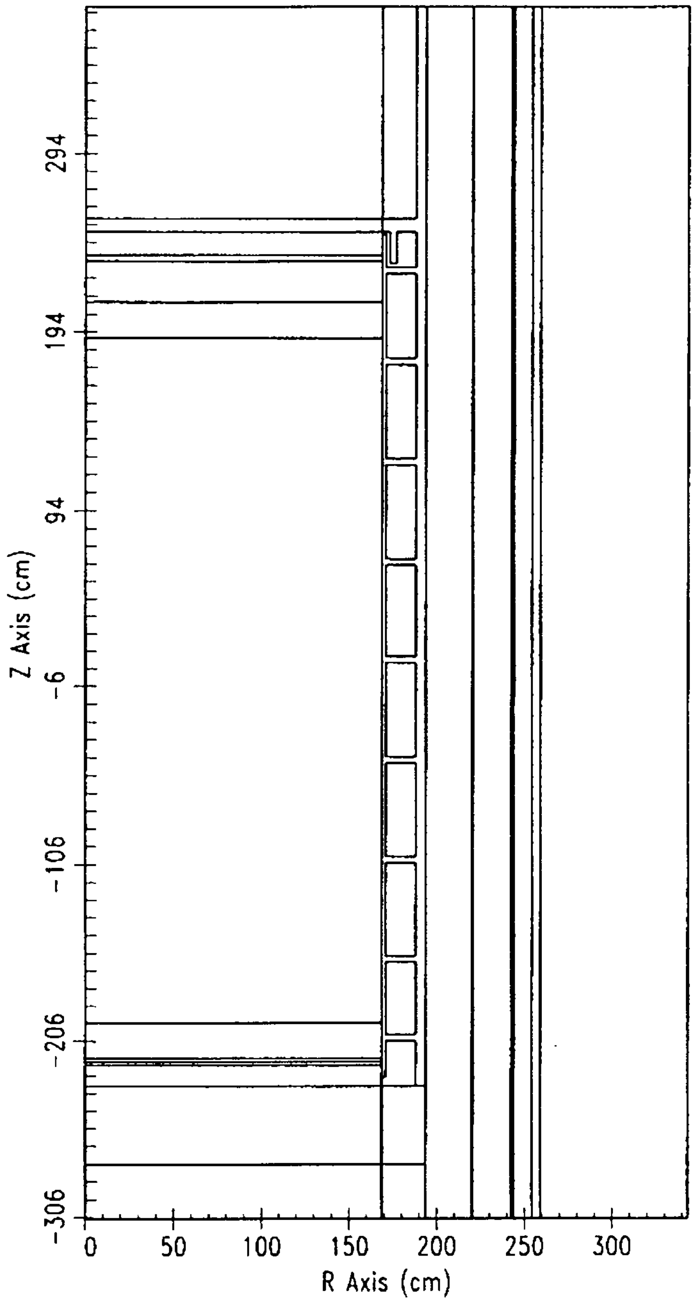

Note: This model was used in the assessment of the reactor vessel neutron exposures at the 0°, 15°, and 30° azimuthal locations only.

Table 6-1

Calculated Neutron Exposure Rates And Integrated Exposures
At The Surveillance Capsule Center

Neutrons (E > 1.0 MeV)

Cycle	Cycle Length [EFPS]	Cumulative Irradiation Time [EFPS]	Cumulative Irradiation Time [EFPY]	Neutron Flux (E > 1.0 MeV) [n/cm^2-s]		
				Dual 29°	Dual 31.5°	Single 31.5°
1	2.47E+07	2.47E+07	0.78	9.63E+10	1.05E+11	1.03E+11
2	1.23E+07	3.70E+07	1.17	7.52E+10	7.76E+10	7.66E+10
3	1.07E+07	4.77E+07	1.51	8.76E+10	9.50E+10	9.40E+10
4	4.25E+07	9.02E+07	2.86	8.00E+10	8.56E+10	8.46E+10
5	3.08E+07	1.21E+08	3.84	8.07E+10	8.32E+10	8.22E+10
6	3.36E+07	1.55E+08	4.90	8.32E+10	8.71E+10	8.61E+10
7	3.90E+07	1.94E+08	6.14	7.13E+10	7.75E+10	7.68E+10
8	4.53E+07	2.39E+08	7.57	6.50E+10	7.27E+10	7.20E+10
9	2.58E+07	2.65E+08	8.39	7.13E+10	8.08E+10	8.00E+10
10	4.37E+07	3.08E+08	9.77	6.43E+10	7.12E+10	7.05E+10
11	4.26E+07	3.51E+08	11.13	6.79E+10	7.18E+10	7.10E+10
12 (Prj.)	4.71E+07	3.98E+08	12.62	6.59E+10	7.13E+10	7.05E+10
Future	1.07E+08	5.05E+08	16.00	6.59E+10	7.13E+10	7.05E+10
Future	5.05E+08	1.01E+09	32.00	6.59E+10	7.13E+10	7.05E+10
Future	5.05E+08	1.51E+09	48.00	6.59E+10	7.13E+10	7.05E+10
Future	1.89E+08	1.70E+09	54.00	6.59E+10	7.13E+10	7.05E+10

Note: Neutron exposure values reported for the surveillance capsules are centered at the core midplane.

Table 6-1 cont'd

Calculated Neutron Exposure Rates And Integrated Exposures
At The Surveillance Capsule Center

Neutrons (E > 1.0 MeV)

Cycle	Cycle Length [EFPS]	Cumulative Irradiation Time [EFPS]	Cumulative Irradiation Time [EFPY]	Neutron Fluence (E > 1.0 MeV) [n/cm²]		
				Dual 29°	Dual 31.5°	Single 31.5°
1	2.47E+07	2.47E+07	0.78	2.38E+18	2.58E+18	2.56E+18
2	1.23E+07	3.70E+07	1.17	3.31E+18	3.54E+18	3.50E+18
3	1.07E+07	4.77E+07	1.51	4.24E+18	4.55E+18	4.50E+18
4	4.25E+07	9.02E+07	2.86	7.64E+18	8.19E+18	8.10E+18
5	3.08E+07	1.21E+08	3.84	1.01E+19	1.08E+19	1.06E+19
6	3.36E+07	1.55E+08	4.90	1.29E+19	1.37E+19	1.35E+19
7	3.90E+07	1.94E+08	6.14	1.57E+19	1.67E+19	1.65E+19
8	4.53E+07	2.39E+08	7.57	1.87E+19	2.00E+19	1.98E+19
9	2.58E+07	2.65E+08	8.39	2.05E+19	2.21E+19	2.19E+19
10	4.37E+07	3.08E+08	9.77	2.33E+19	2.52E+19	2.49E+19
11	4.26E+07	3.51E+08	11.13	2.62E+19	2.83E+19	2.80E+19
12 (Prj.)	4.71E+07	3.98E+08	12.62	2.93E+19	3.16E+19	3.13E+19
Future	1.07E+08	5.05E+08	16.00	3.63E+19	3.92E+19	3.88E+19
Future	5.05E+08	1.01E+09	32.00	6.96E+19	7.52E+19	7.44E+19
Future	5.05E+08	1.51E+09	48.00	1.03E+20	1.11E+20	1.10E+20
Future	1.89E+08	1.70E+09	54.00	1.15E+20	1.25E+20	1.23E+20

Note: Neutron exposure values reported for the surveillance capsules are centered at the core midplane.

Table 6-1 cont'd

Calculated Neutron Exposure Rates And Integrated Exposures
At The Surveillance Capsule Center

Iron Atom Displacements

Cycle	Cycle Length [EFPS]	Cumulative Irradiation Time [EFPS]	Cumulative Irradiation Time [EFPY]	Displacement Rate [dpa/s]		
				Dual 29°	Dual 31.5°	Single 31.5°
1	2.47E+07	2.47E+07	0.78	1.88E-10	2.04E-10	2.01E-10
2	1.23E+07	3.70E+07	1.17	1.47E-10	1.52E-10	1.49E-10
3	1.07E+07	4.77E+07	1.51	1.71E-10	1.85E-10	1.83E-10
4	4.25E+07	9.02E+07	2.86	1.56E-10	1.66E-10	1.64E-10
5	3.08E+07	1.21E+08	3.84	1.57E-10	1.62E-10	1.59E-10
6	3.36E+07	1.55E+08	4.90	1.62E-10	1.69E-10	1.67E-10
7	3.90E+07	1.94E+08	6.14	1.38E-10	1.50E-10	1.48E-10
8	4.53E+07	2.39E+08	7.57	1.26E-10	1.40E-10	1.39E-10
9	2.58E+07	2.65E+08	8.39	1.38E-10	1.56E-10	1.55E-10
10	4.37E+07	3.08E+08	9.77	1.25E-10	1.38E-10	1.36E-10
11	4.26E+07	3.51E+08	11.13	1.31E-10	1.39E-10	1.37E-10
12 (Prj.)	4.71E+07	3.98E+08	12.62	1.28E-10	1.38E-10	1.36E-10
Future	1.07E+08	5.05E+08	16.00	1.28E-10	1.38E-10	1.36E-10
Future	5.05E+08	1.01E+09	32.00	1.28E-10	1.38E-10	1.36E-10
Future	5.05E+08	1.51E+09	48.00	1.28E-10	1.38E-10	1.36E-10
Future	1.89E+08	1.70E+09	54.00	1.28E-10	1.38E-10	1.36E-10

Note: Neutron exposure values reported for the surveillance capsules are centered at the core midplane.

Table 6-1 cont'd

Calculated Neutron Exposure Rates And Integrated Exposures
At The Surveillance Capsule Center

Iron Atom Displacements

Cycle	Cycle Length [EFPS]	Cumulative Irradiation Time [EFPS]	Cumulative Irradiation Time [EFPY]	Displacements [dpa]		
				Dual 29°	Dual 31.5°	Single 31.5°
1	2.47E+07	2.47E+07	0.78	4.65E-03	5.05E-03	4.98E-03
2	1.23E+07	3.70E+07	1.17	6.46E-03	6.91E-03	6.81E-03
3	1.07E+07	4.77E+07	1.51	8.29E-03	8.89E-03	8.77E-03
4	4.25E+07	9.02E+07	2.86	1.49E-02	1.60E-02	1.57E-02
5	3.08E+07	1.21E+08	3.84	1.97E-02	2.09E-02	2.06E-02
6	3.36E+07	1.55E+08	4.90	2.52E-02	2.66E-02	2.62E-02
7	3.90E+07	1.94E+08	6.14	3.06E-02	3.25E-02	3.20E-02
8	4.53E+07	2.39E+08	7.57	3.62E-02	3.88E-02	3.83E-02
9	2.58E+07	2.65E+08	8.39	3.98E-02	4.29E-02	4.23E-02
10	4.37E+07	3.08E+08	9.77	4.52E-02	4.89E-02	4.82E-02
11	4.26E+07	3.51E+08	11.13	5.08E-02	5.48E-02	5.41E-02
12 (Prj.)	4.71E+07	3.98E+08	12.62	5.69E-02	6.13E-02	6.05E-02
Future	1.07E+08	5.05E+08	16.00	7.05E-02	7.60E-02	7.50E-02
Future	5.05E+08	1.01E+09	32.00	1.35E-01	1.46E-01	1.44E-01
Future	5.05E+08	1.51E+09	48.00	1.99E-01	2.15E-01	2.12E-01
Future	1.89E+08	1.70E+09	54.00	2.24E-01	2.41E-01	2.38E-01

Note: Neutron exposure values reported for the surveillance capsules are centered at the core midplane.

Table 6-2

Calculated Azimuthal Variation Of Maximum Exposure Rates
And Integrated Exposures At The Reactor Vessel
Clad/Base Metal Interface

Cycle	Cycle Length [EFPS]	Cumulative Irradiation Time [EFPS]	Cumulative Irradiation Time [EFPY]	Neutron Flux (E > 1.0 MeV) [n/cm^2-s]			
				0°	15°	30°	45°
1	2.47E+07	2.47E+07	0.78	1.37E+10	2.08E+10	2.42E+10	2.91E+10
2	1.23E+07	3.70E+07	1.17	1.38E+10	2.01E+10	1.94E+10	2.47E+10
3	1.07E+07	4.77E+07	1.51	1.22E+10	1.87E+10	2.15E+10	2.98E+10
4	4.25E+07	9.02E+07	2.86	1.14E+10	1.78E+10	1.98E+10	2.48E+10
5	3.08E+07	1.21E+08	3.84	1.31E+10	1.96E+10	1.97E+10	2.38E+10
6	3.36E+07	1.55E+08	4.90	1.22E+10	1.85E+10	2.01E+10	2.43E+10
7	3.90E+07	1.94E+08	6.14	9.53E+09	1.50E+10	1.74E+10	2.48E+10
8	4.53E+07	2.39E+08	7.57	8.09E+09	1.20E+10	1.60E+10	2.23E+10
9	2.58E+07	2.65E+08	8.39	8.68E+09	1.30E+10	1.76E+10	2.75E+10
10	4.37E+07	3.08E+08	9.77	8.46E+09	1.26E+10	1.66E+10	2.51E+10
11	4.26E+07	3.51E+08	11.13	1.02E+10	1.42E+10	1.70E+10	2.06E+10
12 (Prj.)	4.71E+07	3.98E+08	12.62	8.92E+09	1.33E+10	1.68E+10	2.22E+10
Future	1.07E+08	5.05E+08	16.00	8.92E+09	1.33E+10	1.68E+10	2.22E+10
Future	5.05E+08	1.01E+09	32.00	8.92E+09	1.33E+10	1.68E+10	2.22E+10
Future	5.05E+08	1.51E+09	48.00	8.92E+09	1.33E+10	1.68E+10	2.22E+10
Future	1.89E+08	1.70E+09	54.00	8.92E+09	1.33E+10	1.68E+10	2.22E+10

Table 6-2 cont'd

Calculated Azimuthal Variation Of Maximum Exposure Rates
And Integrated Exposures At The Reactor Vessel
Clad/Base Metal Interface

Cycle	Cycle Length [EFPS]	Cumulative Irradiation Time [EFPS]	Cumulative Irradiation Time [EFPY]	Neutron Fluence (E > 1.0 MeV) [n/cm²]			
				0°	15°	30°	45°
1	2.47E+07	2.47E+07	0.78	3.40E+17	5.14E+17	5.99E+17	7.19E+17
2	1.23E+07	3.70E+07	1.17	4.97E+17	7.42E+17	8.19E+17	1.02E+18
3	1.07E+07	4.77E+07	1.51	6.28E+17	9.42E+17	1.05E+18	1.34E+18
4	4.25E+07	9.02E+07	2.86	1.11E+18	1.70E+18	1.89E+18	2.40E+18
5	3.08E+07	1.21E+08	3.84	1.51E+18	2.30E+18	2.50E+18	3.13E+18
6	3.36E+07	1.55E+08	4.90	1.91E+18	2.91E+18	3.15E+18	3.94E+18
7	3.90E+07	1.94E+08	6.14	2.29E+18	3.49E+18	3.83E+18	4.90E+18
8	4.53E+07	2.39E+08	7.57	2.65E+18	4.03E+18	4.56E+18	5.91E+18
9	2.58E+07	2.65E+08	8.39	2.88E+18	4.37E+18	5.01E+18	6.63E+18
10	4.37E+07	3.08E+08	9.77	3.24E+18	4.91E+18	5.72E+18	7.72E+18
11	4.26E+07	3.51E+08	11.13	3.67E+18	5.51E+18	6.44E+18	8.60E+18
12 (Prj.)	4.71E+07	3.98E+08	12.62	4.08E+18	6.13E+18	7.22E+18	9.65E+18
Future	1.07E+08	5.05E+08	16.00	5.02E+18	7.53E+18	9.00E+18	1.20E+19
Future	5.05E+08	1.01E+09	32.00	9.49E+18	1.42E+19	1.74E+19	2.32E+19
Future	5.05E+08	1.51E+09	48.00	1.40E+19	2.09E+19	2.59E+19	3.44E+19
Future	1.89E+08	1.70E+09	54.00	1.57E+19	2.34E+19	2.90E+19	3.86E+19

Table 6-2 cont'd

Calculated Azimuthal Variation Of Fast Neutron Exposure Rates And Iron Atom Displacement Rates At The Reactor Vessel Clad/Base Metal Interface

Cycle	Cycle Length [EFPS]	Cumulative Irradiation Time [EFPS]	Cumulative Irradiation Time [EFPY]	Iron Atom Displacement Rate [dpa/s]			
				0°	15°	30°	45°
1	2.47E+07	2.47E+07	0.78	2.13E-11	3.19E-11	3.73E-11	4.50E-11
2	1.23E+07	3.70E+07	1.17	2.14E-11	3.08E-11	2.98E-11	3.79E-11
3	1.07E+07	4.77E+07	1.51	1.90E-11	2.87E-11	3.31E-11	4.59E-11
4	4.25E+07	9.02E+07	2.86	1.77E-11	2.73E-11	3.05E-11	3.83E-11
5	3.08E+07	1.21E+08	3.84	2.03E-11	3.01E-11	3.04E-11	3.66E-11
6	3.36E+07	1.55E+08	4.90	1.90E-11	2.84E-11	3.10E-11	3.74E-11
7	3.90E+07	1.94E+08	6.14	1.48E-11	2.30E-11	2.69E-11	3.82E-11
8	4.53E+07	2.39E+08	7.57	1.26E-11	1.85E-11	2.47E-11	3.43E-11
9	2.58E+07	2.65E+08	8.39	1.35E-11	2.00E-11	2.71E-11	4.23E-11
10	4.37E+07	3.08E+08	9.77	1.31E-11	1.94E-11	2.56E-11	3.87E-11
11	4.26E+07	3.51E+08	11.13	1.58E-11	2.18E-11	2.61E-11	3.18E-11
12 (Prj.)	4.71E+07	3.98E+08	12.62	1.38E-11	2.05E-11	2.58E-11	3.42E-11
Future	1.07E+08	5.05E+08	16.00	1.38E-11	2.05E-11	2.58E-11	3.42E-11
Future	5.05E+08	1.01E+09	32.00	1.38E-11	2.05E-11	2.58E-11	3.42E-11
Future	5.05E+08	1.51E+09	48.00	1.38E-11	2.05E-11	2.58E-11	3.42E-11
Future	1.89E+08	1.70E+09	54.00	1.38E-11	2.05E-11	2.58E-11	3.42E-11

Table 6-2 cont'd

Calculated Azimuthal Variation Of Maximum Exposure Rates
And Integrated Exposures At The Reactor Vessel
Clad/Base Metal Interface

Cycle	Cycle Length [EFPS]	Cumulative Irradiation Time [EFPS]	Cumulative Irradiation Time [EFPY]	Iron Atom Displacements [dpa]			
				0°	15°	30°	45°
1	2.47E+07	2.47E+07	0.78	5.27E-04	7.89E-04	9.22E-04	1.11E-03
2	1.23E+07	3.70E+07	1.17	7.71E-04	1.14E-03	1.26E-03	1.57E-03
3	1.07E+07	4.77E+07	1.51	9.73E-04	1.45E-03	1.61E-03	2.06E-03
4	4.25E+07	9.02E+07	2.86	1.72E-03	2.60E-03	2.91E-03	3.69E-03
5	3.08E+07	1.21E+08	3.84	2.35E-03	3.53E-03	3.85E-03	4.82E-03
6	3.36E+07	1.55E+08	4.90	2.97E-03	4.46E-03	4.86E-03	6.07E-03
7	3.90E+07	1.94E+08	6.14	3.55E-03	5.36E-03	5.91E-03	7.55E-03
8	4.53E+07	2.39E+08	7.57	4.12E-03	6.20E-03	7.03E-03	9.10E-03
9	2.58E+07	2.65E+08	8.39	4.47E-03	6.71E-03	7.73E-03	1.02E-02
10	4.37E+07	3.08E+08	9.77	5.03E-03	7.54E-03	8.82E-03	1.19E-02
11	4.26E+07	3.51E+08	11.13	5.70E-03	8.47E-03	9.93E-03	1.32E-02
12 (Prj.)	4.71E+07	3.98E+08	12.62	6.34E-03	9.42E-03	1.11E-02	1.48E-02
Future	1.07E+08	5.05E+08	16.00	7.81E-03	1.16E-02	1.39E-02	1.85E-02
Future	5.05E+08	1.01E+09	32.00	1.47E-02	2.18E-02	2.68E-02	3.58E-02
Future	5.05E+08	1.51E+09	48.00	2.17E-02	3.21E-02	3.98E-02	5.30E-02
Future	1.89E+08	1.70E+09	54.00	2.43E-02	3.60E-02	4.47E-02	5.95E-02

Table 6-3

Calculated Integrated Exposures for KeyVessel Plate and Weld Materials
At The Reactor Vessel Clad/Base Metal Interface

Material	Location	Neutron Fluence (E > 1.0 MeV), n/cm^2					
		11.13 EFPY	12.62 EFPY	16 EFPY	32 EFPY	48 EFPY	54 EFPY
Upper-to-Intermediate Shell Circumferential Weld	45°	8.64E+16	9.54E+16	1.16E+17	2.12E+17	3.09E+17	3.45E+17
Intermediate Shell Basemetal	45°	6.46E+18	7.23E+18	8.96E+18	1.72E+19	2.54E+19	2.85E+19
Intermediate Shell Longitudinal Weld 0° Azimuth	0°	3.60E+18	4.01E+18	4.93E+18	9.30E+18	1.37E+19	1.53E+19
Intermediate-to-Lower Shell Circumferential Weld	45°	6.46E+18	7.23E+18	8.96E+18	1.71E+19	2.53E+19	2.84E+19
Lower Shell Basemetal	45°	8.60E+18	9.65E+18	1.20E+19	2.32E+19	3.44E+19	3.86E+19
Lower Shell Longitudinal Weld 90° Azimuth	0°	3.67E+18	4.08E+18	5.02E+18	9.49E+18	1.40E+19	1.57E+19
Lower Shell Longitudinal Weld 210° and 330° Azimuth 12.5° Neutron Pad	30°	8.45E+18	9.50E+18	1.19E+19	2.31E+19	3.44E+19	3.86E+19
Lower Shell-to-Lower Head Circumferential Weld	45°	8.45E+16	9.34E+16	1.14E+17	2.09E+17	3.05E+17	3.41E+17

Notes:

(1) The Intermediate Shell Longitudinal Weld, 120° Azimuth, 20° Neutron Pad results at the 30° location are bounded by the Intermediate Shell Basemetal values at the 45° location.

(2) The Intermediate Shell Longitudinal Weld, 240° Azimuth, 22.5° Neutron Pad results at the 30° location are bounded by the Intermediate Shell Basemetal values at the 45° location.

Table 6-3 cont'd

Calculated Integrated Exposures for KeyVessel Plate and Weld Materials
At The Reactor Vessel Clad/Base Metal Interface

Iron Atom Displacements, dpa

Material	Location	11.13 EFPY	12.62 EFPY	16 EFPY	32 EFPY	48 EFPY	54 EFPY
Upper-to-Intermediate Shell Circumferential Weld	45°	1.50E-04	1.66E-04	2.02E-04	3.70E-04	5.39E-04	6.03E-04
Intermediate Shell Basemetal	45°	1.02E-02	1.15E-02	1.42E-02	2.72E-02	4.03E-02	4.52E-02
Intermediate Shell Longitudinal Weld 0° Azimuth	0°	5.60E-03	6.23E-03	7.66E-03	1.45E-02	2.12E-02	2.38E-02
Intermediate-to-Lower Shell Circumferential Weld	45°	1.02E-02	1.15E-02	1.42E-02	2.72E-02	4.02E-02	4.50E-02
Lower Shell Basemetal	45°	1.32E-02	1.48E-02	1.85E-02	3.58E-02	5.30E-02	5.95E-02
Lower Shell Longitudinal Weld 90° Azimuth	0°	5.70E-03	6.34E-03	7.81E-03	1.47E-02	2.17E-02	2.43E-02
Lower Shell Longitudinal Weld 210° and 330° Azimuth 12.5° Neutron Pad	30°	1.27E-02	1.43E-02	1.78E-02	3.47E-02	5.16E-02	5.80E-02
Lower Shell-to-Lower Head Circumferential Weld	45°	1.52E-04	1.68E-04	2.04E-04	3.77E-04	5.50E-04	6.15E-04

Notes:

(3) The Intermediate Shell Longitudinal Weld, 120° Azimuth, 20° Neutron Pad results at the 30° location are bounded by the Intermediate Shell Basemetal values at the 45° location.

(4) The Intermediate Shell Longitudinal Weld, 240° Azimuth, 22.5° Neutron Pad results at the 30° location are bounded by the Intermediate Shell Basemetal values at the 45° location.

Table 6-4

Relative Radial Distribution Of Neutron Fluence (E > 1.0 MeV) Within The Reactor Vessel Wall

RADIUS (cm)	AZIMUTHAL ANGLE			
	0°	15°	30°	45°
220.350	1.000	1.000	1.000	1.000
225.868	0.563	0.559	0.553	0.550
231.385	0.277	0.272	0.268	0.264
236.903	0.131	0.127	0.125	0.122
242.420	0.063	0.058	0.057	0.055

Note:
Base Metal Inner Radius = 220.350 cm
Base Metal 1/4T = 225.868 cm
Base Metal 1/2T = 231.385 cm
Base Metal 3/4T = 236.903 cm
Base Metal Outer Radius = 242.420 cm

Table 6-5

Relative Radial Distribution Of Iron Atom Displacements (dpa) Within The Reactor Vessel Wall

RADIUS (cm)	AZIMUTHAL ANGLE			
	0°	15°	30°	45°
220.350	1.000	1.000	1.000	1.000
225.868	0.639	0.633	0.632	0.642
231.385	0.389	0.380	0.381	0.393
236.903	0.236	0.227	0.229	0.236
242.420	0.143	0.129	0.130	0.134

Note:
Base Metal Inner Radius = 220.350 cm
Base Metal 1/4T = 225.868 cm
Base Metal 1/2T = 231.385 cm
Base Metal 3/4T = 236.903 cm
Base Metal Outer Radius = 242.420 cm

Table 6-6

Calculated Fast Neutron Exposure of Surveillance Capsules
Withdrawn from South Texas Project Unit 1

Capsule	Irradiation Time [EFPY]	Fluence (E > 1.0 MeV) [n/cm^2]	Iron Displacements [dpa]
U	0.78	2.58E+18	5.05E-03
Y	4.90	1.29E+19	2.52E-02
V	11.13	2.62E+19	5.08E-02

Table 6-7

Calculated Surveillance Capsule Lead Factors

Capsule ID And Location	Status	Lead Factor
U (31.5° dual)	Withdrawn EOC 1	3.59
Y (29° dual)	Withdrawn EOC 6	3.28
V (29° dual)	Withdrawn EOC 11	3.04
X (31.5° dual)	In Reactor	3.28
W (31.5° single)	In Reactor	3.24
Z (31.5° single)	In Reactor	3.24

Note: Lead factors for capsules remaining in the reactor are based on cycle specific exposure calculations through the current operating fuel reload, i.e., Cycle 12.

7 SURVEILLANCE CAPSULE REMOVAL SCHEDULE

The following surveillance capsule removal schedule meets the requirements of ASTM E185-82 and is recommended for future capsules to be removed from the South Texas Unit 1 reactor vessel. This recommended removal schedule is applicable to 34 EFPY of operation.

Table 7-1 Recommended Surveillance Capsule Withdrawal Schedule

Capsule	Capsule Location	Lead Factor [a]	Withdrawal EFPY [b]	Fluence (n/cm^2) [a]
U	58.5°	3.59	0.78	2.58×10^{18} (c)
Y	241°	3.28	4.90	1.29×10^{19} (c)
V	61°	3.04	11.13	2.62×10^{19} (c)
X	238.5°	3.28	Standby	(d)
W	121.5°	3.24	Standby	(d)
Z	301.5°	3.24	Standby	(d)

Notes:

(a) Updated in Capsule V dosimetry analysis.

(b) Effective Full Power Years (EFPY) from plant startup.

(c) Plant specific evaluation.

(d) Section XI.M31, "Reactor Vessel Surveillance," of NUREG-1801 states that any surveillance capsules that are left in the reactor vessel should provide meaningful metallurgical data. The NRC specifically states that anything beyond 60 years of exposure is not meaningful metallurgical data. Hence, it is recommended that Capsules "X", "W" and "Z" be removed at 16 EFPY (3.86×10^{19} n/cm^2, E > 1.0 MeV, i.e., the peak 54 EFPY fluence) and placed in storage. In the event that South Texas Unit 1 obtains license renewal approval for an additional 20 years (i.e., 54 EFPY) then Capsule "X" should be tested instead of placed in storage.

8 REFERENCES

1. Regulatory Guide 1.99, Revision 2, *Radiation Embrittlement of Reactor Vessel Materials,* U.S. Nuclear Regulatory Commission, May, 1988.

2. Code of Federal Regulations, 10CFR50, Appendix G, *Fracture Toughness Requirements*, and Appendix H, *Reactor Vessel Material Surveillance Program Requirements*, U.S. Nuclear Regulatory Commission, Washington, D.C.

3. WCAP-14847, *Analysis of Capsule Y from the Houston Lighting and Power Company South Texas Unit 1 Reactor Vessel Radiation Surveillance Program*, E. Terek, et. al., dated April 1997.

4. WCAP-9492, *South Texas Utilities South Texas Project Unit No. 1 Reactor Vessel Radiation Surveillance Program*, W.T. Kaiser, et. al., dated June 1979.

5. WCAP-12629, *Analysis of Capsule U from the Houston Lighting and Power Company South Texas Unit 1 Reactor Vessel Radiation Surveillance Program*, E. Terek, et. al., dated August 1990.

6. ASTM E208, *Standard Test Method for Conducting Drop-Weight Test to Determine Nil-Ductility Transition Temperature of Ferritic Steels*, in ASTM Standards, Section 3, American Society for Testing and Materials, Philadelphia, PA.

7. Section XI of the ASME Boiler and Pressure Vessel Code, Appendix G, *Fracture Toughness Criteria for Protection Against Failure*

8. ASTM E185-82, *Standard Practice for Conducting Surveillance Tests for Light-Water Cooled Nuclear Power Reactor Vessels,* in ASTM Standards, Section 3, American Society for Testing and Materials, Philadelphia, PA.

9. Procedure RMF 8402, *Surveillance Capsule Testing Program*, Revision 2.

10. Procedure RMF 8102, *Tensile Testing*, Revision 1.

11. Procedure RMF 8103, *Charpy Impact Testing*, Revision 1.

12. ASTM E23-98, *Standard Test Method for Notched Bar Impact Testing of Metallic Materials*, in ASTM Standards, Section 3, American Society for Testing and Materials, Philadelphia, PA, 1998.

13. ASTM A370-97a, *Standard Test Methods and Definitions for Mechanical Testing of Steel Products*, in ASTM Standards, Section 3, American Society for Testing and Materials, Philadelphia, PA, 1997.

14. ASTM E8-99, *Standard Test Methods for Tension Testing of Metallic Materials*, in ASTM Standards, Section 3, American Society for Testing and Materials, Philadelphia, PA, 1999.

15. ASTM E21-92 (1998), *Standard Test Methods for Elevated Temperature Tension Tests of Metallic Materials*, in ASTM Standards, Section 3, American Society for Testing and Materials, Philadelphia, PA, 1998.

16. ASTM E83-93, *Standard Practice for Verification and Classification of Extensometers*, in ASTM Standards, Section 3, American Society for Testing and Materials, Philadelphia, PA, 1993.

17. ASTM E185-79, *Standard Practice for Conducting Surveillance Tests for Light-Water Cooled Nuclear Power Reactor Vessels*

18. WCAP-14370, *Use of the Hyperbolic Tangent Function for Fitting Transition Temperature Toughness Data*, T. R. Mager, et al, May 1995.

19. Regulatory Guide RG-1.190, *Calculational and Dosimetry Methods for Determining Pressure Vessel Neutron Fluence*, U. S. Nuclear Regulatory Commission, Office of Nuclear Regulatory Research, March 2001.

20. WCAP-14040-NP-A, Revision 2, *Methodology Used to Develop Cold Overpressure Mitigating System Setpoints and RCS Heatup and Cooldown Limit Curves*, January 1996.

21. WCAP-15557, Revision 0, *Qualification of the Westinghouse Pressure Vessel Neutron Fluence Evaluation Methodology*, August 2000.

22. RSICC Computer Code Collection CCC-650, *DOORS 3.1, One, Two- and Three-Dimensional Discrete Ordinates Neutron/Photon Transport Code System*, August 1996.

23. RSIC Data Library Collection DLC-185, "BUGLE-96, Coupled 47 Neutron, 20 Gamma-Ray Group Cross Section Library Derived from ENDF/B-VI for LWR Shielding and Pressure Vessel Dosimetry Applications," March 1996.

APPENDIX A

VALIDATION OF THE RADIATION TRANSPORT MODELS BASED ON NEUTRON DOSIMETRY MEASUREMENTS

A.1 Neutron Dosimetry

Comparisons of measured dosimetry results to both the calculated and least squares adjusted values for all surveillance capsules withdrawn from service to date at South Texas Project Unit 1 are described herein. The sensor sets from these capsules have been analyzed in accordance with the current dosimetry evaluation methodology described in Regulatory Guide 1.190, "Calculational and Dosimetry Methods for Determining Pressure Vessel Neutron Fluence."[A-1] One of the main purposes for presenting this material is to demonstrate that the overall measurements agree with the calculated and least squares adjusted values to within ± 20% as specified by Regulatory Guide 1.190, thus serving to validate the calculated neutron exposures previously reported in Section 6.2 of this report. This information may also be useful in the future, in particular, as least squares adjustment techniques become accepted in the regulatory environment.

A.1.1 Sensor Reaction Rate Determinations

In this section, the results of the evaluations of the three neutron sensor sets withdrawn to date as part of the South Texas Project Unit 1 Reactor Vessel Materials Surveillance Program are presented. The capsule designation, location within the reactor, and time of withdrawal of each of these dosimetry sets were as follows:

Capsule ID	Azimuthal Location	Withdrawal Time	Irradiation Time [EFPY]
U	31.5° dual	End of Cycle 1	0.78
Y	29° dual	End of Cycle 6	4.90
V	29° dual	End of Cycle 11	11.13

The azimuthal locations included in the above tabulation represent the first octant equivalent azimuthal angle of the geometric center of the respective surveillance capsules.

The passive neutron sensors included in the evaluations of Survillance Capsules U, Y, and V are summarized as follows:

Sensor Material	Reaction Of Interest	Capsule U	Capsule Y	Capsule V
Copper	$^{63}Cu(n,\alpha)^{60}Co$	X	X	X
Iron	$^{54}Fe(n,p)^{54}Mn$	X	X	X
Nickel	$^{58}Ni(n,p)^{58}Co$	X	X	X
Uranium-238	$^{238}U(n,f)^{137}Cs$	X	X	X
Neptunium-237	$^{237}Np(n,f)^{137}Cs$	X	X	X
Cobalt-Aluminum*	$^{59}Co(n,\gamma)^{60}Co$	X	X	X

* The cobalt-aluminum measurements for this plant include both bare wire and cadmium-covered sensors.

Since all of the dosimetry monitors were accommodated within the dosimeter block centered at the radial, azimuthal, and axial center of the material test specimen array, gradient corrections were not required for these reaction rates. Pertinent physical and nuclear characteristics of the passive neutron sensors are listed in Table A-1.

The use of passive monitors such as those listed above does not yield a direct measure of the energy dependent neutron flux at the point of interest. Rather, the activation or fission process is a measure of the integrated effect that the time and energy dependent neutron flux has on the target material over the course of the irradiation period. An accurate assessment of the average neutron flux level incident on the various monitors may be derived from the activation measurements only if the irradiation parameters are well known. In particular, the following variables are of interest:

- the measured specific activity of each monitor,
- the physical characteristics of each monitor,
- the operating history of the reactor,
- the energy response of each monitor, and
- the neutron energy spectrum at the monitor location.

The radiometric counting of the neutron sensors from Capsule U was carried out by the Westinghouse Analytical Services Laboratory at the Waltz Mill Site.[A-2] The radiometric counting of the sensors from Capsule Y were also performed by the Westinghouse Analytical Services Laboratory[A-3], and the sensors from Capsule V were counted by Pace Analytical Services, Inc., located at the Waltz Mill Site. In all cases, the radiometric counting followed established ASTM procedures. Following sample preparation and weighing, the specific activity of each sensor was determined by means of a high-resolution gamma spectrometer. For the copper, iron, nickel, and cobalt-aluminum sensors, these analyses were performed by direct counting of each of the individual samples. In the case of the uranium and neptunium fission sensors, the analyses were carried out by direct counting preceded by dissolution and chemical separation of cesium from the sensor material.

The irradiation history of the reactor over the irradiation periods experienced by Capsules U, Y, and V was based on the reported monthly power generation of South Texas Project Unit 1 from initial reactor startup through the end of the dosimetry evaluation period. For the sensor sets utilized in the surveillance capsules, the half-lives of the product isotopes are long enough that a monthly histogram describing reactor operation has proven to be an adequate representation for use in radioactive decay corrections for the reactions of interest in the exposure evaluations. The irradiation history applicable to Capsules U, Y, and V is given in Table A-2.

Having the measured specific activities, the physical characteristics of the sensors, and the operating history of the reactor, reaction rates referenced to full-power operation were determined from the following equation:

$$R = \frac{A}{N_0 \, F \, Y \sum \frac{P_j}{P_{ref}} C_j \, [1 - e^{-\lambda t_j}] \, [e^{-\lambda t_d}]}$$

where:

R	=	Reaction rate averaged over the irradiation period and referenced to operation at a core power level of P_{ref} (rps/nucleus).
A	=	Measured specific activity (dps/gm).
N_0	=	Number of target element atoms per gram of sensor.
F	=	Weight fraction of the target isotope in the sensor material.
Y	=	Number of product atoms produced per reaction.
P_j	=	Average core power level during irradiation period j (MW).
P_{ref}	=	Maximum or reference power level of the reactor (MW).
C_j	=	Calculated ratio of $\phi(E > 1.0 \text{ MeV})$ during irradiation period j to the time weighted average $\phi(E > 1.0 \text{ MeV})$ over the entire irradiation period.
λ	=	Decay constant of the product isotope (1/sec).
t_j	=	Length of irradiation period j (sec).
t_d	=	Decay time following irradiation period j (sec).

and the summation is carried out over the total number of monthly intervals comprising the irradiation period.

In the equation describing the reaction rate calculation, the ratio $[P_j]/[P_{ref}]$ accounts for month-by-month variation of reactor core power level within any given fuel cycle as well as over multiple fuel cycles. The ratio C_j, which was calculated for each fuel cycle using the transport methodology discussed in Section 6.2, accounts for the change in sensor reaction rates caused by variations in flux level induced by changes in core spatial power distributions from fuel cycle to fuel cycle. For a single-cycle irradiation, C_j is normally taken to be 1.0. However, for multiple-cycle irradiations, particularly those employing low leakage fuel management, the additional C_j term should be employed. The impact of changing flux levels for constant power operation can be quite significant for sensor sets that have been irradiated for many cycles in a reactor that has transitioned from non-low leakage to low leakage fuel management or for sensor sets contained in surveillance capsules that have been moved from one capsule location to another. The fuel cycle specific neutron flux values along with the computed values for C_j are listed in Table A-3. These flux values represent the cycle dependent results at the radial and azimuthal center of the respective capsules at the axial elevation of the active fuel midplane.

Prior to using the measured reaction rates in the least-squares evaluations of the dosimetry sensor sets, additional corrections were made to the ^{238}U measurements to account for the presence of ^{235}U impurities in the sensors as well as to adjust for the build-in of plutonium isotopes over the course of the irradiation. Corrections were also made to the ^{238}U and ^{237}Np sensor reaction rates to account for gamma ray induced fission reactions that occurred over the course of the capsule irradiations. The correction factors applied to the South Texas Project Unit 1 fission sensor reaction rates are summarized as follows:

Correction	Capsule U	Capsule Y	Capsule V
^{235}U Impurity/Pu Build-in	0.873	0.834	0.789
$^{238}U(\gamma,f)$	0.969	0.969	0.969
Net ^{238}U Correction	0.846	0.808	0.765
$^{237}Np(\gamma,f)$	0.991	0.991	0.991

These factors were applied in a multiplicative fashion to the decay corrected uranium and neptunium fission sensor reaction rates.

Results of the sensor reaction rate determinations for Capsules U, Y, and V are given in Table A-4. In Table A-4, the measured specific activities, decay corrected saturated specific activities, and computed reaction rates for each sensor indexed to the radial center of the capsule are listed. The fission sensor reaction rates are listed both with and without the applied corrections for ^{238}U impurities, plutonium build-in, and gamma ray induced fission effects.

A.1.2 Least Squares Evaluation of Sensor Sets

Least squares adjustment methods provide the capability of combining the measurement data with the corresponding neutron transport calculations resulting in a Best Estimate neutron energy spectrum with associated uncertainties. Best Estimates for key exposure parameters such as $\phi(E > 1.0\ \text{MeV})$ or dpa/s along with their uncertainties are then easily obtained from the adjusted spectrum. In general, the least squares methods, as applied to surveillance capsule dosimetry evaluations, act to reconcile the measured sensor reaction rate data, dosimetry reaction cross-sections, and the calculated neutron energy spectrum within their respective uncertainties. For example,

$$R_i \pm \delta_{R_i} = \sum_g (\sigma_{ig} \pm \delta_{\sigma_{ig}})(\phi_g \pm \delta_{\phi_g})$$

relates a set of measured reaction rates, R_i, to a single neutron spectrum, ϕ_g, through the multigroup dosimeter reaction cross-section, σ_{ig}, each with an uncertainty δ. The primary objective of the least squares evaluation is to produce unbiased estimates of the neutron exposure parameters at the location of the measurement.

For the least squares evaluation of the South Texas Project Unit 1 surveillance capsule dosimetry, the FERRET code[A-4] was employed to combine the results of the plant specific neutron transport calculations and sensor set reaction rate measurements to determine best-estimate values of exposure parameters ($\phi(E > 1.0\ \text{MeV})$ and dpa) along with associated uncertainties for the three in-vessel capsules withdrawn to date.

The application of the least squares methodology requires the following input:

1 - The calculated neutron energy spectrum and associated uncertainties at the measurement location.

2 - The measured reaction rates and associated uncertainty for each sensor contained in the multiple foil set.

3 - The energy dependent dosimetry reaction cross-sections and associated uncertainties for each sensor contained in the multiple foil sensor set.

For the South Texas Project Unit 1 application, the calculated neutron spectrum was obtained from the results of plant specific neutron transport calculations described in Section 6.2 of this report. The sensor reaction rates were derived from the measured specific activities using the procedures described in Section A.1.1. The dosimetry reaction cross-sections and uncertainties were obtained from the SNLRML dosimetry cross-section library[A-5]. The SNLRML library is an evaluated dosimetry reaction cross-section compilation recommended for use in LWR evaluations by ASTM Standard E1018, "Application of ASTM Evaluated Cross-Section Data File, Matrix E 706 (IIB)".

The uncertainties associated with the measured reaction rates, dosimetry cross-sections, and calculated neutron spectrum were input to the least squares procedure in the form of variances and covariances. The assignment of the input uncertainties followed the guidance provided in ASTM Standard E 944, "Application of Neutron Spectrum Adjustment Methods in Reactor Surveillance."

The following provides a summary of the uncertainties associated with the least squares evaluation of the South Texas Project Unit 1 surveillance capsule sensor sets.

Reaction Rate Uncertainties

The overall uncertainty associated with the measured reaction rates includes components due to the basic measurement process, irradiation history corrections, and corrections for competing reactions. A high level of accuracy in the reaction rate determinations is assured by utilizing laboratory procedures that conform to the ASTM National Consensus Standards for reaction rate determinations for each sensor type.

After combining all of these uncertainty components, the sensor reaction rates derived from the counting and data evaluation procedures were assigned the following net uncertainties for input to the least squares evaluation:

Reaction	Uncertainty
$^{63}Cu(n,\alpha)^{60}Co$	5%
$^{54}Fe(n,p)^{54}Mn$	5%
$^{58}Ni(n,p)^{58}Co$	5%
$^{238}U(n,f)^{137}Cs$	10%
$^{237}Np(n,f)^{137}Cs$	10%
$^{59}Co(n,\gamma)^{60}Co$	5%

These uncertainties are given at the 1σ level.

Dosimetry Cross-Section Uncertainties

The reaction rate cross-sections used in the least squares evaluations were taken from the SNLRML library. This data library provides reaction cross-sections and associated uncertainties, including covariances, for 66 dosimetry sensors in common use. Both cross-sections and uncertainties are provided in a fine multigroup structure for use in least squares adjustment applications. These cross-sections were compiled from the most recent cross-section evaluations and they have been tested with respect to their accuracy and consistency for least squares evaluations. Further, the library has been empirically tested for use in fission spectra determination as well as in the fluence and energy characterization of 14 MeV neutron sources.

For sensors included in the South Texas Project Unit 1 surveillance program, the following uncertainties in the fission spectrum averaged cross-sections are provided in the SNLRML documentation package.

Reaction	Uncertainty
$^{63}Cu(n,\alpha)^{60}Co$	4.08-4.16%
$^{54}Fe(n,p)^{54}Mn$	3.05-3.11%
$^{58}Ni(n,p)^{58}Co$	4.49-4.56%
$^{238}U(n,f)^{137}Cs$	0.54-0.64%
$^{237}Np(n,f)^{137}Cs$	10.32-10.97%
$^{59}Co(n,\gamma)^{60}Co$	0.79-3.59%

These tabulated ranges provide an indication of the dosimetry cross-section uncertainties associated with the sensor sets used in LWR irradiations.

Calculated Neutron Spectrum

The neutron spectra input to the least squares adjustment procedure were obtained directly from the results of plant specific transport calculations for each surveillance capsule irradiation period and location. The spectrum for each capsule was input in an absolute sense (rather than as simply a relative spectral shape). Therefore, within the constraints of the assigned uncertainties, the calculated data were treated equally with the measurements.

While the uncertainties associated with the reaction rates were obtained from the measurement procedures and counting benchmarks and the dosimetry cross-section uncertainties were supplied directly with the SNLRML library, the uncertainty matrix for the calculated spectrum was constructed from the following relationship:

$$M_{gg'} = R_n^2 + R_g * R_{g'} * P_{gg'}$$

where R_n specifies an overall fractional normalization uncertainty and the fractional uncertainties R_g and $R_{g'}$ specify additional random groupwise uncertainties that are correlated with a correlation matrix given by:

$$P_{gg'} = [1 - \theta]\delta_{gg'} + \theta\, e^{-H}$$

where

$$H = \frac{(g - g')^2}{2\gamma^2}$$

The first term in the correlation matrix equation specifies purely random uncertainties, while the second term describes the short-range correlations over a group range γ (θ specifies the strength of the latter term). The value of δ is 1.0 when g = g', and is 0.0 otherwise.

The set of parameters defining the input covariance matrix for the South Texas Project Unit 1 calculated spectra was as follows:

Flux Normalization Uncertainty (R_n) 15%

Flux Group Uncertainties (R_g, $R_{g'}$)

(E > 0.0055 MeV)	15%
(0.68 eV < E < 0.0055 MeV)	29%
(E < 0.68 eV)	52%

Short Range Correlation (θ)

(E > 0.0055 MeV)	0.9
(0.68 eV < E < 0.0055 MeV)	0.5
(E < 0.68 eV)	0.5

Flux Group Correlation Range (γ)

(E > 0.0055 MeV)	6
(0.68 eV < E < 0.0055 MeV)	3
(E < 0.68 eV)	2

A.1.3 Comparisons of Measurements and Calculations

Results of the least squares evaluations of the dosimetry from the South Texas Project Unit 1 surveillance capsules withdrawn to date are provided in Tables A-5 and A-6. In Table A-5, measured, calculated, and best-estimate values for sensor reaction rates are given for each capsule. Also provided in this tabulation are ratios of the measured reaction rates to both the calculated and least squares adjusted reaction rates. These ratios of M/C and M/BE illustrate the consistency of the fit of the calculated neutron energy spectra to the measured reaction rates both before and after adjustment. In Table A-6, comparison of the calculated and best estimate values of neutron flux (E > 1.0 MeV) and iron atom displacement rate are tabulated along with the BE/C ratios observed for each of the capsules.

The data comparisons provided in Tables A-5 and A-6 show that the adjustments to the calculated spectra are relatively small and well within the assigned uncertainties for the calculated spectra, measured sensor reaction rates, and dosimetry reaction cross-sections. Further, these results indicate that the use of the least squares evaluation results in a reduction in the uncertainties associated with the exposure of the surveillance capsules. From Section 6.4 of this report, it may be noted that the uncertainty associated with the unadjusted calculation of neutron fluence (E > 1.0 MeV) and iron atom displacements at the surveillance capsule locations is specified as 12% at the 1σ level. From Table A-6, it is noted that the corresponding uncertainties associated with the least squares adjusted exposure parameters have been reduced to 6% for neutron flux (E > 1.0 MeV) and 8% for iron atom displacement rate. Again, the uncertainties from the least squares evaluation are at the 1σ level.

Further comparisons of the measurement results with calculations are given in Tables A-7 and A-8. These comparisons are given on two levels. In Table A-7, calculations of individual threshold sensor reaction rates are compared directly with the corresponding measurements. These threshold reaction rate comparisons provide a good evaluation of the accuracy of the fast neutron portion of the calculated energy spectra. In Table A-8, calculations of fast neutron exposure rates in terms of ϕ(E > 1.0 MeV) and dpa/s are compared with the best estimate results obtained from the least squares evaluation of the capsule dosimetry results. These two levels of comparison yield consistent and similar results with all measurement-to-calculation comparisons falling well within the 20% limits specified as the acceptance criteria in Regulatory Guide 1.190.

In the case of the direct comparison of measured and calculated sensor reaction rates, the M/C comparisons for fast neutron reactions range from 0.95–1.21 for the 15 samples included in the data set. The overall average M/C ratio for the entire set of South Texas Project Unit 1 data is 1.07 with an associated standard deviation of 7.2%.

In the comparisons of best estimate and calculated fast neutron exposure parameters, the corresponding BE/C comparisons for the capsule data sets range from 1.01–1.07 for neutron flux (E > 1.0 MeV) and from 1.02 to 1.07 for iron atom displacement rate. The overall average BE/C ratios for neutron flux (E > 1.0 MeV) and iron atom displacement rate are 1.05 with a standard deviation of 3.1% and 1.05 with a standard deviation of 2.7%, respectively.

Based on these comparisons, it is concluded that the calculated fast neutron exposures provided in Section 6.2 of this report are validated for use in the assessment of the condition of the materials comprising the beltline region of the South Texas Project Unit 1 reactor pressure vessel.

Table A-1

Nuclear Parameters Used In The Evaluation Of Neutron Sensors

Monitor Material	Reaction of Interest	Target Atom Fraction	90% Response Range (MeV)	Product Half-life	Fission Yield (%)
Copper	^{63}Cu (n,α)	0.6917	4.9 – 11.9	5.271 y	
Iron	^{54}Fe (n,p)	0.0585	2.1 – 8.5	312.3 d	
Nickel	^{58}Ni (n,p)	0.6808	1.5 – 8.3	70.82 d	
Uranium-238	^{238}U (n,f)	1.0000	1.3 – 6.9	30.07 y	6.02
Neptunium-237	^{237}Np (n,f)	1.0000	0.3 – 3.8	30.07 y	6.17
Cobalt-Aluminum	^{59}Co (n,γ)	0.0015	non-threshold	5.271 y	

Note: The 90% response range is defined such that, in the neutron spectrum characteristic of the South Texas Project Unit 1 surveillance capsules, approximately 90% of the sensor response is due to neutrons in the energy range specified with approximately 5% of the total response due to neutrons with energies below the lower limit and 5% of the total response due to neutrons with energies above the upper limit.

Table A-2

Monthly Thermal Generation During The First Eleven Fuel Cycles
Of The South Texas Project Unit 1 Reactor
(Reactor Power of 3800 MWt through mid-Cycle 11; 3853 MWt thereafter)

Year	Month	Thermal Generation (MWt-hr)	Year	Month	Thermal Generation (MWt-hr)	Year	Month	Thermal Generation (MWt-hr)
1988	3	3439	1991	3	0	1994	3	463078
1988	4	663115	1991	4	1648852	1994	4	2614950
1988	5	41693	1991	5	2827023	1994	5	2735140
1988	6	443688	1991	6	2674129	1994	6	2746591
1988	7	1543286	1991	7	2837649	1994	7	2839115
1988	8	200458	1991	8	2782043	1994	8	2839207
1988	9	1828286	1991	9	2458759	1994	9	2410390
1988	10	1993115	1991	10	1789196	1994	10	2843421
1988	11	2506212	1991	11	2695565	1994	11	2747874
1988	12	2277375	1991	12	2762897	1994	12	2833893
1989	1	1368165	1992	1	2837741	1995	1	2476989
1989	2	0	1992	2	2651777	1995	2	2518396
1989	3	2502364	1992	3	2470851	1995	3	264197
1989	4	2625943	1992	4	1965083	1995	4	1266206
1989	5	2671014	1992	5	2833435	1995	5	2839390
1989	6	2736789	1992	6	2739812	1995	6	2748057
1989	7	2372372	1992	7	2817038	1995	7	2839665
1989	8	313757	1992	8	2728178	1995	8	2650586
1989	9	0	1992	9	1342973	1995	9	2747507
1989	10	783890	1992	10	0	1995	10	2843604
1989	11	2728544	1992	11	0	1995	11	2733949
1989	12	1761072	1992	12	49285	1995	12	2394967
1990	1	2526182	1993	1	1765744	1996	1	2783050
1990	2	2561818	1993	2	309269	1996	2	2644490
1990	3	2614217	1993	3	0	1996	3	2659793
1990	4	0	1993	4	0	1996	4	2731768
1990	5	0	1993	5	0	1996	5	1540167
1990	6	357271	1993	6	0	1996	6	1797096
1990	7	2091044	1993	7	0	1996	7	2827109
1990	8	2615866	1993	8	0	1996	8	2827200
1990	9	2174774	1993	9	0	1996	9	2736000
1990	10	1901324	1993	10	0	1996	10	2831030
1990	11	2157277	1993	11	0	1996	11	2734450
1990	12	0	1993	12	0	1996	12	2827200
1991	1	0	1994	1	0	1997	1	2591813
1991	2	0	1994	2	82814	1997	2	2553600

Table A-2 cont'd

Monthly Thermal Generation During The First Eleven Fuel Cycles
Of The South Texas Project Unit 1 Reactor
(Reactor Power of 3800 MWt through mid-Cycle 11; 3853 MWt thereafter)

Year	Month	Thermal Generation (MWt-hr)	Year	Month	Thermal Generation (MWt-hr)	Year	Month	Thermal Generation (MWt-hr)
1997	3	2824646	1999	4	82354	2001	4	2731805
1997	4	2589442	1999	5	2699976	2001	5	2826653
1997	5	2827109	1999	6	2560622	2001	6	2735179
1997	6	2504990	1999	7	2827109	2001	7	2827018
1997	7	2826926	1999	8	2827109	2001	8	2826926
1997	8	2826744	1999	9	2512013	2001	9	2652278
1997	9	1081997	1999	10	2830939	2001	10	735072
1997	10	2170195	1999	11	2735726	2001	11	2736000
1997	11	2324414	1999	12	2826014	2001	12	2827200
1997	12	2826470	2000	1	2825741	2002	1	2827200
1998	1	2826926	2000	2	2538826	2002	2	2548128
1998	2	2553509	2000	3	9	2002	3	2827200
1998	3	2827109	2000	4	0	2002	4	2731440
1998	4	2732078	2000	5	1379765	2002	5	2808960
1998	5	2827109	2000	6	2732534	2002	6	2735088
1998	6	2690400	2000	7	2826835	2002	7	2827200
1998	7	2827200	2000	8	2827109	2002	8	2827200
1998	8	2787528	2000	9	2735726	2002	9	2736000
1998	9	2554147	2000	10	2830848	2002	10	2830848
1998	10	2827474	2000	11	2735818	2002	11	1989984
1998	11	2735818	2000	12	2469514	2002	12	2827200
1998	12	2823643	2001	1	2826562	2003	1	2827200
1999	1	2826926	2001	2	2552779	2003	2	2553600
1999	2	2553144	2001	3	2826653	2003	3	1935264
1999	3	2144659						

Table A-3

Calculated C_j Factors at the Surveillance Capsule Center
Core Midplane Elevation

Fuel. Cycle	$\phi(E > 1.0\ MeV)$ [n/cm^2-s]			C_j		
	Capsule U	Capsule Y	Capsule V	U	Y	V
1	1.05E+11	9.63E+10	9.63E+10	1.000	1.153	1.291
2		7.52E+10	7.52E+10		0.899	1.008
3		8.76E+10	8.76E+10		1.049	1.175
4		8.00E+10	8.00E+10		0.957	1.072
5		8.07E+10	8.07E+10		0.965	1.081
6		8.32E+10	8.32E+10		0.995	1.115
7			7.13E+10			0.955
8			6.50E+10			0.871
9			7.13E+10			0.955
10			6.43E+10			0.862
11			6.79E+10			0.911
Average	1.05E+11	8.36E+10	7.46E+10	1.000	1.000	1.000

Table A-4
Measured Sensor Activities And Reaction Rates

Surveillance Capsule U

Reaction	Location	Measured Activity (dps/g)	Saturated Activity (dps/g)	Radially Adjusted Saturated Activity (dps/g)	Radially Adjusted Reaction Rate (rps/atom)
$^{63}Cu\ (n,\alpha)\ ^{60}Co$	Top	3.63E+04	4.20E+05	4.20E+05	6.40E-17
	Middle	3.55E+04	4.10E+05	4.10E+05	6.26E-17
	Bottom	3.64E+04	4.21E+05	4.21E+05	6.42E-17
	Average				**6.36E-17**
$^{54}Fe\ (n,p)\ ^{54}Mn$	Top	9.06E+05	4.05E+06	4.05E+06	6.42E-15
	Middle	8.69E+05	3.88E+06	3.88E+06	6.16E-15
	Bottom	8.75E+05	3.91E+06	3.91E+06	6.20E-15
	Average				**6.26E-15**
$^{58}Ni\ (n,p)\ ^{58}Co$	Top	2.61E+06	6.05E+07	6.05E+07	8.67E-15
	Middle	2.55E+06	5.91E+07	5.91E+07	8.47E-15
	Bottom	2.44E+06	5.66E+07	5.66E+07	8.10E-15
	Average				**8.41E-15**
$^{238}U\ (n,f)\ ^{137}Cs$ (Cd)	Middle	1.18E+05	6.74E+06	6.74E+06	4.43E-14
$^{238}U\ (n,f)\ ^{137}Cs$ (Cd)		Including ^{235}U, ^{239}Pu, and γ,fission corrections:			**3.74E-14**
$^{237}Np\ (n,f)\ ^{137}Cs$ (Cd)	Middle	1.05E+06	6.00E+07	6.00E+07	3.83E-13
$^{237}Np\ (n,f)\ ^{137}Cs$ (Cd)			Including γ,fission correction:		**3.79E-13**
$^{59}Co\ (n,\gamma)\ ^{60}Co$	Top	8.09E+06	9.35E+07	9.35E+07	6.10E-12
	Top	6.86E+06	7.93E+07	7.93E+07	5.17E-12
	Middle	6.92E+06	8.00E+07	8.00E+07	5.22E-12
	Middle	8.36E+06	9.66E+07	9.66E+07	6.30E-12
	Bottom	7.54E+06	8.71E+07	8.71E+07	5.69E-12
	Bottom	8.61E+06	9.95E+07	9.95E+07	6.49E-12
	Average				**5.83E-12**
$^{59}Co\ (n,\gamma)\ ^{60}Co$ (Cd)	Top	4.20E+06	4.85E+07	4.85E+07	3.17E-12
	Middle	4.33E+06	5.00E+07	5.00E+07	3.27E-12
	Bottom	4.40E+06	5.09E+07	5.09E+07	3.32E-12
	Average				**3.25E-12**

Notes:
1) Measured specific activities are indexed to a counting date of May 31, 1990.
2) The average ^{238}U (n,f) reaction rate of 3.74E-14 includes a correction factor of 0.873 to account for plutonium build-in and an additional factor of 0.969 to account for photo-fission effects in the sensor.
3) The average ^{237}Np (n,f) reaction rate of 3.79E-13 includes a correction factor of 0.991 to account for photo-fission effects in the sensor.

Table A-4 cont'd
Measured Sensor Activities And Reaction Rates

Surveillance Capsule Y

Reaction	Location	Measured Activity (dps/g)	Saturated Activity (dps/g)	Radially Adjusted Saturated Activity (dps/g)	Radially Adjusted Reaction Rate (rps/atom)
$^{63}Cu\ (n,\alpha)\ ^{60}Co$	Top	1.27E+05	3.30E+05	3.30E+05	5.03E-17
	Middle	1.24E+05	3.22E+05	3.22E+05	4.91E-17
	Bottom	1.19E+05	3.09E+05	3.09E+05	4.71E-17
	Average				**4.88E-17**
$^{54}Fe\ (n,p)\ ^{54}Mn$	Top	1.65E+06	3.07E+06	3.07E+06	4.87E-15
	Middle	1.59E+06	2.96E+06	2.96E+06	4.69E-15
	Bottom	1.54E+06	2.86E+06	2.86E+06	4.54E-15
	Average				**4.70E-15**
$^{58}Ni\ (n,p)\ ^{58}Co$	Top	7.99E+06	4.73E+07	4.73E+07	6.78E-15
	Middle	7.64E+06	4.53E+07	4.53E+07	6.48E-15
	Bottom	7.56E+06	4.48E+07	4.48E+07	6.41E-15
	Average				**6.56E-15**
$^{238}U\ (n,f)\ ^{137}Cs$ (Cd)	Middle	5.69E+05	5.56E+06	5.56E+06	3.65E-14
$^{238}U\ (n,f)\ ^{137}Cs$ (Cd)		Including ^{235}U, ^{239}Pu, and γ,fission corrections:			**2.95E-14**
$^{237}Np\ (n,f)\ ^{137}Cs$ (Cd)	Middle	4.50E+06	4.39E+07	4.39E+07	2.80E-13
$^{237}Np\ (n,f)\ ^{137}Cs$ (Cd)			Including γ,fission correction:		**2.78E-13**
$^{59}Co\ (n,\gamma)\ ^{60}Co$	Top	2.31E+07	5.99E+07	5.99E+07	3.91E-12
	Middle	2.08E+07	5.40E+07	5.40E+07	3.52E-12
	Middle	2.41E+07	6.25E+07	6.25E+07	4.08E-12
	Bottom	2.46E+07	6.38E+07	6.38E+07	4.17E-12
	Bottom	2.12E+07	5.50E+07	5.50E+07	3.59E-12
	Average				**3.85E-12**
$^{59}Co\ (n,\gamma)\ ^{60}Co$ (Cd)	Top	1.29E+07	3.35E+07	3.35E+07	2.18E-12
	Middle	1.33E+07	3.45E+07	3.45E+07	2.25E-12
	Bottom	1.35E+07	3.50E+07	3.50E+07	2.29E-12
	Average				**2.24E-12**

Notes: 1) Measured specific activities are indexed to a counting date of November 11, 1996.
2) The average ^{238}U (n,f) reaction rate of 2.95E-14 includes a correction factor of 0.834 to account for plutonium build-in and an additional factor of 0.969 to account for photo-fission effects in the sensor.
3) The average ^{237}Np (n,f) reaction rate of 2.78E-13 includes a correction factor of 0.991 to account for photo-fission effects in the sensor.

Table A-4 cont'd
Measured Sensor Activities And Reaction Rates

Surveillance Capsule V

Reaction	Location	Measured Activity (dps/g)	Saturated Activity (dps/g)	Radially Adjusted Saturated Activity (dps/g)	Radially Adjusted Reaction Rate (rps/atom)
$^{63}Cu\ (n,\alpha)\ ^{60}Co$	Top	1.93E+05	2.92E+05	2.92E+05	4.45E-17
	Middle	1.84E+05	2.78E+05	2.78E+05	4.24E-17
	Bottom	1.77E+05	2.68E+05	2.68E+05	4.08E-17
	Average				**4.26E-17**
$^{54}Fe\ (n,p)\ ^{54}Mn$	Top	2.16E+06	2.94E+06	2.94E+06	4.65E-15
	Middle	2.07E+06	2.81E+06	2.81E+06	4.46E-15
	Bottom	1.99E+06	2.71E+06	2.71E+06	4.29E-15
	Average				**4.47E-15**
$^{58}Ni\ (n,p)\ ^{58}Co$	Top	2.15E+07	4.63E+07	4.63E+07	6.64E-15
	Middle	2.08E+07	4.48E+07	4.48E+07	6.42E-15
	Bottom	1.99E+07	4.29E+07	4.29E+07	6.14E-15
	Average				**6.40E-15**
$^{238}U\ (n,f)\ ^{137}Cs$ (Cd)	Middle	1.21E+06	5.53E+06	5.53E+06	3.63E-14
$^{238}U\ (n,f)\ ^{137}Cs$ (Cd)		Including ^{235}U, ^{239}Pu, and γ,fission corrections:			**2.78E-14**
$^{237}Np\ (n,f)\ ^{137}Cs$ (Cd)	Middle	8.60E+06	3.93E+07	3.93E+07	2.51E-13
$^{237}Np\ (n,f)\ ^{137}Cs$ (Cd)			Including γ,fission correction:		**2.49E-13**
$^{59}Co\ (n,\gamma)\ ^{60}Co$	Top	3.08E+07	4.66E+07	4.66E+07	3.04E-12
	Top	3.59E+07	5.43E+07	5.43E+07	3.54E-12
	Middle	3.14E+07	4.75E+07	4.75E+07	3.10E-12
	Middle	3.72E+07	5.62E+07	5.62E+07	3.67E-12
	Bottom	3.08E+07	4.66E+07	4.66E+07	3.04E-12
	Bottom	3.66E+07	5.53E+07	5.53E+07	3.61E-12
	Average				**3.33E-12**
$^{59}Co\ (n,\gamma)\ ^{60}Co$ (Cd)	Top	1.96E+07	2.96E+07	2.96E+07	1.93E-12
	Middle	2.00E+07	3.02E+07	3.02E+07	1.97E-12
	Bottom	2.03E+07	3.07E+07	3.07E+07	2.00E-12
	Average				**1.97E-12**

Notes:
1) Measured specific activities are indexed to a counting date of May 27, 2003.
2) The average ^{238}U (n,f) reaction rate of 2.78E-14 includes a correction factor of 0.789 to account for plutonium build-in and an additional factor of 0.969 to account for photo-fission effects in the sensor.
3) The average ^{237}Np (n,f) reaction rate of 2.49E-13 includes a correction factor of 0.991 to account for photo-fission effects in the sensor.

Table A-5

Comparison of Measured, Calculated, and Best Estimate
Reaction Rates At The Surveillance Capsule Center

Capsule U

	Reaction Rate [rps/atom]				
Reaction	Measured	Calculated	Best Estimate	M/C	M/BE
$^{63}Cu(n,\alpha)^{60}Co$	6.36E-17	5.27E-17	6.06E-17	1.21	1.05
$^{54}Fe(n,p)^{54}Mn$	6.26E-15	6.04E-15	6.40E-15	1.04	0.98
$^{58}Ni(n,p)^{58}Co$	8.41E-15	8.50E-15	8.86E-15	0.99	0.95
$^{238}U(n,f)^{137}Cs$ (Cd)	3.74E-14	3.31E-14	3.49E-14	1.13	1.07
$^{237}Np(n,f)^{137}Cs$ (Cd)	3.79E-13	3.27E-13	3.62E-13	1.16	1.05
$^{59}Co(n,\gamma)^{60}Co$	5.83E-12	4.59E-12	5.73E-12	1.27	1.02
$^{59}Co(n,\gamma)^{60}Co$ (Cd)	3.25E-12	3.22E-12	3.30E-12	1.01	0.98

Capsule Y

	Reaction Rate [rps/atom]				
Reaction	Measured	Calculated	Best Estimate	M/C	M/BE
$^{63}Cu(n,\alpha)^{60}Co$	4.88E-17	4.39E-17	4.68E-17	1.11	1.04
$^{54}Fe(n,p)^{54}Mn$	4.70E-15	4.90E-15	4.88E-15	0.96	0.96
$^{58}Ni(n,p)^{58}Co$	6.56E-15	6.89E-15	6.81E-15	0.95	0.96
$^{238}U(n,f)^{137}Cs$ (Cd)	2.95E-14	2.66E-14	2.66E-14	1.11	1.11
$^{237}Np(n,f)^{137}Cs$ (Cd)	2.78E-13	2.61E-13	2.70E-13	1.07	1.03
$^{59}Co(n,\gamma)^{60}Co$	3.85E-12	3.57E-12	3.80E-12	1.08	1.01
$^{59}Co(n,\gamma)^{60}Co$ (Cd)	2.24E-12	2.53E-12	2.27E-12	0.89	0.99

Capsule V

	Reaction Rate [rps/atom]				
Reaction	Measured	Calculated	Best Estimate	M/C	M/BE
$^{63}Cu(n,\alpha)^{60}Co$	4.26E-17	4.01E-17	4.20E-17	1.06	1.01
$^{54}Fe(n,p)^{54}Mn$	4.47E-15	4.43E-15	4.59E-15	1.01	0.97
$^{58}Ni(n,p)^{58}Co$	6.40E-15	6.21E-15	6.47E-15	1.03	0.99
$^{238}U(n,f)^{137}Cs$ (Cd)	2.78E-14	2.38E-14	2.52E-14	1.17	1.10
$^{237}Np(n,f)^{137}Cs$ (Cd)	2.49E-13	2.32E-13	2.48E-13	1.07	1.00
$^{59}Co(n,\gamma)^{60}Co$	3.33E-12	3.16E-12	3.29E-12	1.05	1.01
$^{59}Co(n,\gamma)^{60}Co$ (Cd)	1.97E-12	2.24E-12	2.00E-12	0.88	0.99

Table A-6

Comparison of Calculated and Best Estimate Exposure Rates
At The Surveillance Capsule Center

Capsule ID	ϕ(E > 1.0 MeV) [n/cm^2-s]			
	Calculated	Best Estimate	Uncertainty (1σ)	BE/C
U	1.05E+11	1.11E+11	6%	1.06
Y	8.36E+10	8.46E+10	6%	1.01
V	7.46E+10	8.01E+10	6%	1.07

Note: Calculated results are based on the synthesized transport calculations taken at the core midplane following the completion of each respective capsules irradiation period.

Capsule ID	Iron Atom Displacement Rate [dpa/s]			
	Calculated	Best Estimate	Uncertainty (1σ)	BE/C
U	2.04E-10	2.18E-10	8%	1.07
Y	1.63E-10	1.65E-10	8%	1.02
V	1.45E-10	1.53E-10	8%	1.06

Note: Calculated results are based on the synthesized transport calculations taken at the core midplane following the completion of each respective capsules irradiation period.

Table A-7

Comparison of Measured/Calculated (M/C) Sensor Reaction Rate Ratios Including all Fast Neutron Threshold Reactions

Reaction	M/C Ratio		
	Capsule U	Capsule Y	Capsule V
$^{63}Cu(n,\alpha)^{60}Co$	1.21	1.11	1.06
$^{54}Fe(n,p)^{54}Mn$	1.04	0.96	1.01
$^{58}Ni(n,p)^{58}Co$	0.99	0.95	1.03
$^{238}U(n,p)^{137}Cs$ (Cd)	1.13	1.11	1.17
$^{237}Np(n,f)^{137}Cs$ (Cd)	1.16	1.07	1.07
Average	1.10	1.04	1.07
% Standard Deviation	8.1	7.6	5.7

Note: The overall average M/C ratio for the set of 15 sensor measurements is 1.07 with an associated standard deviation of 7.2%.

Table A-8

Comparison of Best Estimate/Calculated (BE/C) Exposure Rate Ratios

Capsule ID	BE/C Ratio	
	$\phi(E > 1.0\ MeV)$	dpa/s
U	1.06	1.07
Y	1.01	1.02
V	1.07	1.06
Average	1.05	1.05
% Standard Deviation	3.1	2.7

Appendix A References

A-1. Regulatory Guide RG-1.190, "Calculational and Dosimetry Methods for Determining Pressure Vessel Neutron Fluence," U. S. Nuclear Regulatory Commission, Office of Nuclear Regulatory Research, March 2001.

A-2. WCAP-12629, Revision 0, "Analysis of Capsule U from the Houston Lighting and Power Company South Texas Unit 1 Reactor Vessel Radiation Surveillance Program," August 1990.

A-3. WCAP-14847, Revision 0, "Analysis of Capsule Y from the Houston Lighting and Power Company South Texas Unit 1 Reactor Vessel Radiation Surveillance Program," April 1997.

A-4. A. Schmittroth, *FERRET Data Analysis Core*, HEDL-TME 79-40, Hanford Engineering Development Laboratory, Richland, WA, September 1979.

A-5. RSIC Data Library Collection DLC-178, "SNLRML Recommended Dosimetry Cross-Section Compendium", July 1994.

APPENDIX B

LOAD-TIME RECORDS FOR CHARPY SPECIMEN TESTS

- Specimen prefix "GL" denotes Intermediate Shell Plate, Longitudinal Orientation
- Specimen prefix "GT" denotes Intermediate Shell Plate, Transverse Orientation
- Specimen prefix "GW" denotes Weld Material
- Specimen prefix "GH" denotes Heat-Affected Zone material
- Load (1) is in units of lbs
- Time (1) is in units of milli seconds

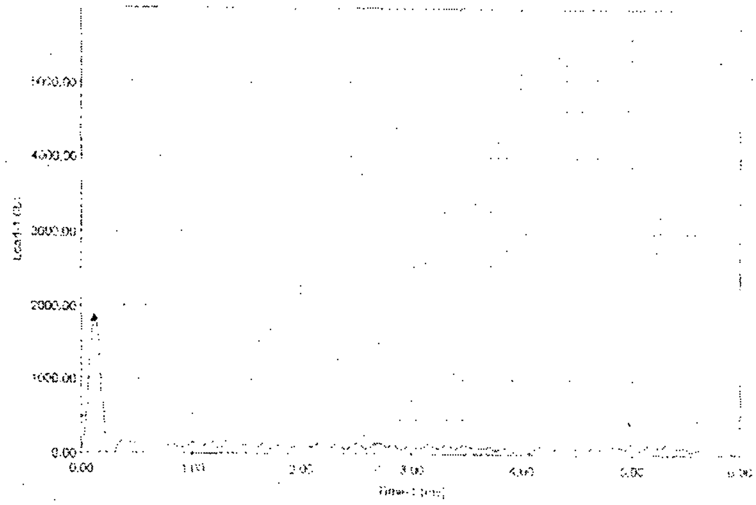

GL29, -75°F

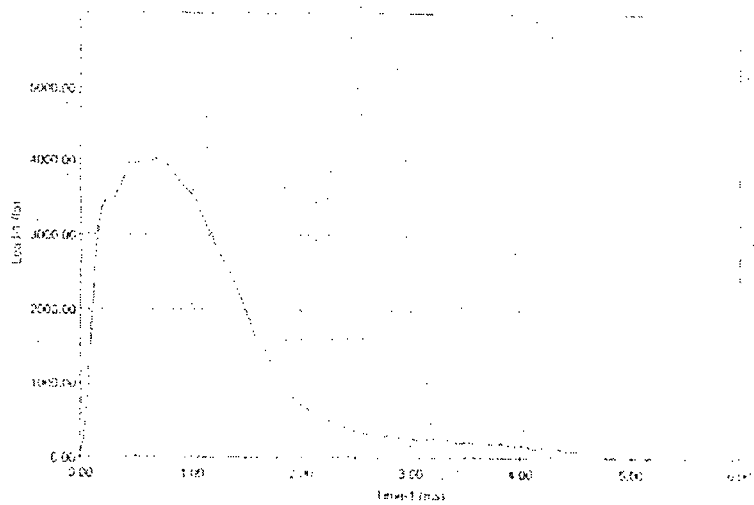

GL16, -25°F

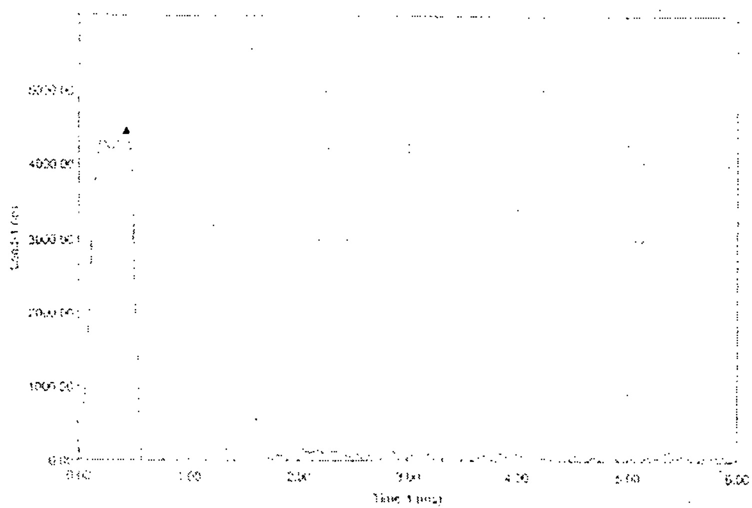

GL21, -25°F

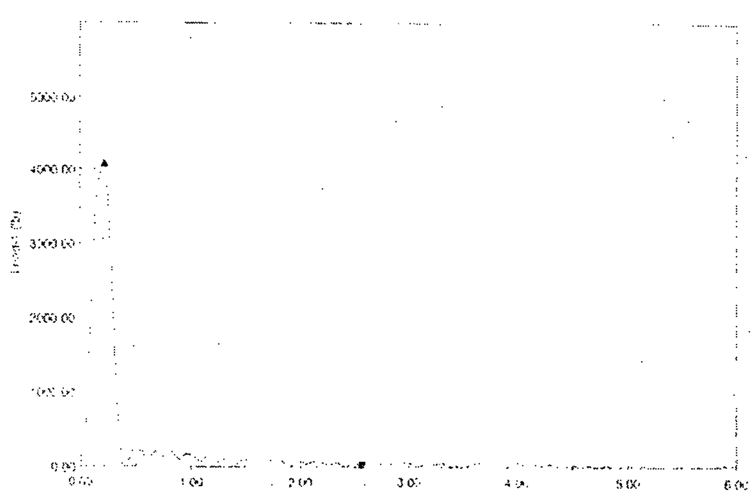

GL17, 0°F

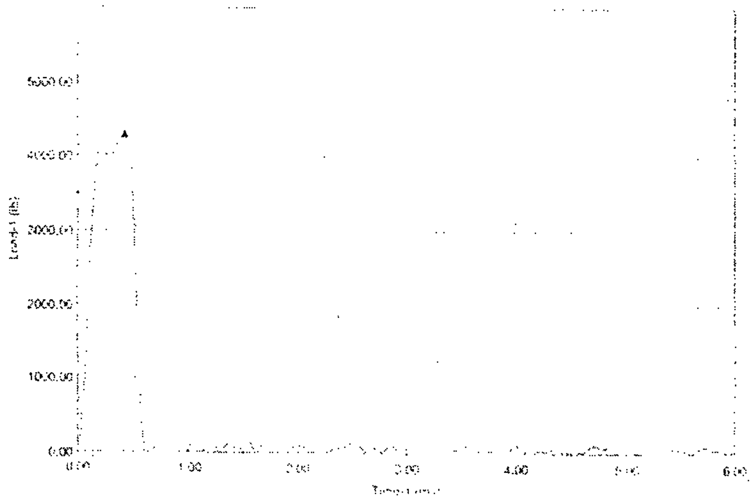

GL24, 10°F

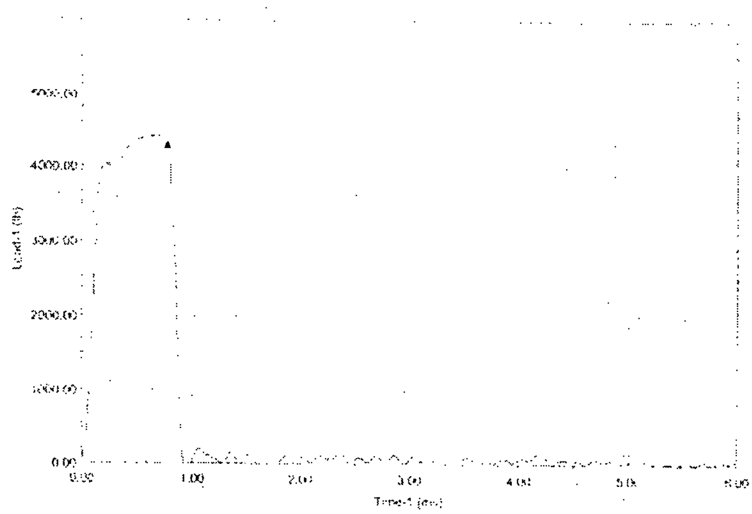

GL23, 25°F

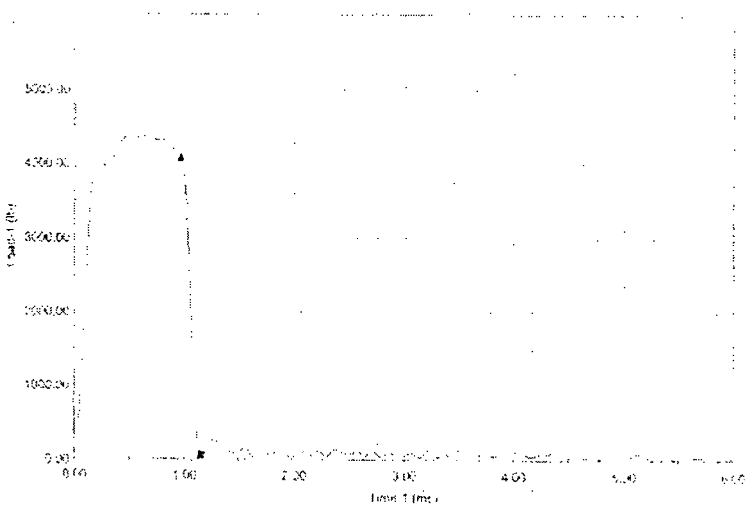

GL18, 30°F

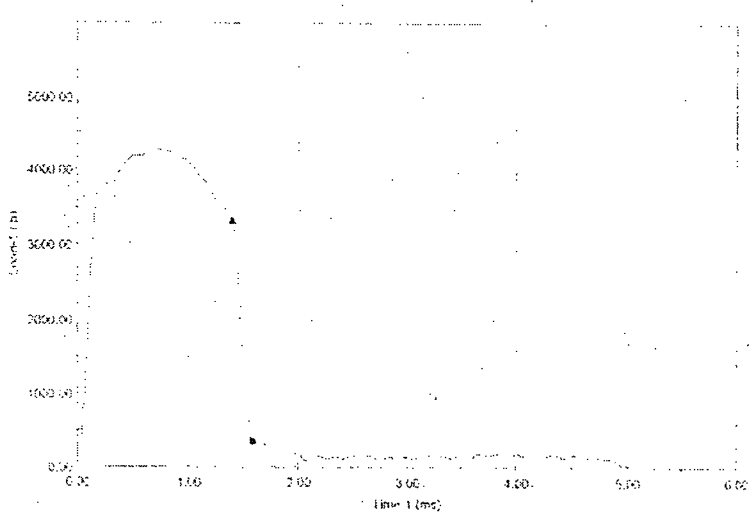

GL19, 50°F

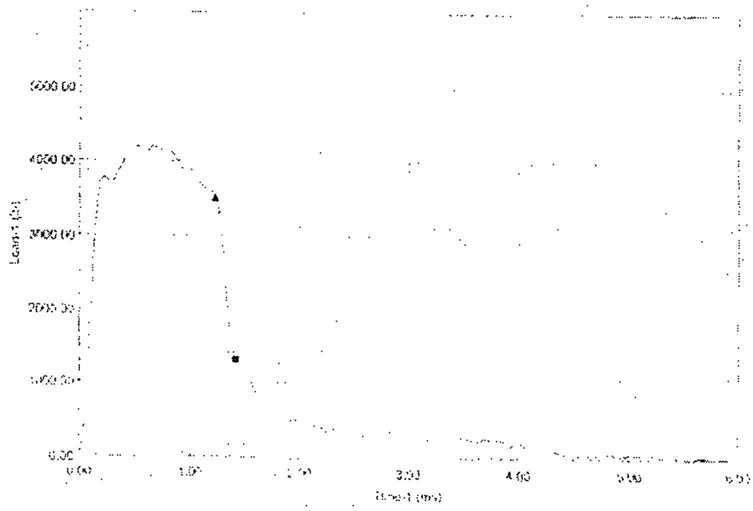

GL25, 100°F

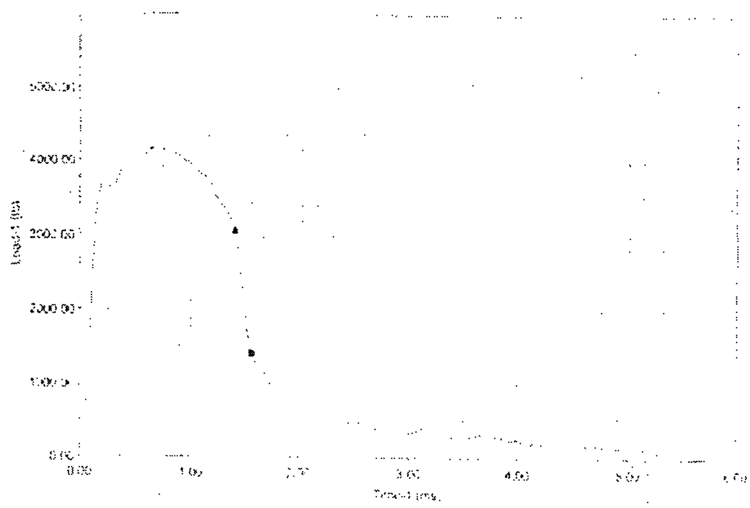

GL20, 125°F

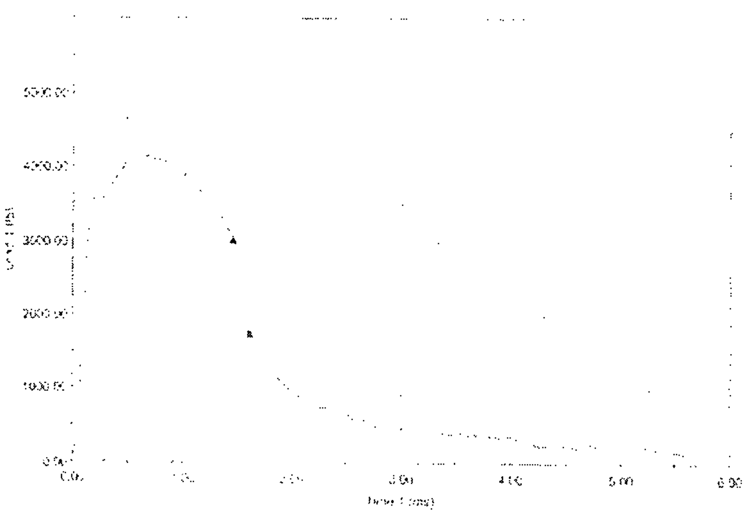

GL27, 150°F

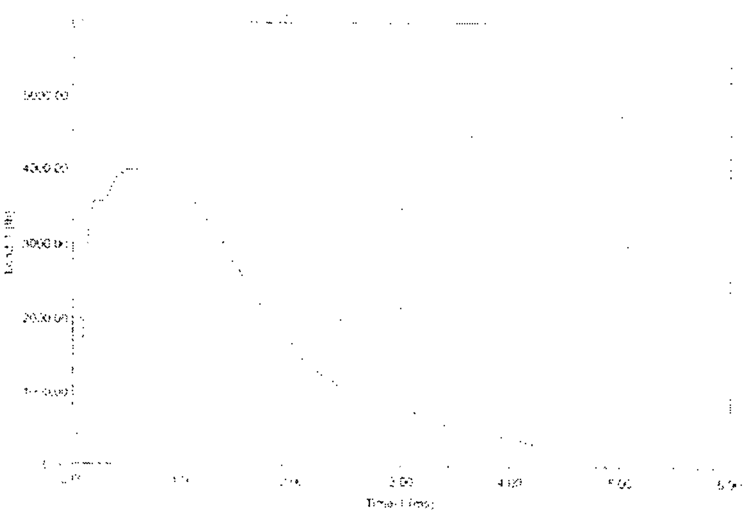

GL22, 175°F

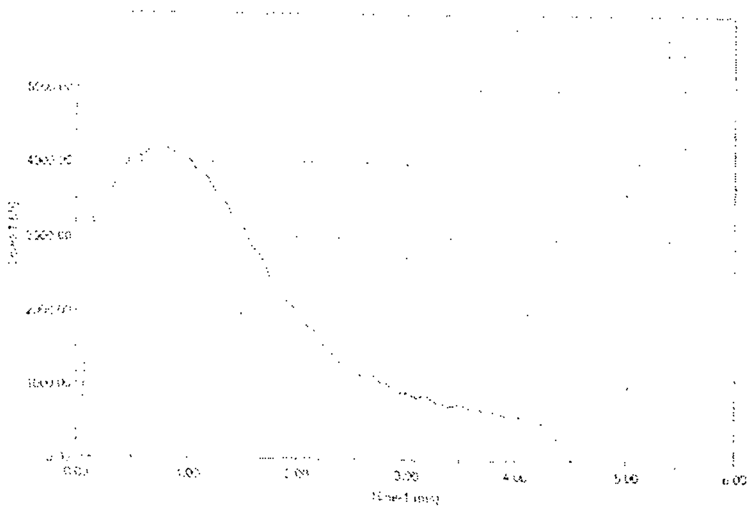

GL30, 225°F

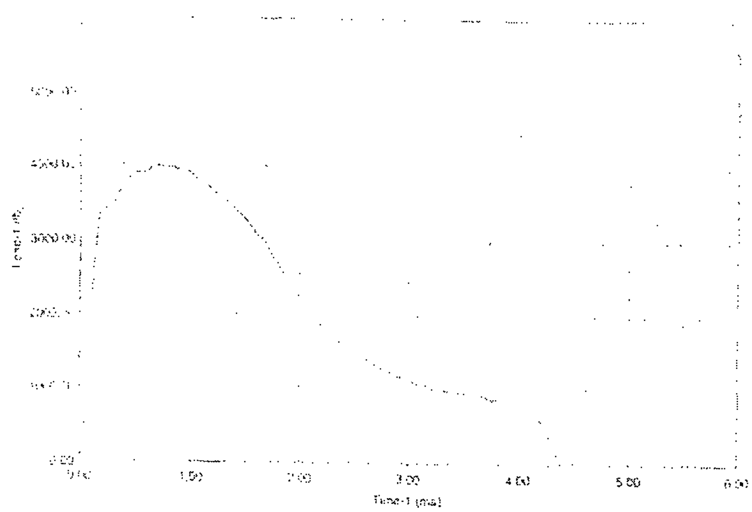

GL28, 250°F

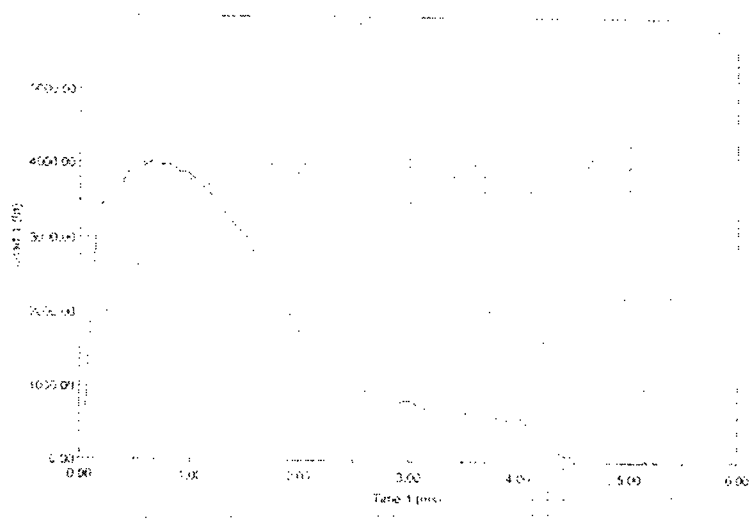

GL26, 250°F

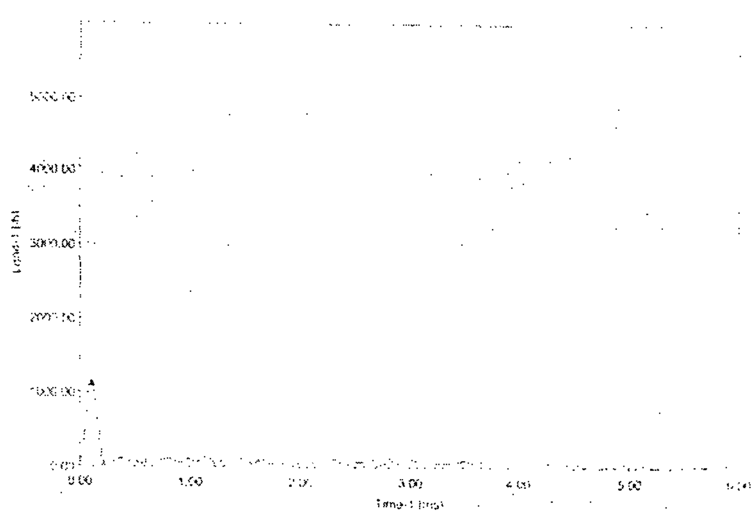

GT28, -100°F

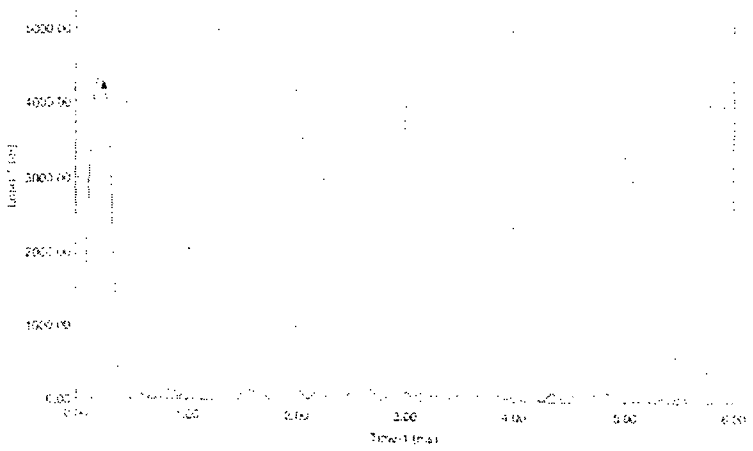

GT25, -50°F

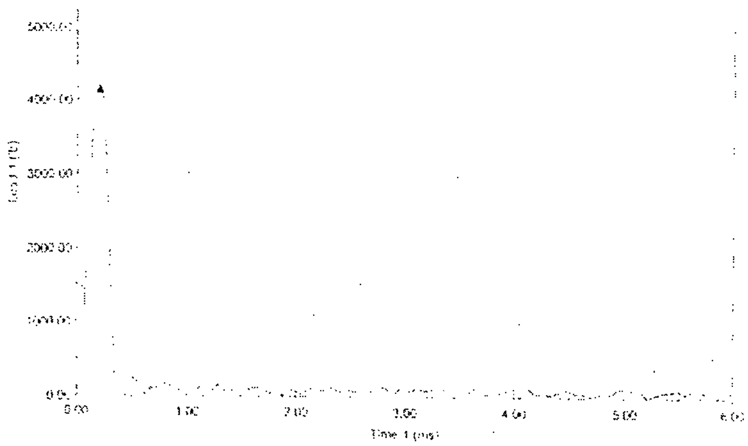

GT21, -25°F

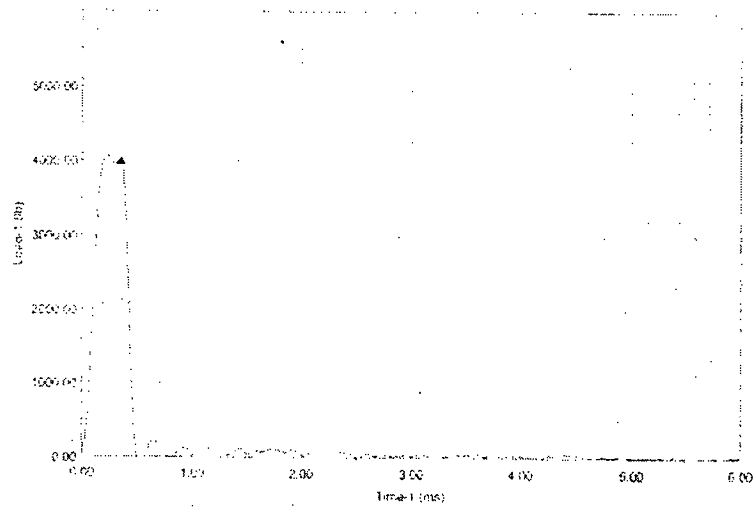

GT20, 0°F

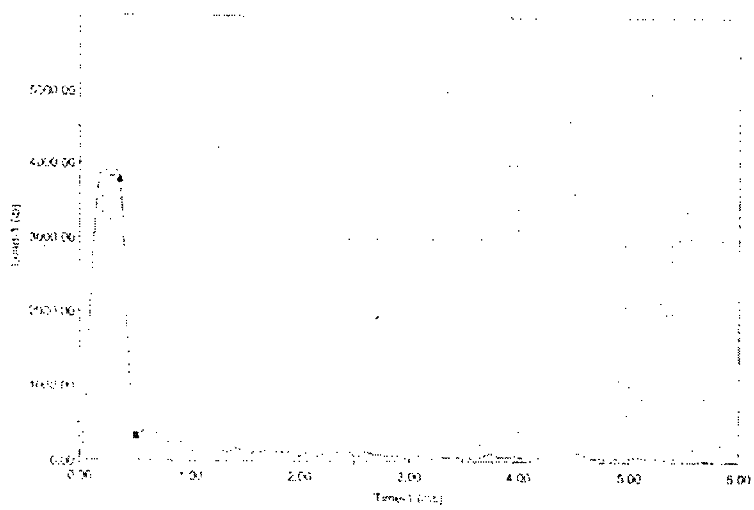

GT30, 25°F

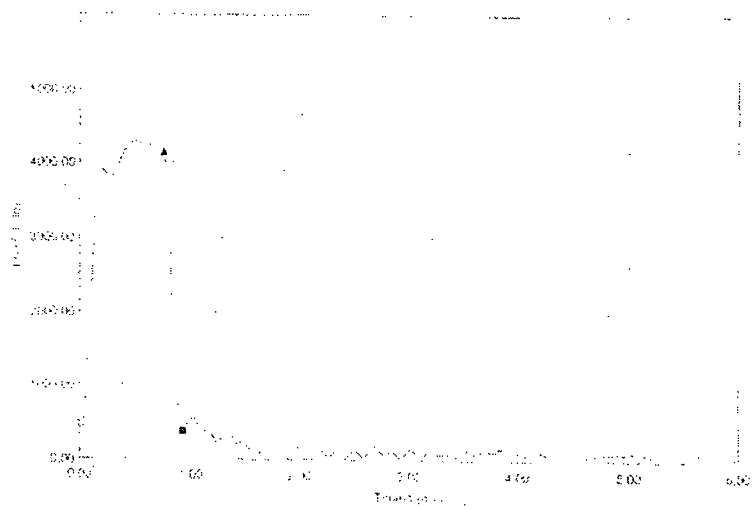

GT22, 40°F

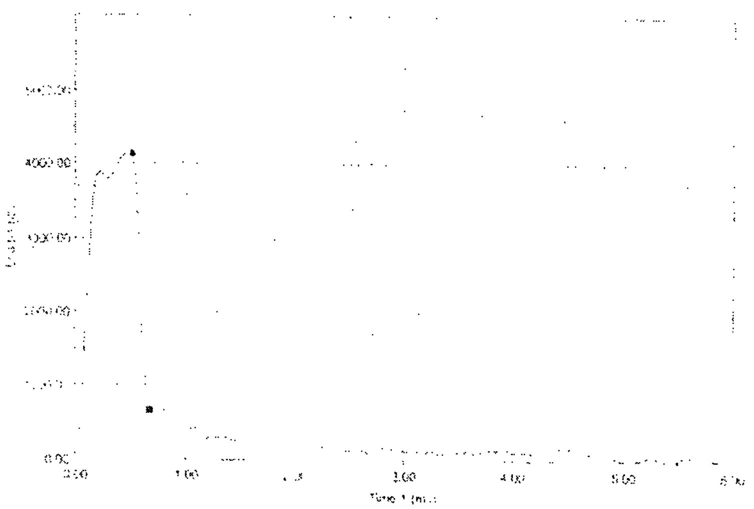

GT24, 50°F

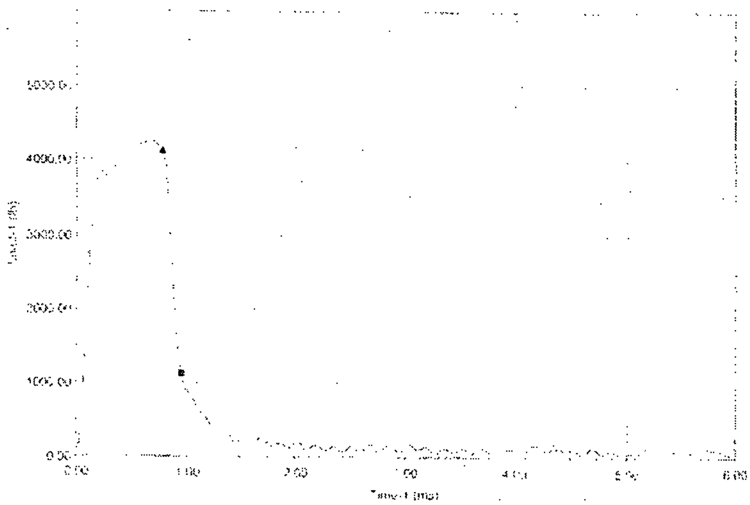

GT29, 75°F

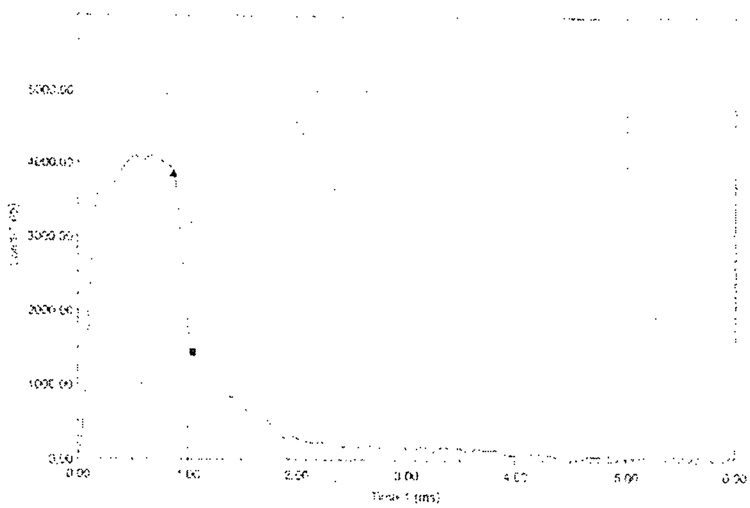

GT26, 100°F

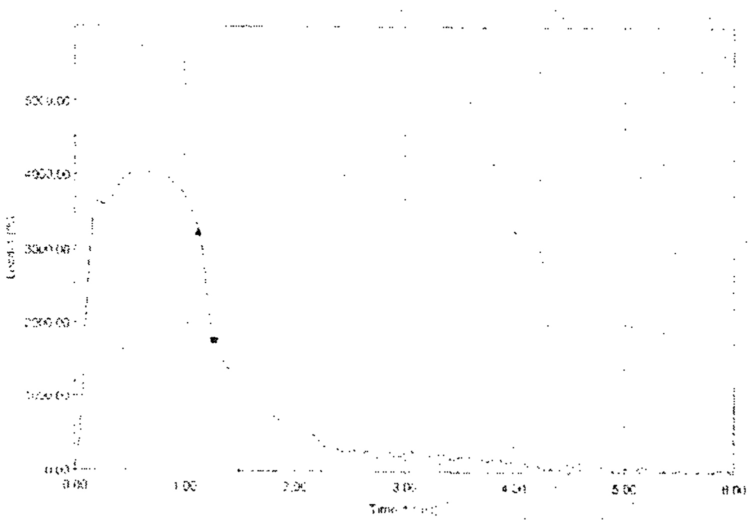

GT27, 125°F

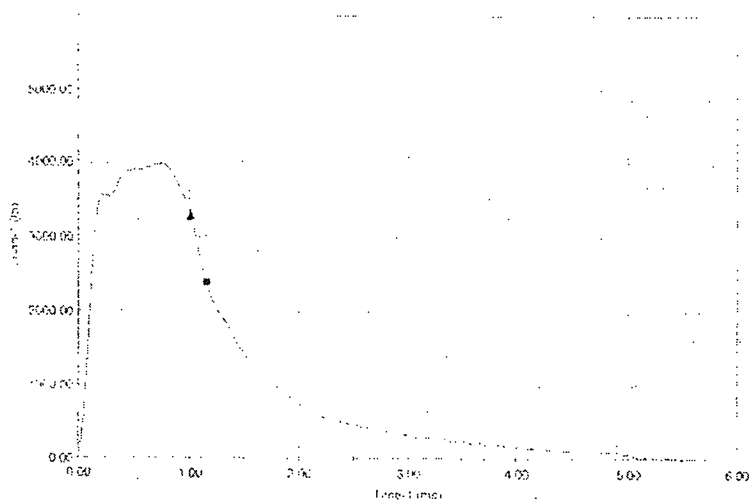

GT17, 150°F

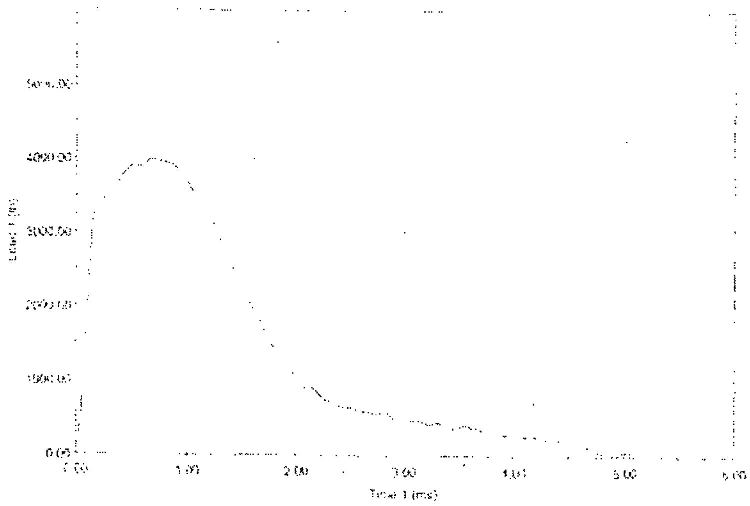

GT18, 200°F

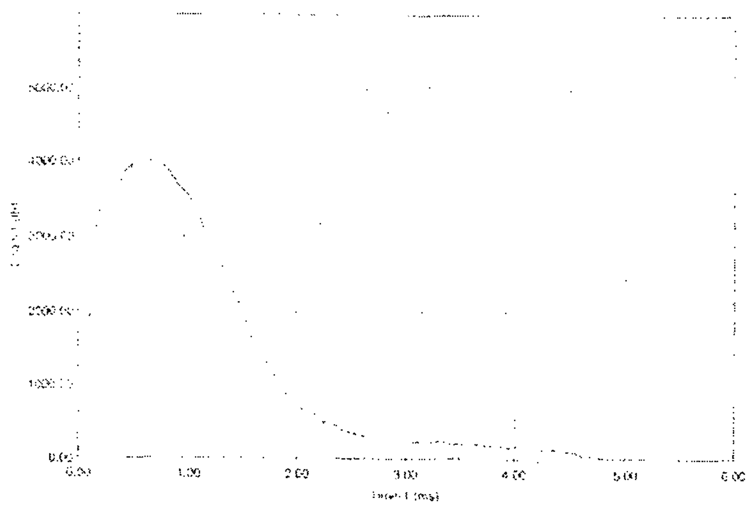

GT16, 225°F

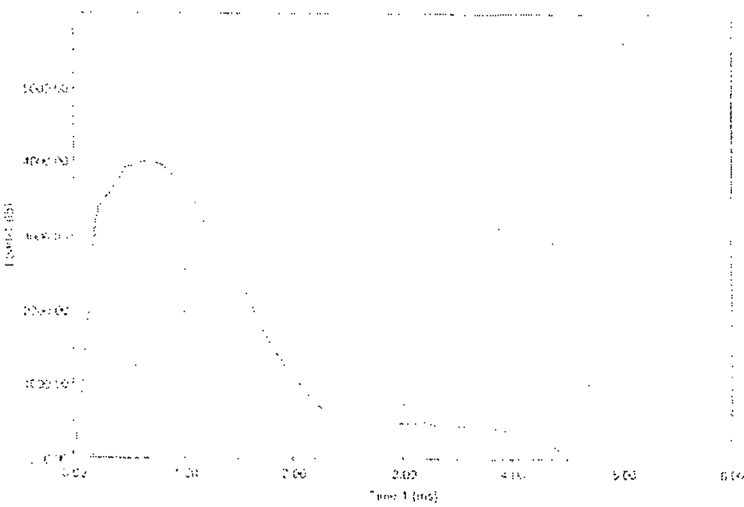

GT19, 250°F

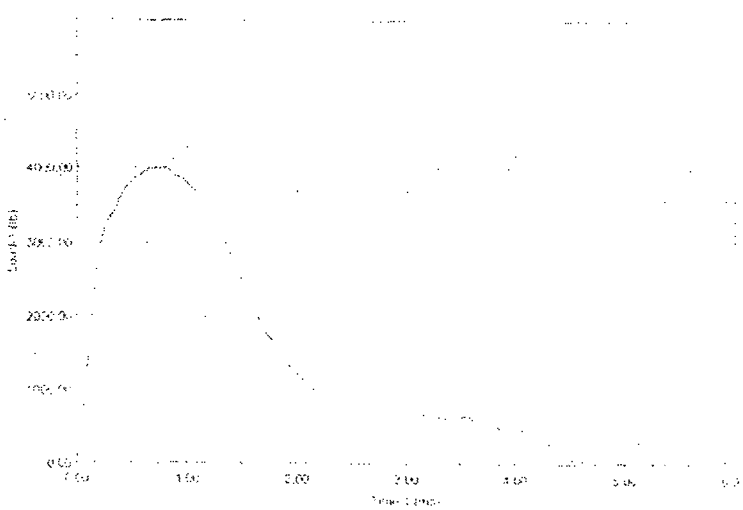

GT23, 260°F

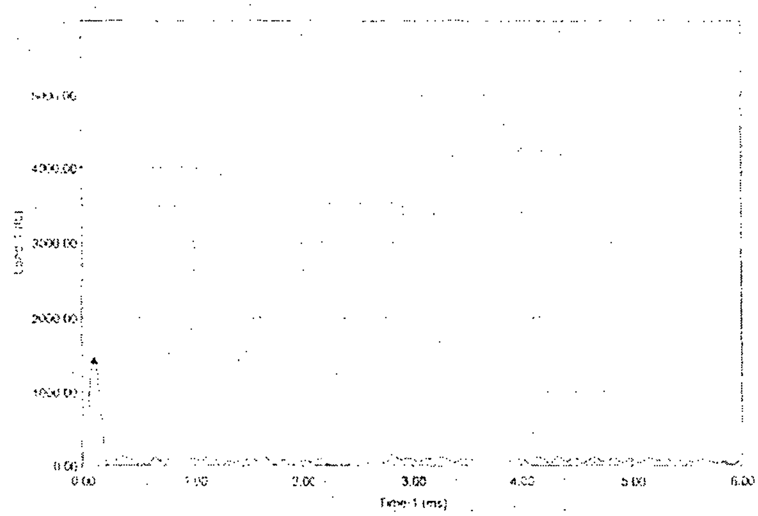

GW16, -125°F

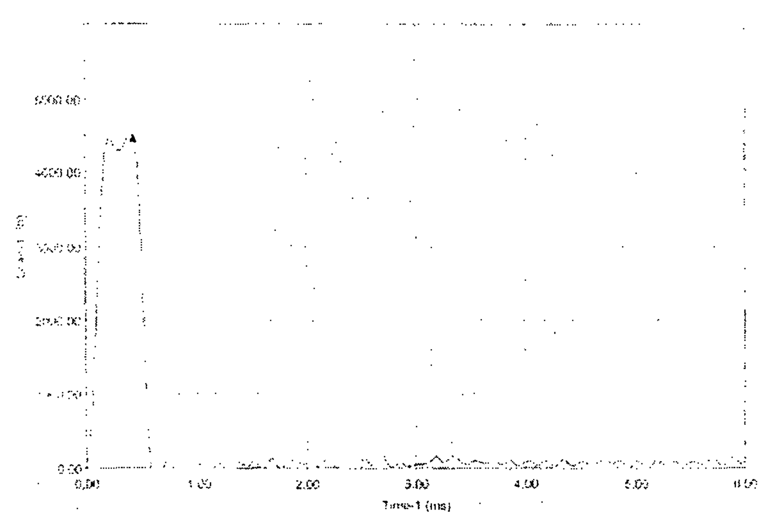

GW17, -75°F

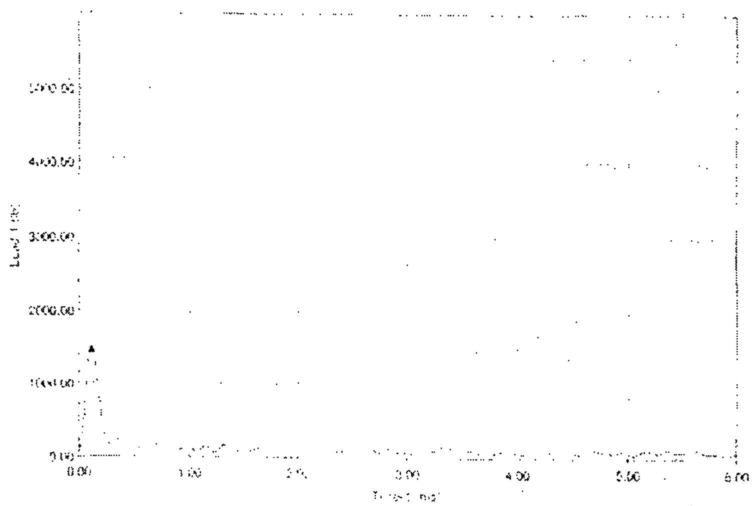

GW25, -75°F

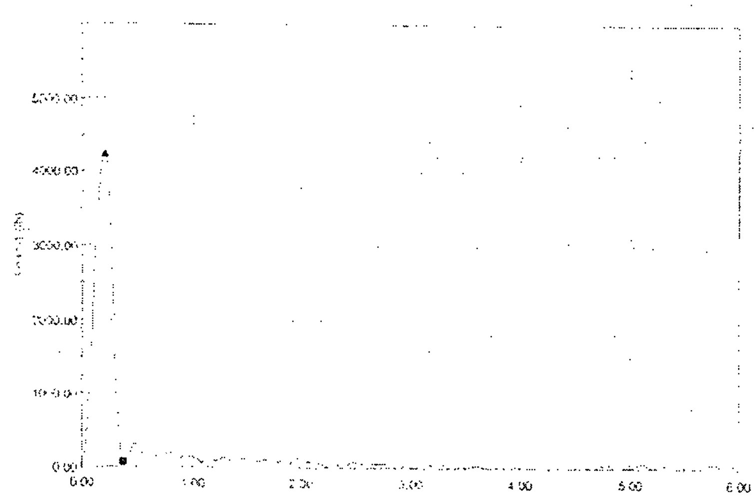

GW26, -50°F

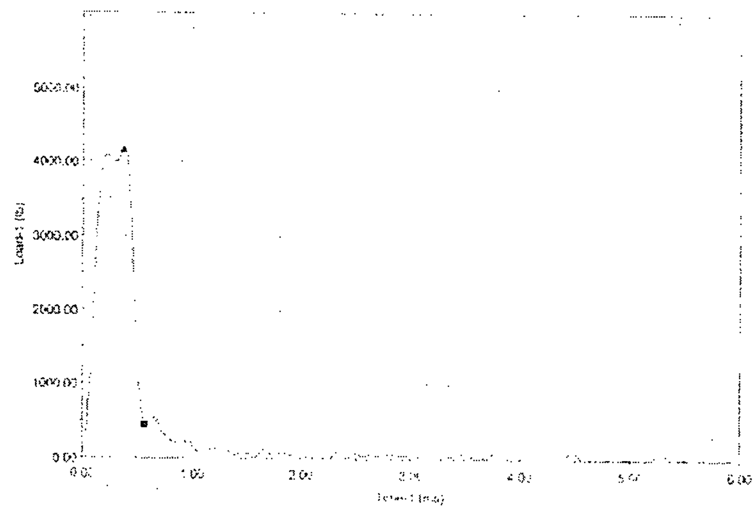

GW19, -25°F

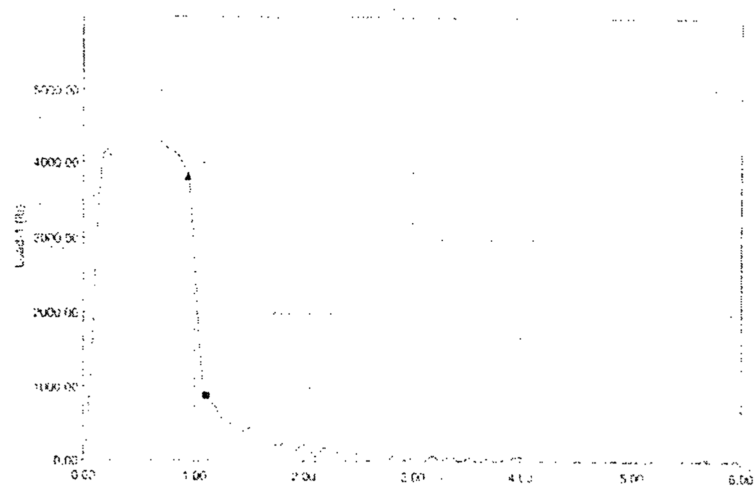

GW28, 0°F

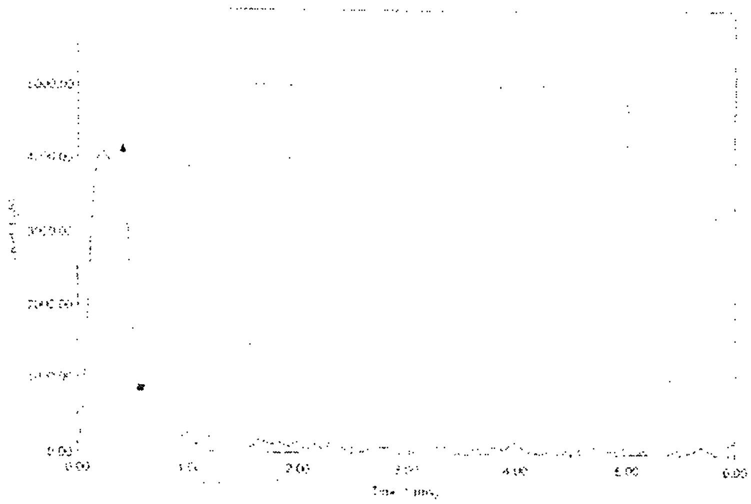

GW27, 0°F

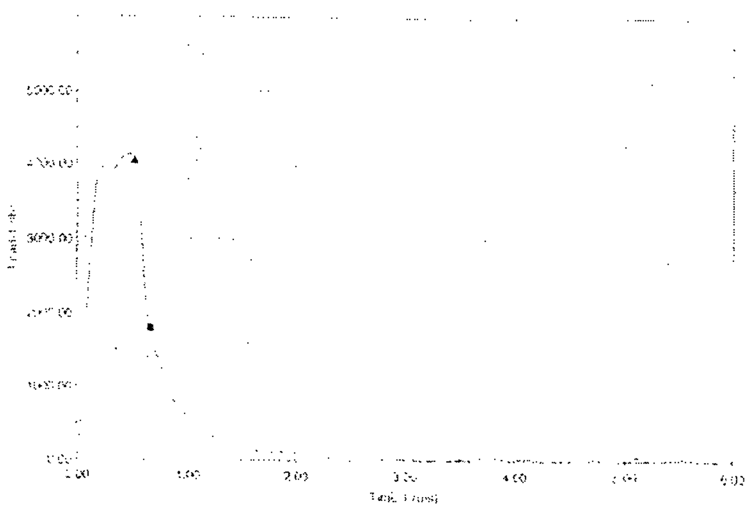

GW20, 25°F

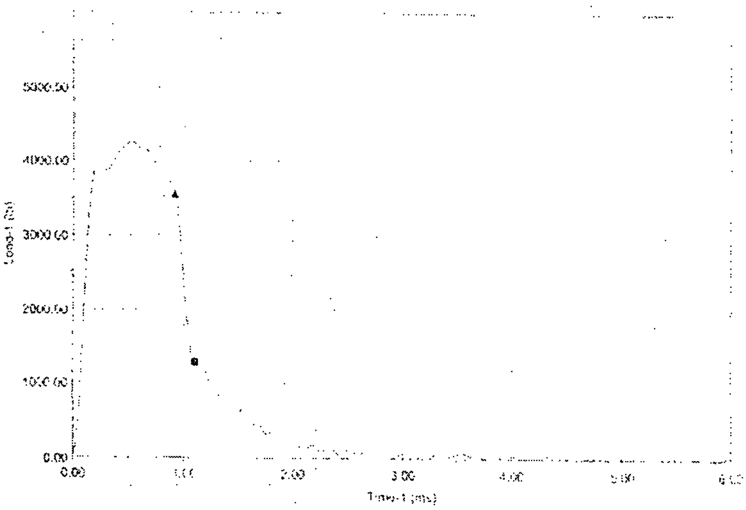

GW24, 50°F

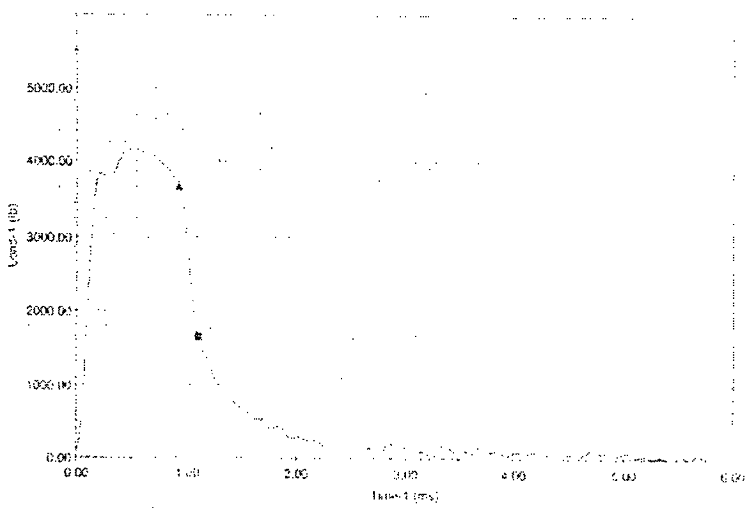

GW22, 75°F

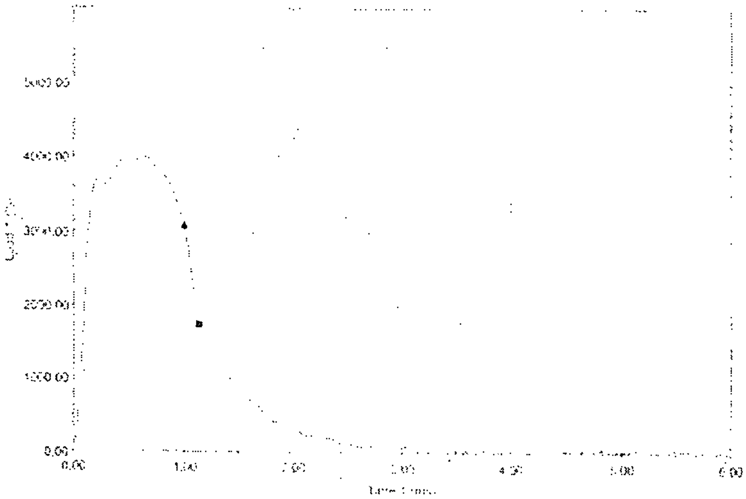

GW29, 100°F

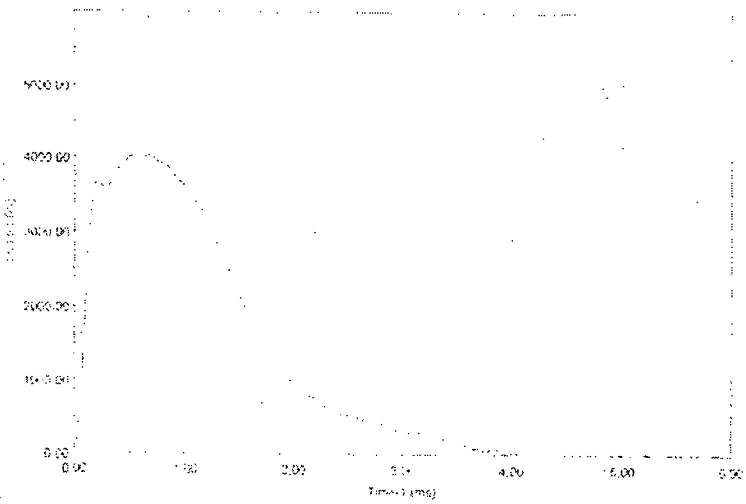

GW21, 150°F

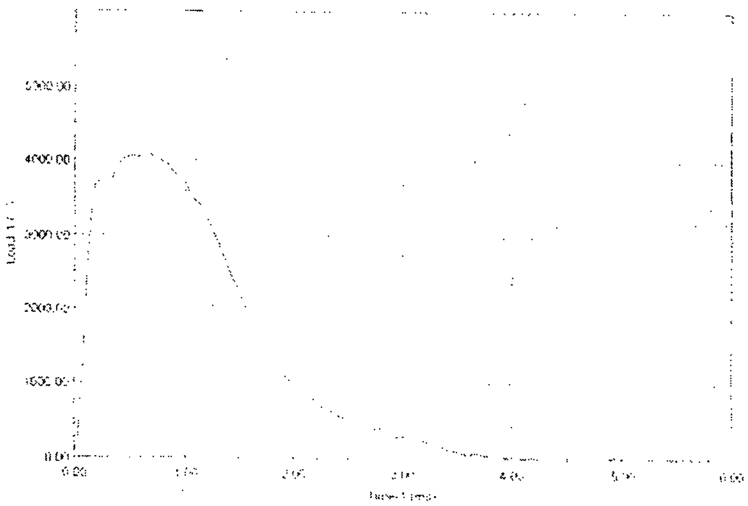

GW18, 175°F

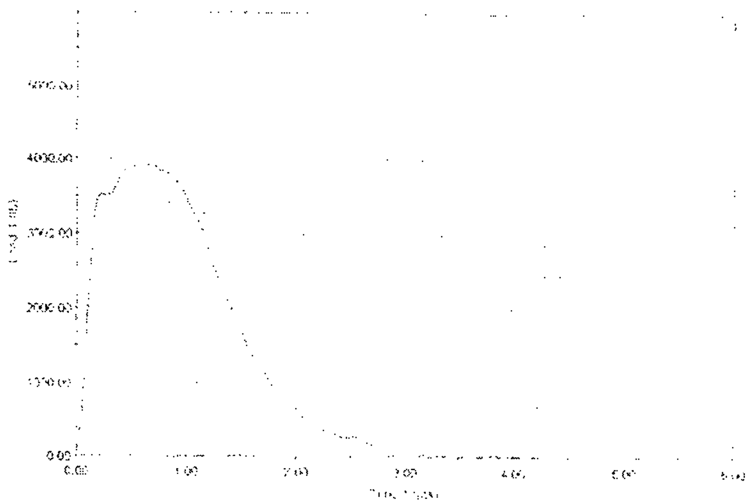

GW23, 200°F

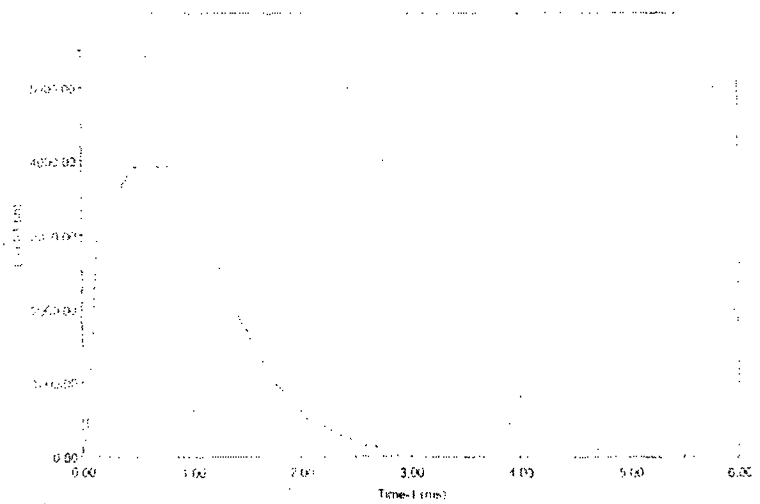

GW30, 200°F

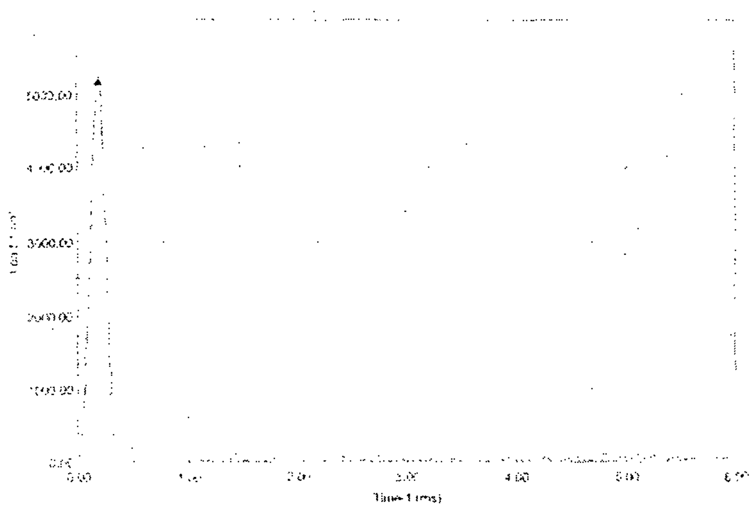

GH22, -150°F

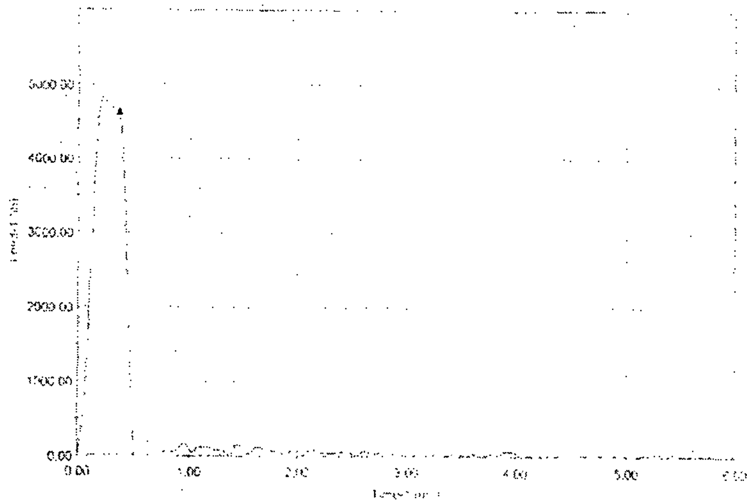

GH30, -75°F

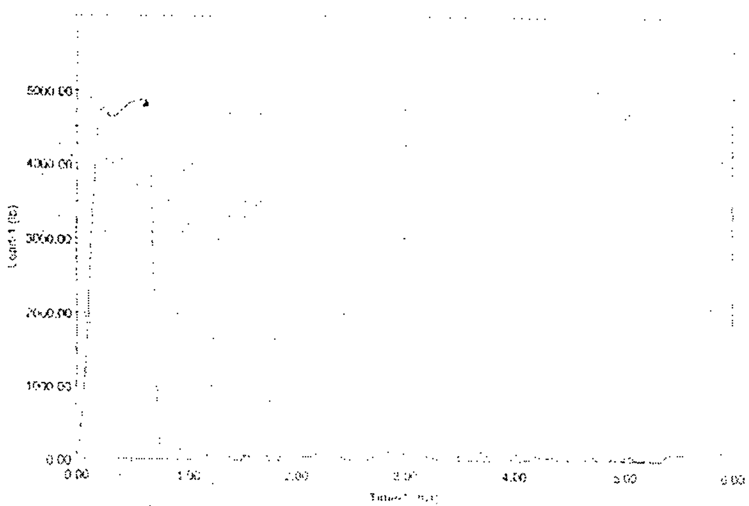

GH28, -50°F

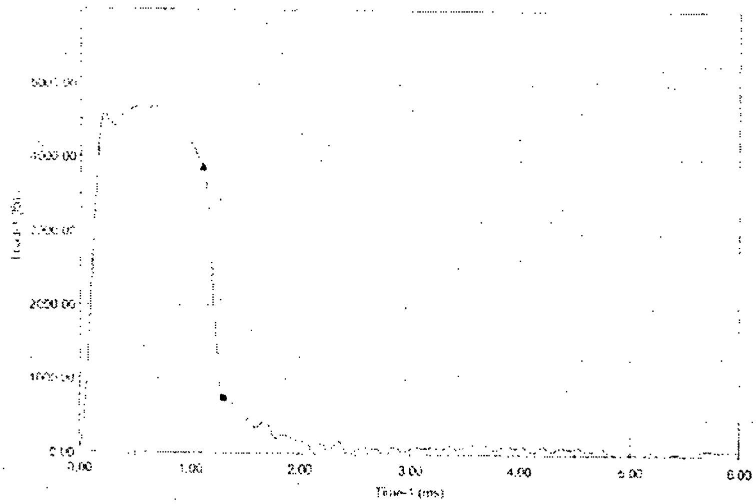

GH18, -25°F

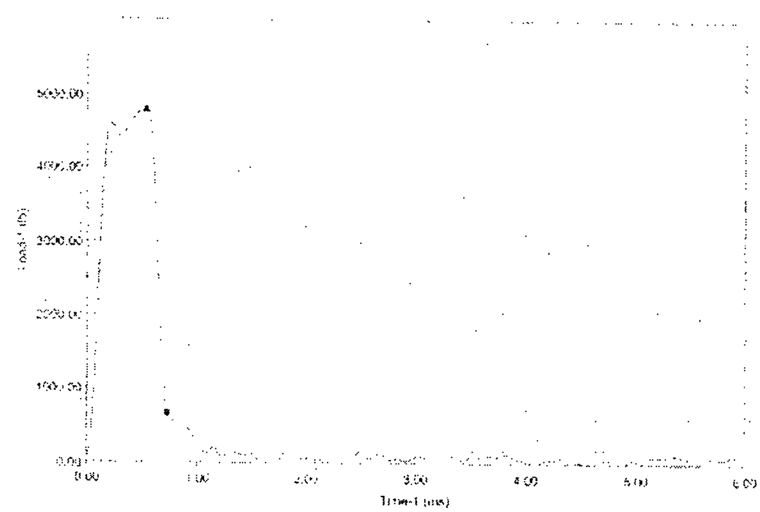

GH20, -25°F

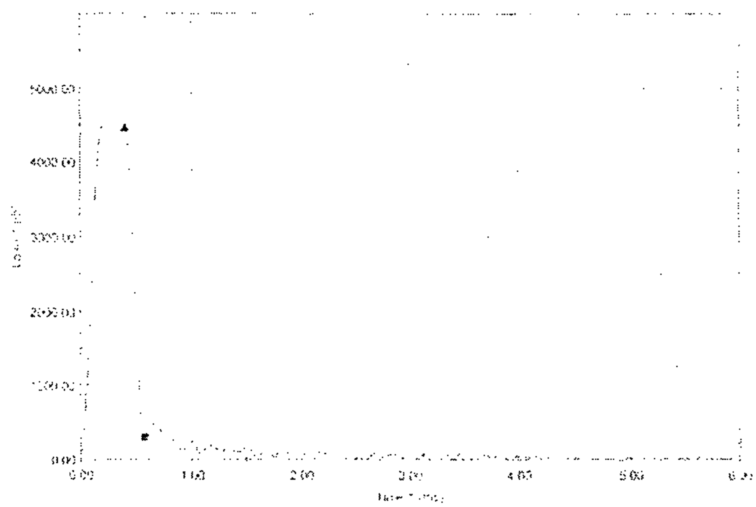

GH16, 0°F

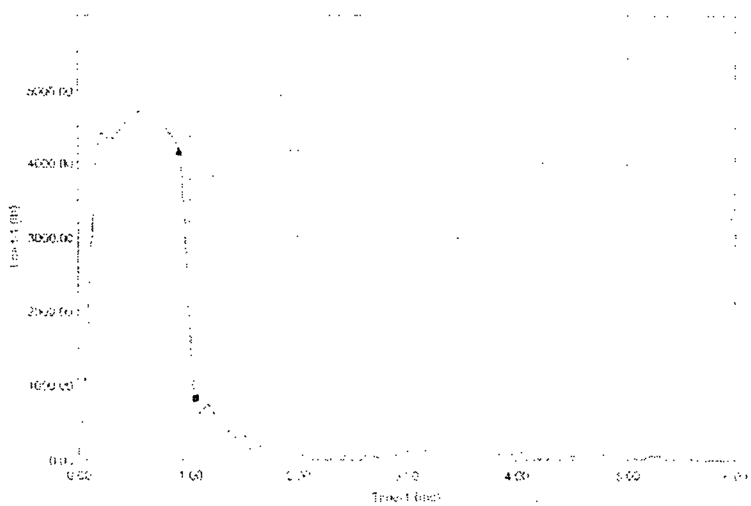

GH21, 10°F

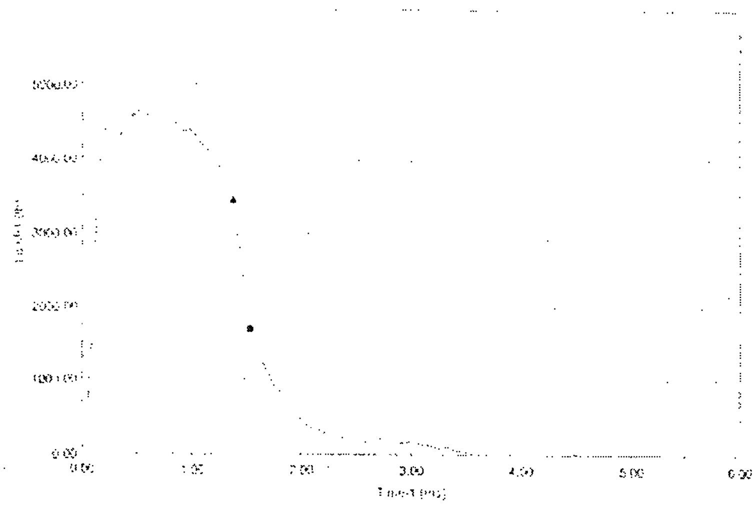

GH24, 25°F

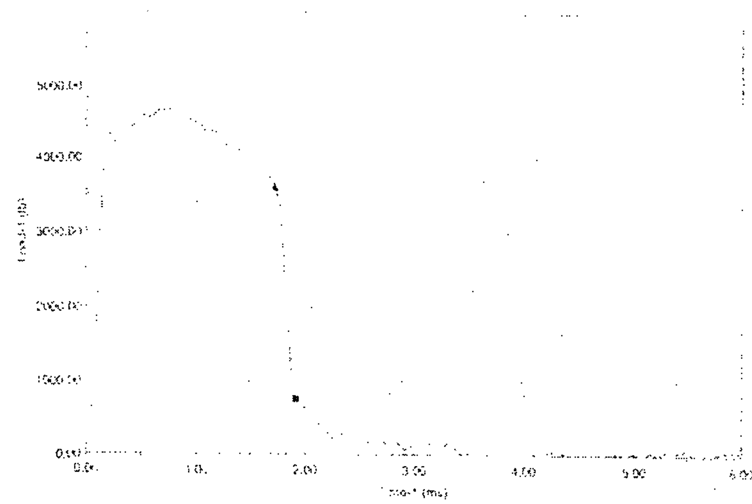

GH26, 25°F

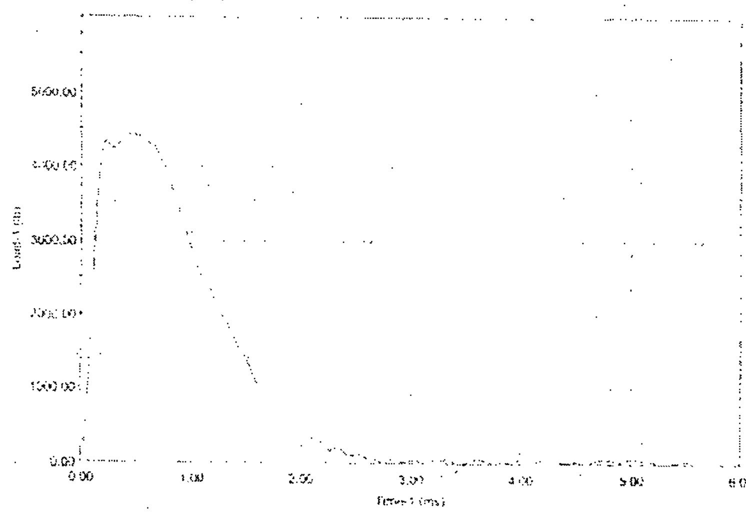

GH17, 40°F

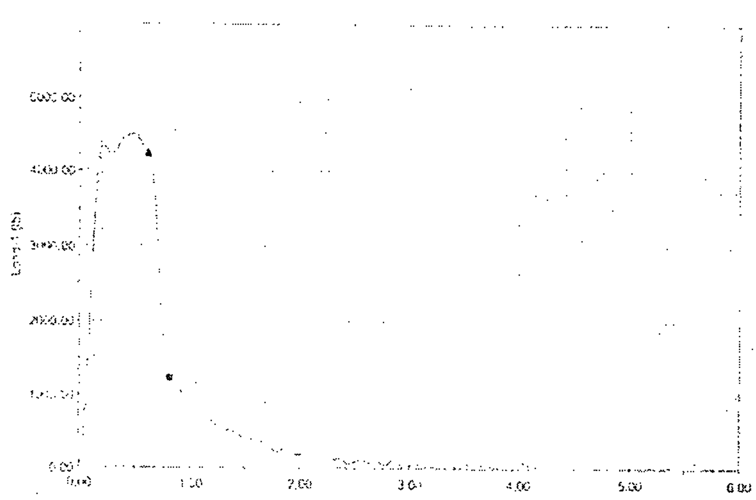

GH23, 50°F

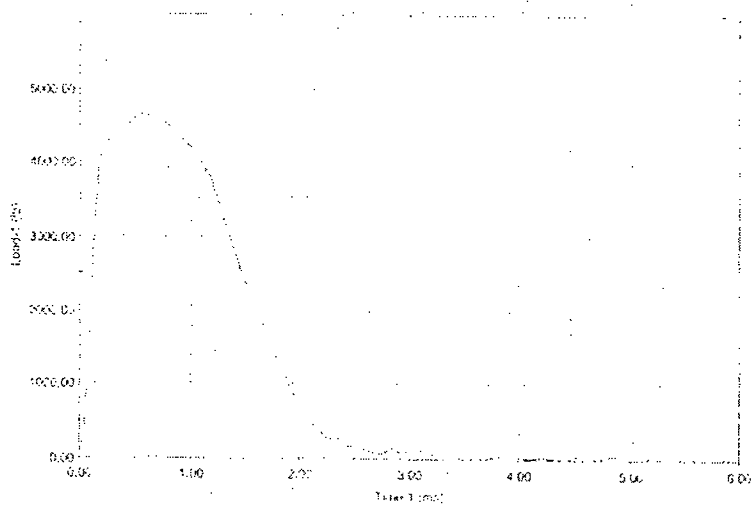

GH29, 75°F

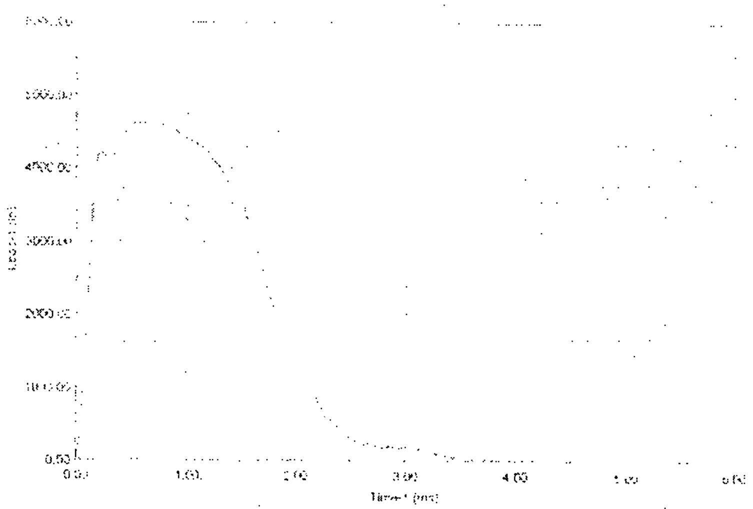

GH27, 100°F

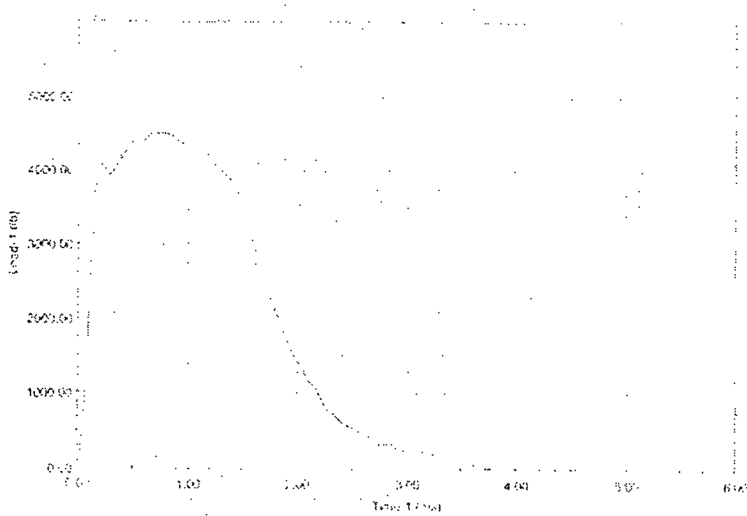

GH19, 125°F

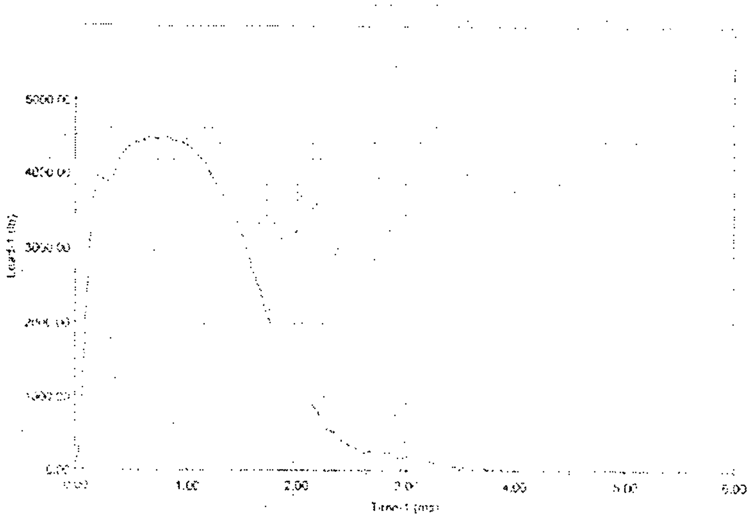

GH25, 150°F

APPENDIX C

CHARPY V-NOTCH PLOTS FOR CAPSULE V USING SYMMETRIC HYPERBOLIC TANGENT CURVE-FITTING METHOD

Contained in Table C-1 are the upper shelf energy values used as input for the generation of the Charpy V-notch plots using CVGRAPH, Version 4.1. The definition for Upper Shelf Energy (USE) is given in ASTM E185-82, Section 4.18, and reads as follows:

> "*upper shelf energy level* – the average energy value for all Charpy specimens (normally three) whose test temperature is above the upper end of the transition region. For specimens tested in sets of three at each test temperature, the set having the highest average may be regarded as defining the upper shelf energy."

If there are specimens tested in set of three at each temperature Westinghouse reports the set having the highest average energy as the USE (usually unirradiated material). If the specimens were not tested in sets of three at each temperature Westinghouse reports the average of all 100% shear Charpy data as the USE. Hence, the USE values reported in Table C-1 and used to generate the Charpy V-notch curves were determined utilizing this methodology.

The lower shelf energy values were fixed at 2.2 ft-lb for all cases.

Table C-1 Upper Shelf Energy Values Fixed in CVGRAPH [ft-lb]

Material	Unirradiated (ft-lbs)	Capsule U (ft-lbs)	Capsule Y (ft-lbs)	Capsule V (ft-lbs)
Intermediate Shell Plate R1606-2 (Long.)	138	127	137	131
Intermediate Shell Plate R1606-2 (Trans.)	113	104	111	106
Weld Metal (heat # V89476)	86	87	96	95
HAZ Material	105	129	130	114

PLATE R1606-2 CAPSULE V

CVGRAPH 4.1 Hyperbolic Tangent Curve Printed at 12:34:21 on 08-15-2003

Page 1

Coefficients of Curve 4

A = 66.59	B = 64.4	C = 87.9	T0 = 44.53

Equation is: CVN = A + B * [tanh((T - T0)/C)]

Upper Shelf Energy: 131 Fixed   Temp. at 30 ft-lbs: -12.1   Temp. at 50 ft-lbs: 21.3   Lower Shelf Energy: 2.19 Fixed

Material: PLATE SA533B1   Heat Number: B8120-1   Orientation: LT

Capsule: V   Total Fluence:

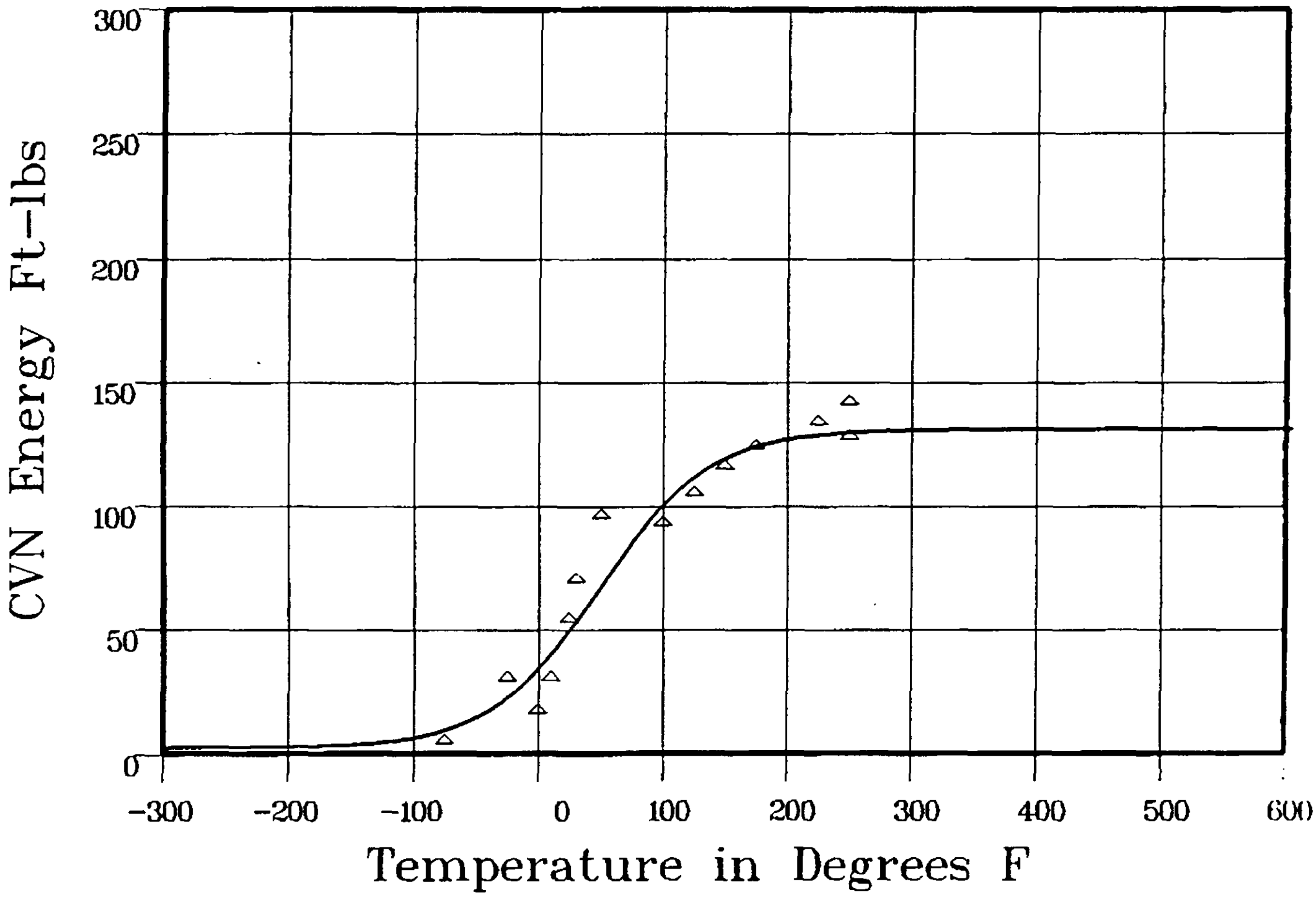

Data Set(s) Plotted

Plant: ST1   Cap.: V   Material: PLATE SA533B1   Ori.: LT   Heat #: B8120-1

Charpy V-Notch Data

Temperature	Input CVN Energy	Computed CVN Energy	Differential
-75	4	10.16	-6.16
-25	29	24.16	4.83
-25	29	24.16	4.83
0	16	36.5	-20.5
10	29	42.52	-13.52
25	53	52.52	.47
30	69	56.05	12.94

**** Data continued on next page ****

PLATE R1606-2 CAPSULE V

Page 2

Material: PLATE SA533B1 Heat Number: B8120-1 Orientation: LT

Capsule: V Total Fluence:

Charpy V-Notch Data (Continued)

Temperature	Input CVN Energy	Computed CVN Energy	Differential
50	95	70.6	24.39
100	92	102.58	-10.58
125	104	113.2	-9.2
150	115	120.28	-5.28
175	123	124.7	-1.7
225	133	128.91	4.08
250	141	129.8	11.19
250	127	129.8	-2.8

SUM of RESIDUALS = -7

PLATE 1606–2 CAPSULE V

CVGRAPH 4.1 Hyperbolic Tangent Curve Printed at 12:40:57 on 08-15-2003
Page 1
Coefficients of Curve 4

A = 36.42	B = 35.42	C = 51.65	T0 = 28.12

Equation is: L.E. = A + B * [tanh((T - T0)/C)]

Upper Shelf L.E.: 71.84 Temperature at L.E. 35: 26 Lower Shelf L.E.: 1 Fixed

Material: PLATE SA533B1 Heat Number: B8120-1 Orientation: LT

Capsule: V Total Fluence:

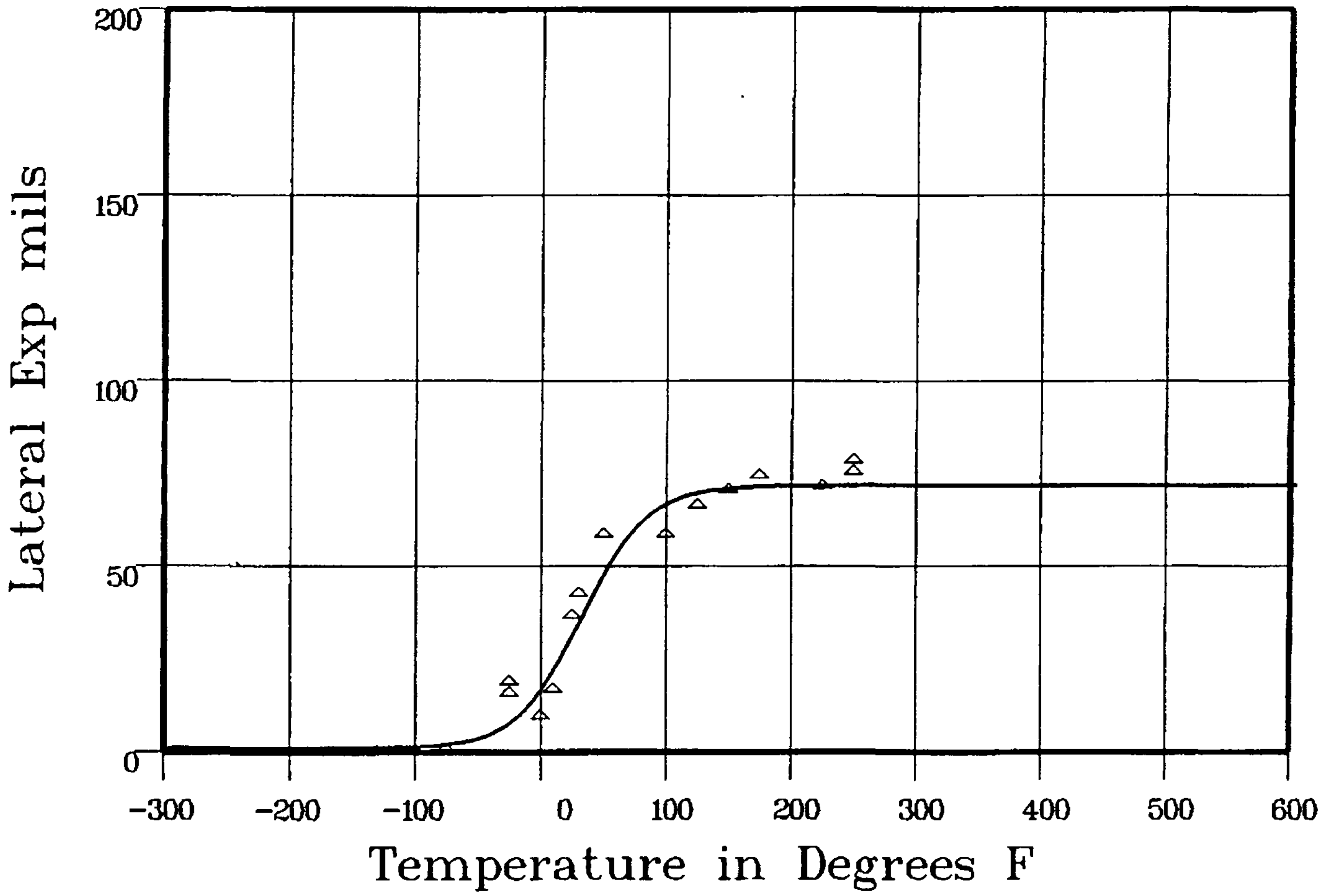

Data Set(s) Plotted
Plant: ST1 Cap.: V Material: PLATE SA533B1 Ori.: LT Heat #: B8120-1

Charpy V-Notch Data

Temperature	Input Lateral Expansion	Computed L.E.	Differential
-75	0	2.28	-2.28
-25	15	9.03	5.96
-25	18	9.03	8.96
0	9	18.84	-9.84
10	16	24.48	-8.48
25	36	34.28	1.71
30	42	37.7	4.29

**** Data continued on next page ****

PLATE 1606-2 CAPSULE V

Page 2

Material: PLATE SA533B1 Heat Number: B8120-1 Orientation: LT

Capsule: V Total Fluence:

Charpy V-Notch Data (Continued)

Temperature	Input Lateral Expansion	Computed L.E.	Differential
50	58	50.58	7.41
100	58	67.71	-9.71
125	66	70.21	-4.21
150	70	71.21	-1.21
175	74	71.6	2.39
225	71	71.81	-.81
250	75	71.83	3.16
250	78	71.83	6.16

SUM of RESIDUALS = 3.52

PLATE 1606-2 CAPSULE V

CVGRAPH 4.1 Hyperbolic Tangent Curve Printed at 12:44:28 on 08-15-2003

Page 1

Coefficients of Curve 4

A = 50	B = 50	C = 75.97	T0 = 58.59

Equation is: Shear% = A + B * [tanh((T - T0)/C)]

Temperature at 50% Shear: 58.5

Material: PLATE SA533B1 Heat Number: B8120-1 Orientation: LT

Capsule: V Total Fluence:

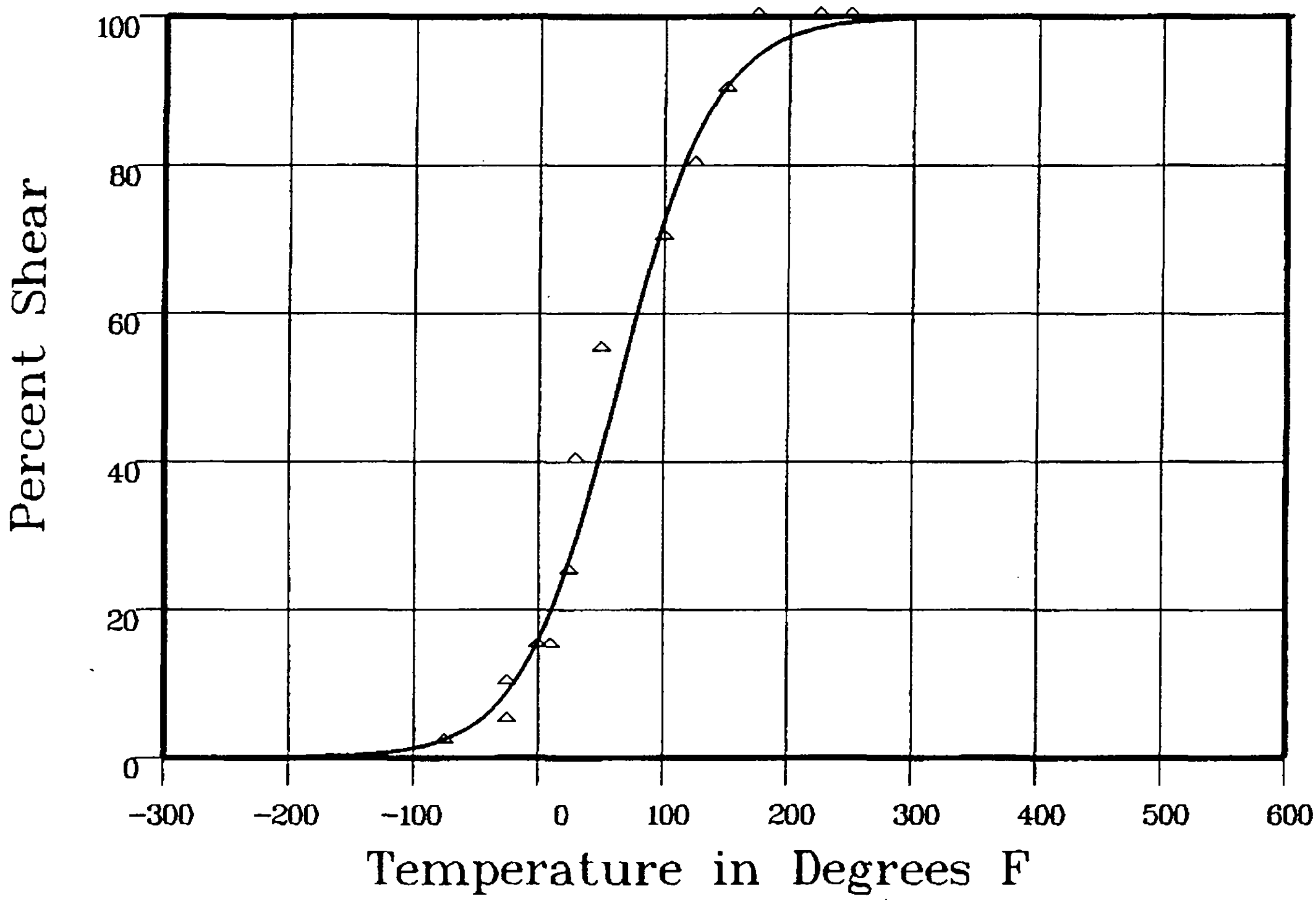

Data Set(s) Plotted

Plant: ST1 Cap.: V Material: PLATE SA533B1 Ori.: LT Heat #: B8120-1

Charpy V-Notch Data

Temperature	Input Percent Shear	Computed Percent Shear	Differential
-75	2	2.88	-.88
-25	10	9.97	.02
-25	5	9.97	-4.97
0	15	17.61	-2.61
10	15	21.76	-6.76
25	25	29.22	-4.22
30	40	32.02	7.97

**** Data continued on next page ****

PLATE 1606-2 CAPSULE V

Material: PLATE SA533B1 Heat Number: B8120-1 Orientation: LT

Capsule: V Total Fluence:

Charpy V-Notch Data (Continued)

Temperature	Input Percent Shear	Computed Percent Shear	Differential
50	55	44.36	10.63
100	70	74.83	-4.83
125	80	85.17	-5.17
150	90	91.72	-1.72
175	100	95.53	4.46
225	100	98.76	1.23
250	100	99.35	.64
250	100	99.35	.64

SUM of RESIDUALS = -5.58

PLATE 1606-2 CAPSULE V

CVGRAPH 4.1 Hyperbolic Tangent Curve   Printed at 12:51:36 on 08-15-2003

Page 1

Coefficients of Curve 4

A = 54.09	B = 51.9	C = 90.48	T0 = 63.28

Equation is: CVN = A + B * [tanh((T - T0)/C)]

Upper Shelf Energy: 106 Fixed   Temp. at 30 ft-lbs: 17.7   Temp. at 50 ft-lbs: 56.1   Lower Shelf Energy: 2.19 Fixed

Material: PLATE SA533B1   Heat Number: B8120-1   Orientation: TL

Capsule: V   Total Fluence:

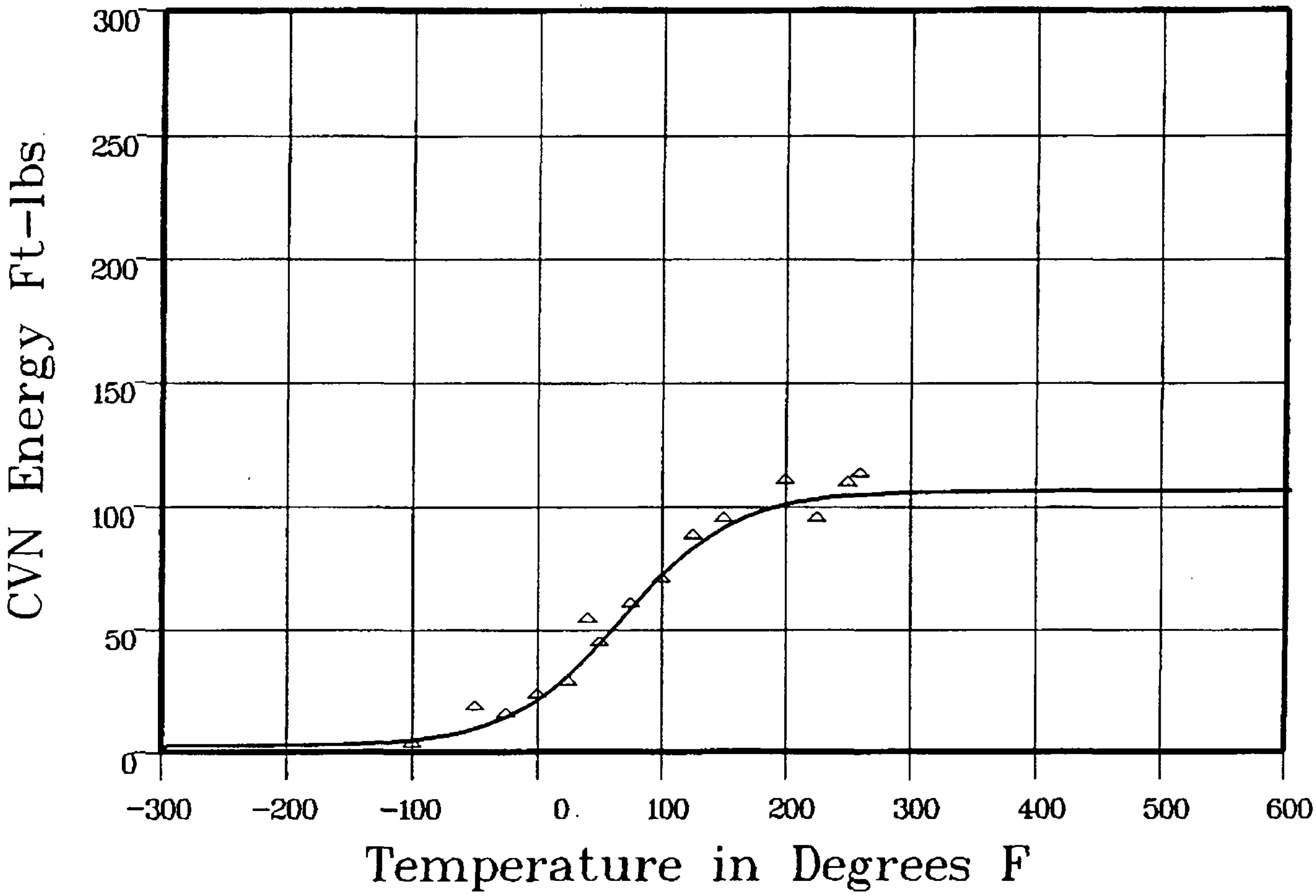

Data Set(s) Plotted

Plant: ST1   Cap: V   Material: PLATE SA533B1   Ori: TL   Heat #: B8120-1

Charpy V-Notch Data

Temperature	Input CVN Energy	Computed CVN Energy	Differential
-100	2	4.93	-2.93
-50	17	10.04	6.95
-25	14	15.11	-1.11
0	22	22.75	-.75
25	27	33.36	-6.36
40	53	41.03	11.96
50	43	46.53	-3.53

**** Data continued on next page ****

PLATE 1606-2 CAPSULE V

Page 2

Material: PLATE SA533B1 Heat Number: B8120-1 Orientation: TL

Capsule: V Total Fluence:

Charpy V-Notch Data (Continued)

Temperature	Input CVN Energy	Computed CVN Energy	Differential
75	59	60.78	-1.78
100	69	74.07	-5.07
125	87	84.87	2.12
150	94	92.69	1.3
200	109	101.17	7.82
225	94	103.17	-9.17
250	108	104.35	3.64
260	112	104.67	7.32

SUM of RESIDUALS = 10.41

PLATE R1606-2 CAPSULE V

CVGRAPH 4.1 Hyperbolic Tangent Curve Printed at 13:28:48 on 08-15-2003

Page 1

Coefficients of Curve 4

A = 35.09	B = 34.09	C = 81.42	T0 = 60

Equation is: L.E. = A + B * [tanh((T - T0)/C)]

Upper Shelf L.E.: 69.18 Temperature at L.E. 35: 59.7 Lower Shelf L.E.: 1 Fixed

Material: PLATE SA533B1 Heat Number: B8120-1 Orientation: TL

Capsule: V Total Fluence:

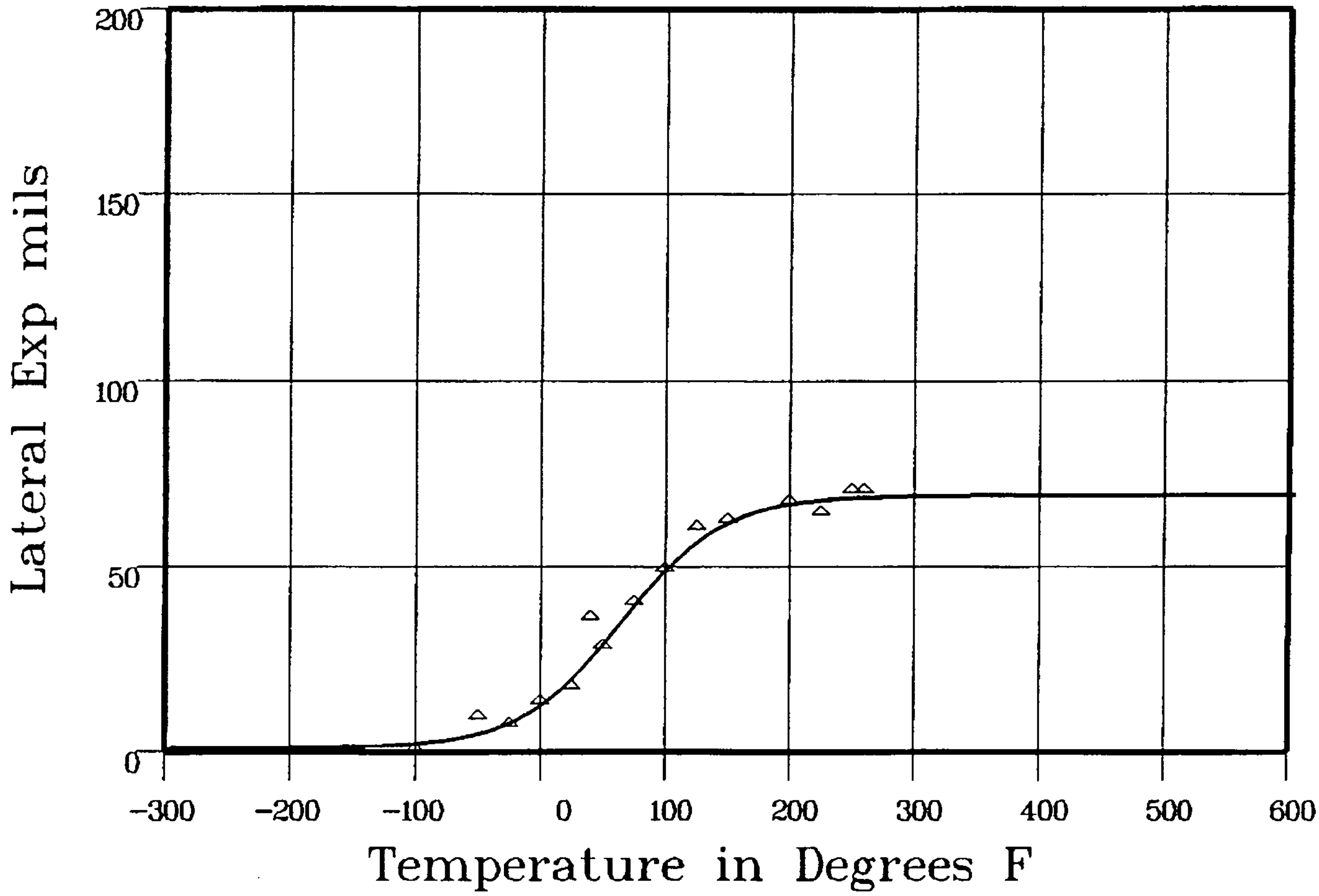

Data Set(s) Plotted

Plant: ST1 Cap.: V Material: PLATE SA533B1 Ori.: TL Heat #: B8120-1

Charpy V-Notch Data

Temperature	Input Lateral Expansion	Computed L.E.	Differential
-100	0	2.31	-2.31
-50	9	5.28	3.71
-25	7	8.52	-1.52
0	13	13.7	-.7
25	17	21.27	-4.27
40	36	26.88	9.11
50	28	30.92	-2.92

**** Data continued on next page ****

PLATE R1606-2 CAPSULE V

Page 2

Material: PLATE SA533B1 Heat Number: B8120-1 Orientation: TL

Capsule: V Total Fluence:

Charpy V-Notch Data (Continued)

Temperature	Input Lateral Expansion	Computed LE	Differential
75	40	41.3	-1.3
100	49	50.61	-1.61
125	60	57.69	2.3
150	62	62.44	-.44
200	67	67.06	-.06
225	64	68.02	-4.02
250	70	68.54	1.45
260	70	68.68	1.31

SUM of RESIDUALS = -1.29

PLATE R1606-2 CAPSULE V

CVGRAPH 4.1 Hyperbolic Tangent Curve Printed at 13:34:11 on 08-15-2003
Page 1
Coefficients of Curve 4

A = 50	B = 50	C = 83.01	T0 = 78.28

Equation is: Shear% = A + B * [tanh((T - T0)/C)]

Temperature at 50% Shear: 78.2

Material: PLATE SA533B1 Heat Number: B8120-1 Orientation: TL

Capsule: V Total Fluence:

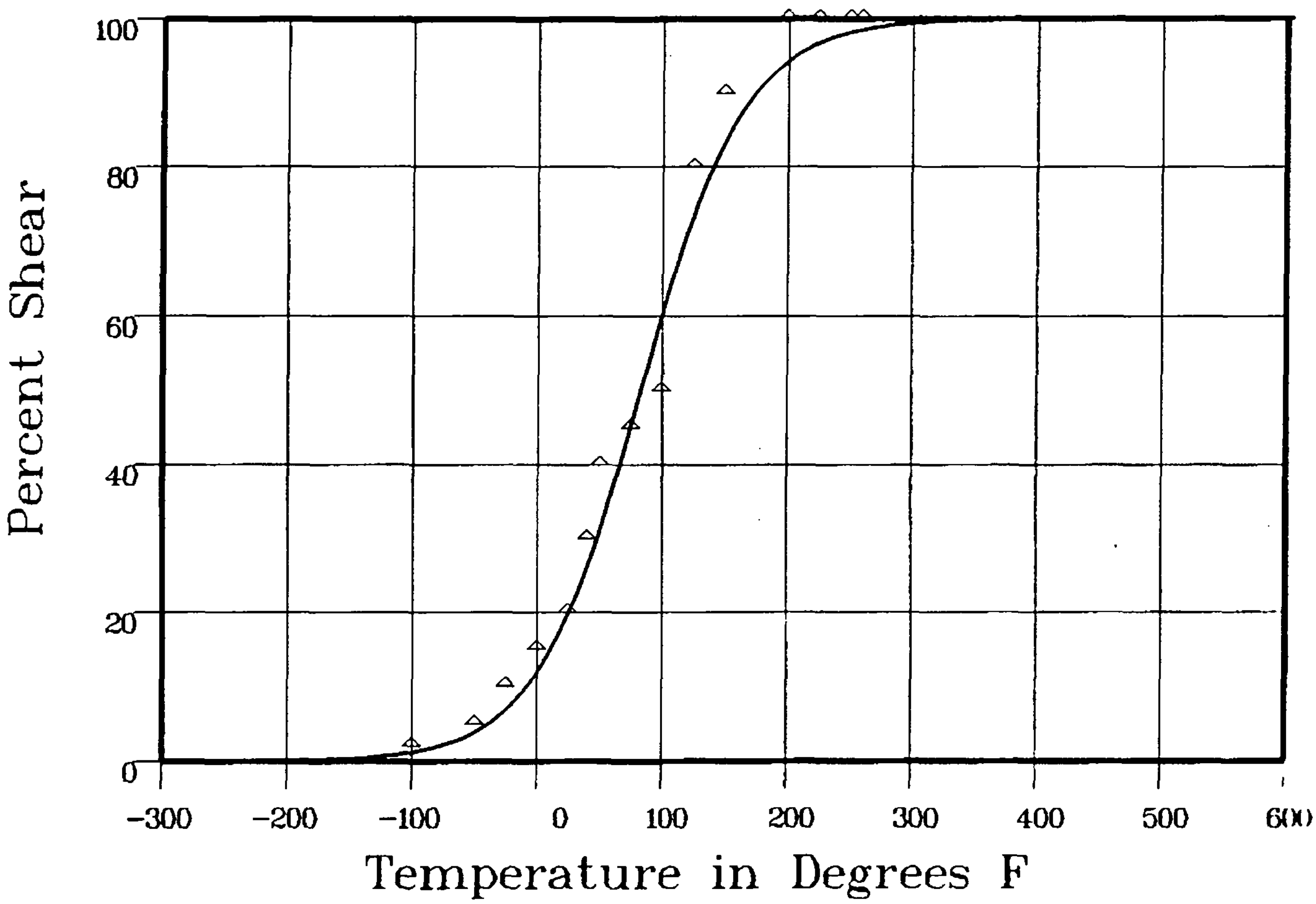

Data Set(s) Plotted
Plant: ST1 Cap.: V Material: PLATE SA533B1 Ori.: TL Heat #: B8120-1

Charpy V-Notch Data

Temperature	Input Percent Shear	Computed Percent Shear	Differential
-100	2	1.34	.65
-50	5	4.35	.64
-25	10	7.66	2.33
0	15	13.17	1.82
25	20	21.69	-1.69
40	30	28.44	1.55
50	40	33.59	6.4

**** Data continued on next page ****

PLATE R1606-2 CAPSULE V

Page 2

Material: PLATE SA533B1 Heat Number: B8120-1 Orientation: TL

Capsule: V Total Fluence:

Charpy V-Notch Data (Continued)

Temperature	Input Percent Shear	Computed Percent Shear	Differential
75	45	48.02	-3.02
100	50	62.79	-12.79
125	80	75.5	4.49
150	90	84.91	5.08
200	100	94.94	5.05
225	100	97.16	2.83
250	100	98.42	1.57
260	100	98.76	1.23

SUM of RESIDUALS = 16.19

WELD METAL CAPSULE V

CVGRAPH 4.1 Hyperbolic Tangent Curve Printed at 13:44:41 on 08-15-2003

Page 1

Coefficients of Curve 4

A = 48.59	B = 46.4	C = 99.07	T0 = 12.65

Equation is: CVN = A + B * [tanh((T - T0)/C)]

Upper Shelf Energy: 95 Fixed Temp. at 30 ft-lbs: -29.4 Temp. at 50 ft-lbs: 15.6 Lower Shelf Energy: 2.19 Fixed

Material: WELD Heat Number: V89476 Orientation:

Capsule: V Total Fluence:

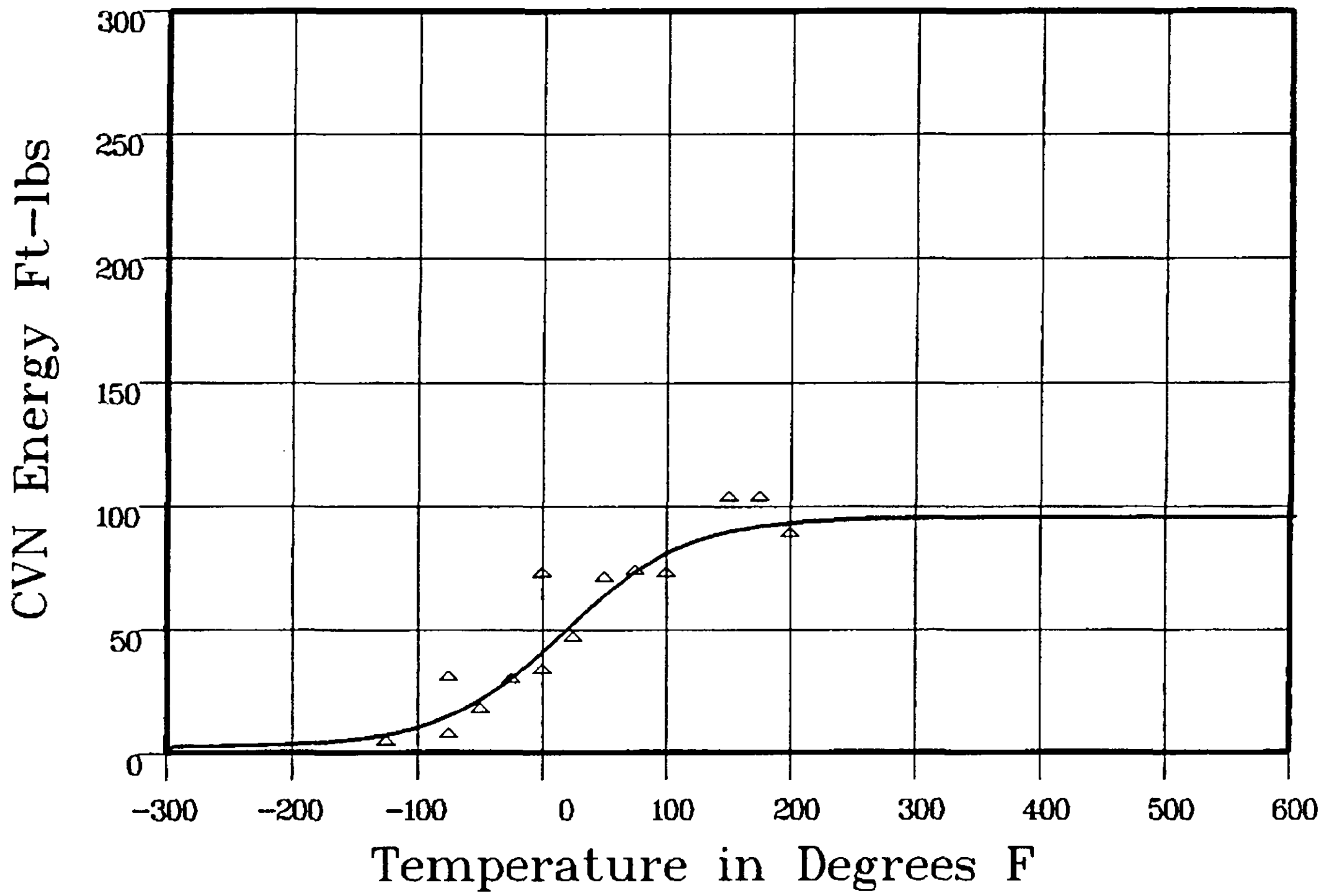

Data Set(s) Plotted

Plant: ST1 Cap.: V Material: WELD Ori.: Heat #: V89476

Charpy V-Notch Data

Temperature	Input CVN Energy	Computed CVN Energy	Differential
-125	3	7.62	-4.62
-75	29	15.71	13.28
-75	6	15.71	-9.71
-50	16	22.62	-6.62
-25	28	31.76	-3.76
0	32	42.7	-10.7
0	71	42.7	28.29

**** Data continued on next page ****

WELD METAL CAPSULE V

Page 2

Material: WELD Heat Number: V89476 Orientation:

Capsule: V Total Fluence:

Charpy V-Notch Data (Continued)

Temperature	Input CVN Energy	Computed CVN Energy	Differential
25	45	54.35	-9.35
50	69	65.3	3.69
75	72	74.46	-2.46
100	71	81.41	-10.41
150	102	89.54	12.45
175	102	91.62	10.37
200	87	92.93	-5.93
200	87	92.93	-5.93

SUM of RESIDUALS = -1.43

WELD METAL CAPSULE V

CVGRAPH 4.1 Hyperbolic Tangent Curve Printed at 13:47:33 on 08-15-2003

Page 1

Coefficients of Curve 4

A = 33.99	B = 32.99	C = 79.44	T0 = 12.18

Equation is: L.E. = A + B * [tanh((T - T0)/C)]

Upper Shelf L.E.: 66.98 Temperature at L.E. 35: 14.6 Lower Shelf L.E.: 1 Fixed

Material: WELD Heat Number: V89476 Orientation:

Capsule: V Total Fluence:

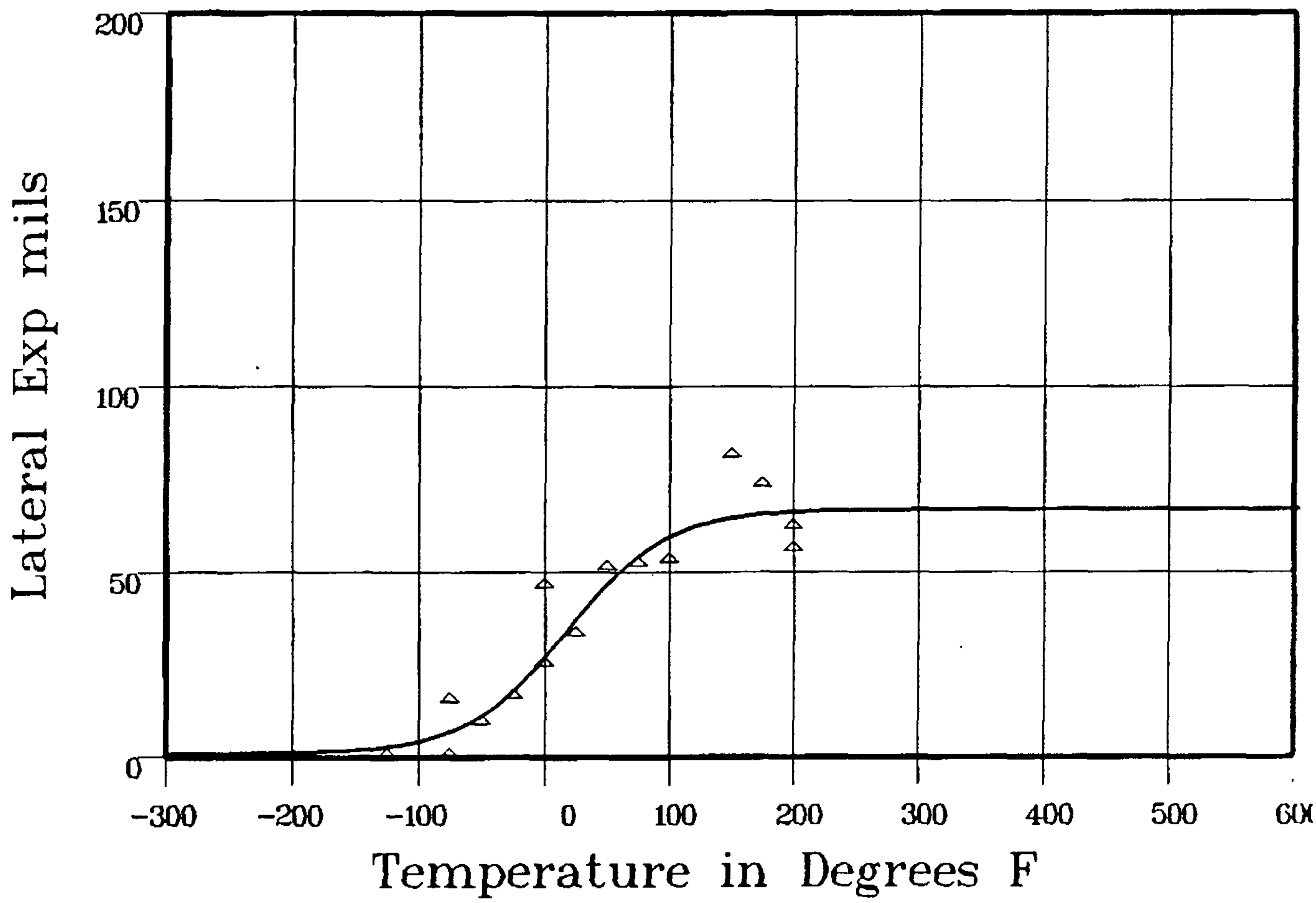

Data Set(s) Plotted

Plant: ST1 Cap.: V Material: WELD Ori.: Heat #: V89476

Charpy V-Notch Data

Temperature	Input Lateral Expansion	Computed L.E.	Differential
-125	0	3.02	-3.02
-75	15	7.61	7.38
-75	0	7.61	-7.61
-50	9	12.4	-3.4
-25	16	19.58	-3.58
0	25	28.97	-3.97
0	46	28.97	17.02

**** Data continued on next page ****

WELD METAL CAPSULE V

Page 2

Material: WELD Heat Number: V89476 Orientation:

Capsule: V Total Fluence:

Charpy V-Notch Data (Continued)

Temperature	Input Lateral Expansion	Computed L.E.	Differential
25	33	39.26	-6.26
50	51	48.6	2.39
75	52	55.72	-3.72
100	53	60.46	-7.46
150	81	64.99	16
175	73	65.9	7.09
200	62	66.4	-4.4
200	56	66.4	-10.4

SUM of RESIDUALS = -3.97

WELD METAL CAPSULE V

CVGRAPH 4.1 Hyperbolic Tangent Curve Printed at 13:51:02 on 08-15-2003

Page 1

Coefficients of Curve 4

A = 50	B = 50	C = 86.85	T0 = 4.21

Equation is: Shear% = A + B * [tanh((T - T0)/C)]

Temperature at 50% Shear: 4.2

Material: WELD Heat Number: V89476 Orientation:

Capsule: V Total Fluence:

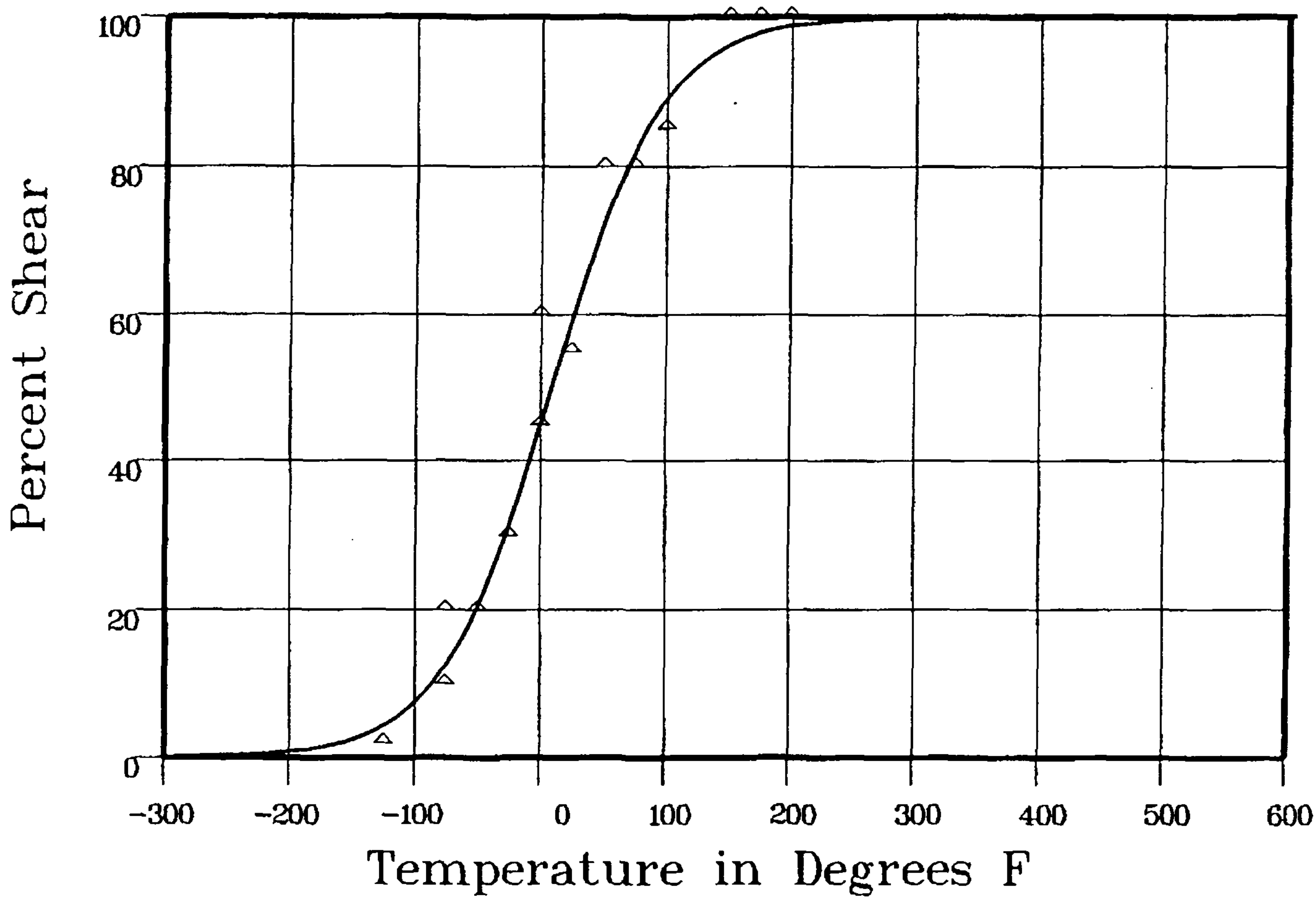

Data Set(s) Plotted

Plant: ST1 Cap.: V Material: WELD Ori.: Heat #: V89476

Charpy V-Notch Data

Temperature	Input Percent Shear	Computed Percent Shear	Differential
-125	2	4.85	-2.85
-75	10	13.89	-3.89
-75	20	13.89	6.1
-50	20	22.29	-2.29
-25	30	33.78	-3.78
0	45	47.57	-2.57
0	60	47.57	12.42

**** Data continued on next page ****

WELD METAL CAPSULE V

Page 2

Material: WELD Heat Number: V89476 Orientation:

Capsule: V Total Fluence:

Charpy V-Notch Data (Continued)

Temperature	Input Percent Shear	Computed Percent Shear	Differential
25	55	61.74	-6.74
50	80	74.15	5.84
75	80	83.61	-3.61
100	85	90.07	-5.07
150	100	96.63	3.36
175	100	98.07	1.92
200	100	98.91	1.08
200	100	98.91	1.08

SUM of RESIDUALS = 1

HAZ CAPSULE V

CVGRAPH 4.1 Hyperbolic Tangent Curve Printed at 14:06:43 on 08-15-2003

Page 1

Coefficients of Curve 4

A = 58.09	B = 55.9	C = 97.26	T0 = -21.56

Equation is: CVN = A + B * [tanh((T - T0)/C)]

Upper Shelf Energy: 114 Fixed Temp. at 30 ft-lbs: -75.3 Temp. at 50 ft-lbs: -35.7 Lower Shelf Energy: 2.19 Fixed

Material: HEAT AFFD ZONE Heat Number: Orientation:

Capsule: V Total Fluence:

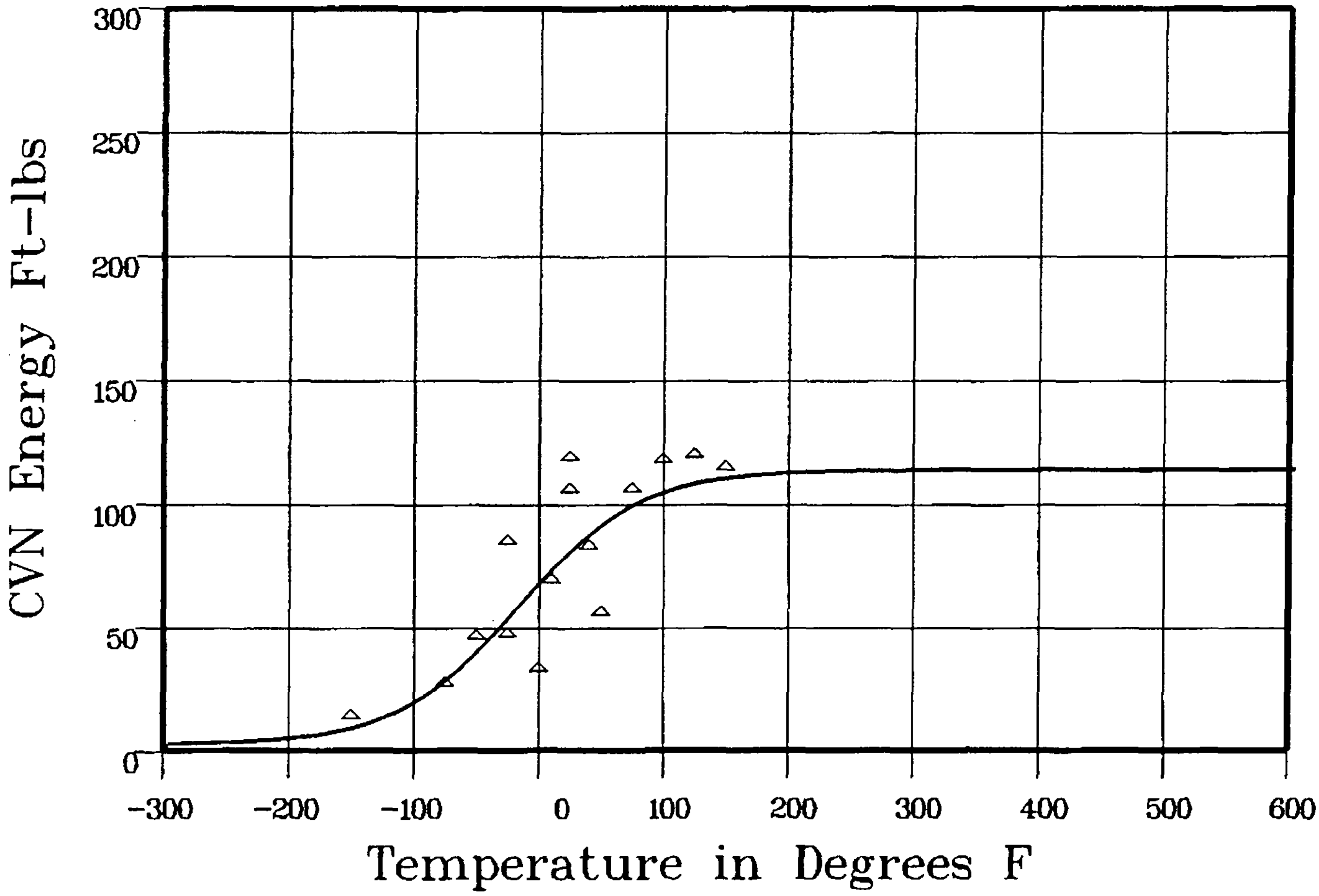

Data Set(s) Plotted

Plant: ST1 Cap.: V Material: HEAT AFFD ZONE Ori.: Heat #:

Charpy V-Notch Data

Temperature	Input CVN Energy	Computed CVN Energy	Differential
-150	13	9.64	3.35
-75	26	30.14	-4.14
-50	45	42.2	2.79
-25	46	56.12	-10.12
-25	84	56.12	27.87
0	32	70.29	-38.29
10	68	75.62	-7.62

**** Data continued on next page ****

HAZ CAPSULE V

Page 2

Material: HEAT AFFD ZONE   Heat Number: Orientation:

Capsule: V   Total Fluence:

Charpy V-Notch Data (Continued)

Temperature	Input CVN Energy	Computed CVN Energy	Differential
25	118	82.98	35.01
25	105	82.98	22.01
40	82	89.4	-7.4
50	55	93.12	-38.12
75	105	100.5	4.49
100	117	105.51	11.48
125	119	108.76	10.23
150	114	110.8	3.19

SUM of RESIDUALS = 14.73

HAZ CAPSULE V

CVGRAPH 4.1 Hyperbolic Tangent Curve Printed at 14:11:50 on 08-15-2003

Page 1

Coefficients of Curve 4

A = 38.73	B = 37.73	C = 93.83	T0 = .46

Equation is: L.E. = A + B * [tanh((T - T0)/C)]

Upper Shelf L.E.: 76.46 Temperature at L.E. 35: -8.8 Lower Shelf L.E.: 1 Fixed

Material: HEAT AFFD ZONE Heat Number: Orientation:

Capsule: V Total Fluence:

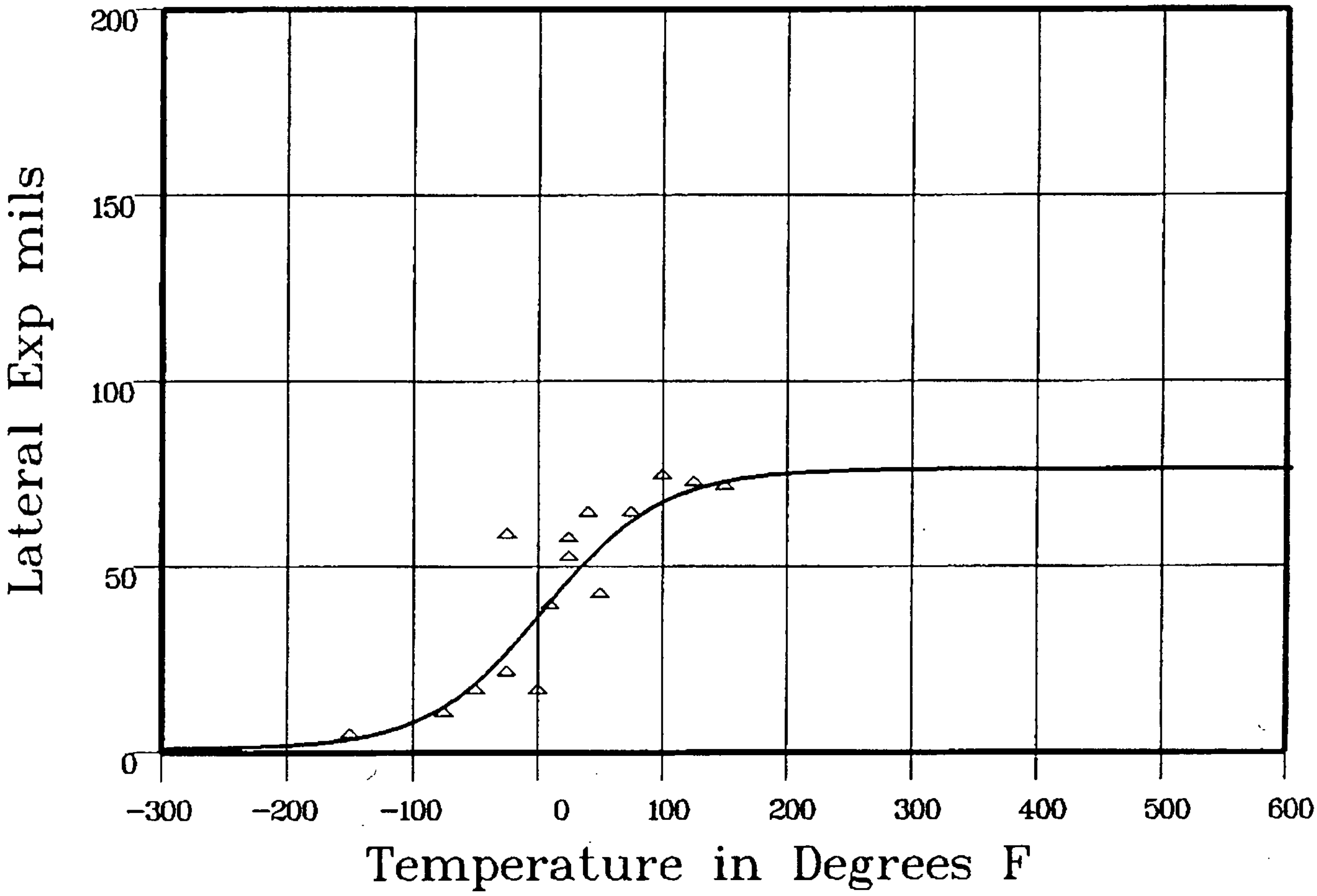

Data Set(s) Plotted

Plant: ST1 Cap: V Material: HEAT AFFD ZONE Ori: Heat #:

Charpy V-Notch Data

Temperature	Input Lateral Expansion	Computed L.E.	Differential
-150	4	3.93	.06
-75	10	13.58	-3.58
-50	16	20.19	-4.19
-25	21	28.73	-7.73
-25	58	28.73	29.26
0	16	38.54	-22.54
10	39	42.55	-3.55

**** Data continued on next page ****

HAZ CAPSULE V

Page 2

Material: HEAT AFFD ZONE   Heat Number: Orientation:

Capsule: V   Total Fluence:

Charpy V-Notch Data (Continued)

Temperature	Input Lateral Expansion	Computed LE.	Differential
25	52	48.37	3.62
25	57	48.37	8.62
40	64	53.75	10.24
50	42	56.98	-14.98
75	64	63.66	.33
100	74	68.38	5.61
125	72	71.5	.49
150	71	73.47	-2.47

SUM of RESIDUALS = -.82

HAZ CAPSULE V

CVGRAPH 4.1 Hyperbolic Tangent Curve Printed at 14:14:08 on 08-15-2003

Page 1

Coefficients of Curve 4

A = 50	B = 50	C = 66.93	T0 = -14.53

Equation is: Shear% = A + B * [tanh((T - T0)/C)]

Temperature at 50% Shear: -14.5

Material: HEAT AFF'D ZONE Heat Number: Orientation:

Capsule: V Total Fluence:

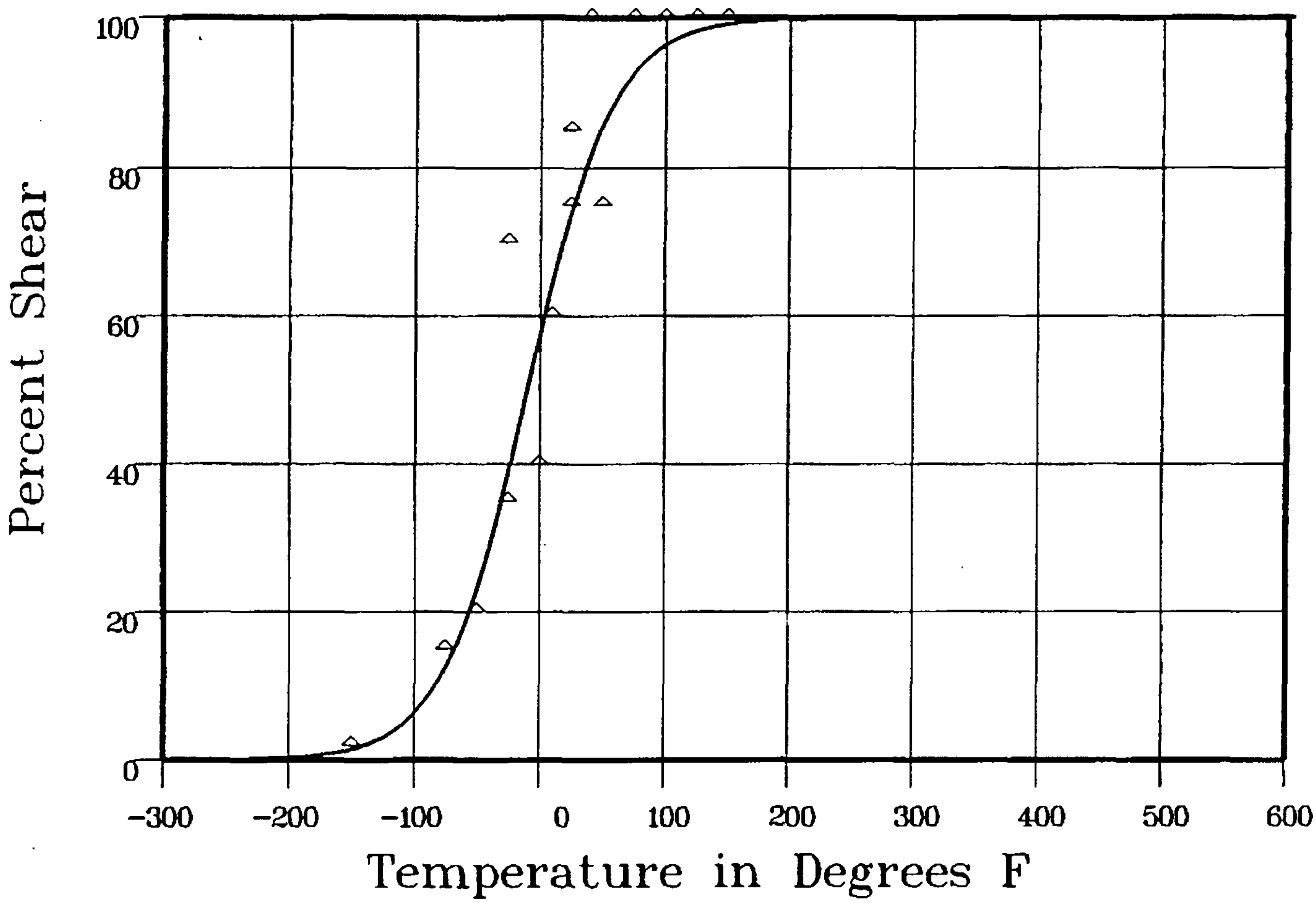

Data Set(s) Plotted

Plant: ST1 Cap: V Material: HEAT AFF'D ZONE Ori: Heat #:

Charpy V-Notch Data

Temperature	Input Percent Shear	Computed Percent Shear	Differential
-150	2	1.71	.28
-75	15	14.1	.89
-50	20	25.73	-5.73
-25	35	42.24	-7.24
-25	70	42.24	27.75
0	40	60.68	-20.68
10	60	67.54	-7.54

**** Data continued on next page ****

HAZ CAPSULE V

Page 2

Material: HEAT AFFD ZONE   Heat Number: Orientation:

Capsule: V   Total Fluence:

Charpy V-Notch Data (Continued)

Temperature	Input Percent Shear	Computed Percent Shear	Differential
25	85	76.51	8.48
25	75	76.51	-1.51
40	100	83.6	16.39
50	75	87.3	-12.3
75	100	93.55	6.44
100	100	96.83	3.16
125	100	98.47	1.52
150	100	99.27	.72

SUM of RESIDUALS = 10.64

APPENDIX D

SOUTH TEXAS UNIT 1 SURVEILLANCE PROGRAM CREDIBILITY EVALUATION

INTRODUCTION:

Regulatory Guide 1.99, Revision 2, describes general procedures acceptable to the NRC staff for calculating the effects of neutron radiation embrittlement of the low-alloy steels currently used for light-water-cooled reactor vessels. Position C.2 of Regulatory Guide 1.99, Revision 2, describes the method for calculating the adjusted reference temperature and Charpy upper-shelf energy of reactor vessel beltline materials using surveillance capsule data. The methods of Position C.2 can only be applied when two or more credible surveillance data sets become available from the reactor in question.

To date there has been three surveillance capsules removed from the South Texas Unit 1 reactor vessel. To use these surveillance data sets, they must be shown to be credible. In accordance with the discussion of Regulatory Guide 1.99, Revision 2, there are five requirements that must be met for the surveillance data to be judged credible.

The purpose of this evaluation is to apply the credibility requirements of Regulatory Guide 1.99, Revision 2, to the South Texas Unit 1 reactor vessel surveillance data and determine if the South Texas Unit 1 surveillance data is credible.

EVALUATION:

Criterion 1: Materials in the capsules should be those judged most likely to be controlling with regard to radiation embrittlement.

The South Texas Unit 1 reactor vessel consists of the following beltline region materials:

- Intermediate Shell Plates R1606-1, 2, 3
- Lower Shell Plates R1622-1, 2, 3
- Intermediate & Lower Shell Longitudinal Weld Seams (Heat # 89476),
- Intermediate to Lower Shell Circumferential Weld Seam (Heat # 89476).

At the time when the South Texas Unit 1 surveillance program material was selected it was believed that copper and phosphorus were the elements most important to embrittlement of the reactor vessel steels. The intermediate shell plate R1606-2 had one of the highest initial RT_{NDT} and the lowest USE of all plate materials in the beltline region. In addition, the intermediate shell plate R1606-2 had approximately the same copper and phosphorus content as the other beltline plate materials. Therefore, based on the highest initial RT_{NDT} and the lowest USE, the intermediate shell plate R1606-2 was chosen for the surveillance program.

The weld material in the South Texas Unit 1 surveillance program was made of the same wire as all the reactor vessel beltline welds, thus it was chosen as the surveillance weld material.

Hence, Criterion 1 is met for the South Texas Unit 1 reactor vessel.

Criterion 2: Scatter in the plots of Charpy energy versus temperature for the irradiated and unirradiated conditions should be small enough to permit the determination of the 30 ft-lb temperature and upper shelf energy unambiguously.

Based on engineering judgment, the scatter in the data presented in these plots is small enough to permit the determination of the 30 ft-lb temperature and the upper shelf energy of the South Texas Unit 1 surveillance materials unambiguously. Hence, the South Texas Unit 1 surveillance program meets this criterion.

Criterion 3: When there are two or more sets of surveillance data from one reactor, the scatter of ΔRT_{NDT} values about a best-fit line drawn as described in Regulatory Position 2.1 normally should be less than 28°F for welds and 17°F for base metal. Even if the fluence range is large (two or more orders of magnitude), the scatter should not exceed twice those values. Even if the data fail this criterion for use in shift calculations, they may be credible for determining decrease in upper shelf energy if the upper shelf can be clearly determined, following the definition given in ASTM E185-82.

The functional form of the least squares method as described in Regulatory Position 2.1 will be utilized to determine a best-fit line for this data and to determine if the scatter of these ΔRT_{NDT} values about this line is less than 28°F for welds and less than 17°F for the plate.

Following is the calculation of the best-fit line as described in Regulatory Position 2.1 of Regulatory Guide 1.99, Revision 2. In addition, the recommended NRC methods for determining credibility will be followed. The NRC methods were presented to industry at a meeting held by the NRC on February 12 and 13, 1998. At this meeting the NRC presented five cases. Of the five cases, Case 1 ("Surveillance data available from plant but no other source") most closely represents the situation listed above for South Texas Unit 1 surveillance weld metal and plate materials.

TABLE D-1

Calculation of Chemistry Factors using South Texas Unit 1 Surveillance Capsule Data

Material	Capsule	Capsule f[(a)]	FF[(b)]	ΔRT_{NDT}[(c)]	FF*ΔRT_{NDT}	FF^2
Intermediate Shell	U	0.258	0.632	18.09	11.433	0.399
Plate R1606-2	Y	1.29	1.071	43.98	47.103	1.147
(Longitudinal)	V	2.62	1.258	40.15	50.509	1.583
Intermediate Shell	U	0.258	0.632	23.44	14.814	0.399
Plate R1606-2	Y	1.29	1.071	11.94	12.788	1.147
(Transverse)	V	2.62	1.258	23.84	29.991	1.583
				SUM:	166.638	6.258
	$CF_{R1606-2} = \Sigma(FF * RT_{NDT}) \div \Sigma(FF^2) = (166.638) \div (6.258) =$ **26.6°F**					
Surveillance Weld	U	0.258	0.632	33.58	21.223	0.399
Material	Y	1.29	1.071	37.89	40.580	1.147
	V	2.62	1.258	26.61	33.475	1.583
				SUM:	95.278	3.129
	$CF_{Surv.\ Weld} = \Sigma(FF * RT_{NDT}) \div \Sigma(FF^2) = (95.278) \div (3.129) =$ **30.4°F**					

Notes:

(a) f = fluence. Calculated fluence from Section 6 of this report, [x 10^{19} n/cm^2, E > 1.0 MeV].

(b) FF = fluence factor = $f^{(0.28 - 0.1*\log f)}$.

(c) ΔRT_{NDT} values are the measured 30 ft-lb shift values taken from Appendix C, herein [°F].

The scatter of ΔRT_{NDT} values about the functional form of a best-fit line drawn as described in Regulatory Position 2.1 is presented in Table D-2.

Table D-2:
South Texas Unit 1 Surveillance Capsule Data Scatter about the Best-Fit Line for Surveillance Forging Materials.

Material	Capsule	CF (Slope$_{best\ fit}$)	FF	Measured ΔRT$_{NDT}$	Predicted ΔRT$_{NDT}$	Scatter ΔRT$_{NDT}$ (°F)	<17°F (Base Metals) <28°F (Weld)
Intermediate Shell Plate R1606-2 (Longitudinal)	U	26.6	0.632	18.09	16.81	1.28	Yes
	Y	26.6	1.071	43.98	28.49	15.49	Yes
	V	26.6	1.258	40.15	33.46	6.69	Yes
Intermediate Shell Plate R1606-2 (Transverse)	U	26.6	0.632	23.44	16.81	6.63	Yes
	Y	26.6	1.071	11.94	28.49	-16.55	Yes
	V	26.6	1.258	23.84	33.46	-9.62	Yes
Vessel Beltline Welds (Heat # 89476)	U	30.4	0.632	33.58	19.21	14.37	Yes
	Y	30.4	1.071	37.89	32.56	5.33	Yes
	V	30.4	1.258	26.61	38.24	-11.63	Yes

Table D-2 indicates that no data point falls outside the +/- 1σ of 17°F scatter band for the intermediate shell plate R1606-2 surveillance data. In addition, no data points fall outside the +/- 1σ of 28°F scatter band for the surveillance weld data. Therefore, the intermediate shell plate R1606-2 and the weld data is deemed credible per the third criterion.

Criterion 4: The irradiation temperature of the Charpy specimens in the capsule should match the vessel wall temperature at the cladding/base metal interface within +/- 25°F.

The capsule specimens are located in the reactor between the core barrel and the vessel wall and are positioned opposite the center of the core. The test capsules are in baskets attached to the neutron pad. The location of the specimens with respect to the reactor vessel beltline provides assurance that the reactor vessel wall and the specimens experience equivalent operating conditions such that the temperatures will not differ by more than 25°F. Hence, this criterion is met.

Criterion 5: The surveillance data for the correlation monitor material in the capsule should fall within the scatter band of the database for that material.

The South Texas Unit 1 surveillance program does not contain correlation monitor material. Therefore, this criterion is not applicable to the South Texas Unit 1 surveillance program.

CONCLUSION:

Based on the preceding responses to all five criteria of Regulatory Guide 1.99, Revision 2, Section B and 10 CFR 50.61, the South Texas Unit 1 surveillance plate and weld data is credible.